Glutamic acid metabolism alterations, causes and consequences in ALS

Thesis

Glutamic acid metabolism alterations, causes and consequences in ALS

Nikola Holodkov

A thesis submitted in fulfilment of the requirements of The Open University, United Kingdom, for the degree of Doctor of Philosophy

Neurobiology group, International Centre for Genetic Engineering and Biotechnology (ICGEB), Trieste, Italy

Director of studies: Dr. Fabian Feiguin

External supervisor: Dr. Alessandro Marcello

September 2018

ABSTRACT

Amyotrophic Lateral Sclerosis (ALS) is a progressive and fatal motor system disease that affects motoneurons causing paralysis and muscular atrophy. Recently, it has been discovered that defects in the protein TDP-43 were present in most patients that suffer from ALS. Similar modifications in the *Drosophila melanogaster* conserved protein TBPH reproduced the motor symptoms observed in ALS patients, such as locomotion problems and reduced life expectancy. These phenotypes were mainly originated from alterations in the organization of proteins responsible for synaptic transmission at the neuromuscular junctions (NMJs) in Drosophila.

The objectives of this work are to discover the proteins affected by TBPH function and determine their role in neuronal and non-neuronal tissues. Moreover, I would like to know how they exert their functions and establish whether these pathways are conserved in humans and/or modified in ALS patients. For these experiments, we took advantage of a genome wide proteomic screening to discover that Glutamic Acid Decarboxylase 1 (GAD1), the enzyme that converts Glutamate to GABA, was downregulated in flies lacking the expression of TBPH. We found that this alteration provoked the excessive accumulation of Glutamate, which in turn, promoted defects in the organization of the post-synaptic

proteins Disc Large and GluRIIA. Pharmacological treatments with Glutamate receptor antagonist Memantine was able to recover the motility problems described in TBPH null larvae including the clustering of the GluRIIA at the terminal membranes. Importantly, we discovered that the suppression of TDP-43 provoked the downregulation of GAD67, the GAD1 homolog protein in human neuroblastoma cell lines and analogous modifications were observed in iPSC-derived motoneurons from ALS patients carrying mutations in TDP-43, uncovering conserved disease mechanisms. In conclusion, we show for the first time a connection between Glutamate metabolism disorders and TDP-43 proteinopathy, two pathological mechanisms of primary importance in ALS.

Acknowledgements

In the first place, I would like to dedicate this thesis to my family, which believed in and supported me over the entire length of my studies. Second, I want to thank my principal investigator, Dr. Fabian Feiguin, for accepting me in his laboratory and giving me the possibility to successfully complete my PhD studies. A heartfelt thank I own to Giulia and Raffaella that shared their expertise and helped me during all stages of my scientific growing. I want to thank all the lab members, in particular Chiara, Marina, Alessio, Nina and Monsurat, for the cheerful moments we had together. Finally, I want to thank all the people within ICGEB that made my studies possible, primarily Prof. Giacca, Dr. Venturi, Dr. Marcello, Dr. Banks, Mrs. Argenti, Mrs. Nigris, Mrs. Brandolin and Mrs. Feriani. Thank you!

Table of Contents

List of figures

4.6) The effect of dGAD1 genetic manipulation on the GluRs receptor field at Drosophila's NMJs

4.7) TBPH deletions cause a loss of endogenous protein expression, locomotor impairment and degenerated motoneurons at the NMJ level

4.7) TBPH controls Syntaxin, Synapsin, Cysten String Protein, Disc Large and GluRIIA clustering at the NMJs

5.1) Genome wide proteomic analysis of TBPH null larvae

5.1) Magnification and quantification of the downregulated spot 701 in 2D gel electrophoresis of TBPH null flies

5.1) $GAD1^{MIMIC}$ protein levels in TBPH null larvae

5.1) mRNA levels of GAD1 in TBPH null larvae

6.1) GAD1 overexpression in pan-neuronal tissues in TBPH null larvae

6.2) Motoneuron branching and synaptic boutons shape integrity in TBPH null larvae upon GAD1 overexpression in neurons

6.3) Distribution of pre-synaptic protein Bruchpilot in the NMJ of TBPH null larvae upon GAD1 overexpression in neurons

6.3) Distribution of pre-synaptic protein Syntaxin in the NMJ of TBPH null larvae upon GAD1 overexpression in neurons

6.3) Distribution of post-synaptic protein Disc Large in the NMJ of TBPH null larvae upon GAD1 overexpression in neurons

6.3) Distribution of post-synaptic protein GluRIIA in the NMJ of TBPH null larvae upon GAD1 overexpression in neurons

6.4) Motility assay upon GAD1 silencing in pan-neuronal tissues

6.4) Branching of motoneurons upon GAD1 suppression in neurons

6.4) Bruchpilot distribution in the NMJ upon GAD1 silencing in neurons

6.4) Syntaxin distribution in the NMJ upon GAD1 silencing in neurons

6.4) Distribution of post-synaptic protein Disc Large in the NMJ upon GAD1 silencing in neurons

6.4) Distribution of post-synaptic protein GluRIIA in the NMJ upon GAD1 silencing in neurons

7.1) GAD1 overexpression in the glia of TBPH null larvae

7.1) Glial wrapping and motoneuron branching upon GAD1 overexpression in the glia of TBPH null larvae

7.1) Distribution of pre-synaptic protein Bruchpilot in the NMJ of TBPH null larvae upon GAD1 overexpression in the glia

7.1) Distribution of pre-synaptic protein Syntaxin in the NMJ of TBPH null larvae upon GAD1 overexpression in the glia

7.1) Distribution of post-synaptic protein Disc Large in the NMJ of TBPH null larvae upon GAD1 overexpression in the glia

7.1) Distribution of post-synaptic protein GluRIIA in the NMJ of TBPH null larvae upon GAD1 overexpression in the glia

7.2) larval locomotion upon GAD1 silencing in glial tissues

7.2) Motoneuron branching upon GAD1 silencing in the glia

7.2) Bruchpilot distribution in the NMJ upon GAD1 silencing in the glia

7.2) Distribution of pre-synaptic protein Syntaxin in the NMJ upon GAD1 silencing in the glia

7.2) Distribution of post-synaptic protein Disc Large in the NMJ upon GAD1 silencing in the glia

7.2) Distribution of post-synaptic protein GluRIIA in the NMJ upon GAD1 silencing in the glia

8.1) Glutamate concentration in the haemolymph of TBPH null third instar larvae

8.2) Motility assays of TBPH null larvae after Memantine treatment

8.2) Motility assays of TBPH null third instar larvae after LiCl treatment

8.2) Motility assay after Memantine treatment of larvae with reduced levels of TBPH expression in neurons

8.3) GluRIIA clustering of larvae with TBPH deficiency in neurons after Memantine treatment

8.4) GABA levels in Drosophila's NMJ of TBPH null larvae

8.4) GABA levels in Drosophila's brain of TBPH null larvae

8.5) Motility assays of TBPH null larvae after GABA treatment

9.1) GAD67 expression values upon silencing of TDP-43 in human neuroblastoma cells

9.2) GAD67 protein expression in iPSC derived from ALS patients

9.2) GAD67 protein expression in motoneurons derived from iPSC of ALS patients

9.2) Expression of GAD67 mRNA in motoneurons derived from iPSC of ALS patients

M&M) TDP43 protein mutation scheme

List of abbreviations

Ach – Acetylcholine

AChR – Acetylcholine Receptor

AD – Alzheimer Disease

ADAR2 – Double-Stranded RNA-Specific Adenosine Deaminase 2

AEL – After egg laying

ALS – Amyotrophic Lateral Sclerosis

AMPA – α-Amino-3-Hydroxy-5-Methyl-4-Isoxazolepropionic Acid

ATD – Amino-terminal Domain

ATP – Adenosine Tri Phosphate

Brp - Bruchpilot

C9ORF72 – Chromosome 9 Open Reading Frame

cALS – classic ALS

cAMP – cyclic Adenosine Mono-Phosphate

CAST - Cytoskeletal Matrix Associated with the Active Zone associated Structural Protein

CFTR – Cystic Fibrosis Transmembrane Conductance Regulator

CLIP – Cross-Linked Immunoprecipitation

CNS – Central Nervous system

CSF – Cerebrospinal Fluid

CTD – C-terminal Domain

Ctrl - Contorl

CyO – Curly O

dALS – ALS with Dementia

dGAD1 – Drosophila Glutamate Decarboxylase 1

dGAD2 – Drosophila Glutamate Decarboxylase 2

DLB – Dementia with Lewy's bodies

DLG – Disc Large

DNA – Deoxyribonucleic acid

dNR1/NMDAR-I – NMDA like protein 1

dNR2/NMDAR-II – NMDA like protein 2

EAAT – Excitatory Amino Acid Transporter

EMG – Electromyography

EPSP – Excitatory Post-Synaptic Potential

ESC – Emryonal Stem Cells

EWSR1 – EWS RNA Binding Protein 1

fALS – Familial ALS

FDA – Food and Drug Administration

FTD – Frontotemporal Dementia

FTLD – Frontotemporal Lobar Degeneration

FUS – Fused in Sarcoma

GABA – γ Amino Butyric Acid

GABAR – GABA Receptor

GAD1 – Glutamic Acid Decarboxylase

GAD25 – Glutamate Decarboxylase subunit 25

GAD44 – Glutamate Decarboxylase subunit 44

GAD65 - Glutamic Acid Decarboxylase 65

GAD67 - Glutamic Acid Decarboxylase 67

GADPH – Glyceraldehyde 3-phosphate dehydrogenase

GDH – Glutamate Dehydrogenase

GFP – Green Fluorescent Protein

GLAST – Glutamate and Aspartate Transporter

GLT-1 – Glial Glutamate Transporter 1

GluRIIA – Glutamate Receptor Subunit II A

GluRs – Glutamate Receptors

GOF – Gain of Function

GPCR – G Protein Coupled Receptors

GS – Glutamine Synthetase

hnRNP – hetero nuclear RNA Nuclear Protein

HpSCL – Hippocampal Sclerosis

Hrp – Horseradish Peroxydase

hTDP-43 – human TAR DNA Binding Protein 43 kDA

IEF – Iso Electro Focusing

iGluR – ionotropic Glutamate Receptor

iPSC – induced Pluripotent Stem Cells

ISN – Intersegmental Nerve

LB – Luria Broth

LBD – Ligand Binding Domain

LiCl – Lithium Chloride

LMN – Lower Motoneuron

LOF – Loss of Function

LQ-MS – Liquid Chromatography-Mass Spectrometry

MAGUK – Membrane Associated Guanylate Kinases

MAP1B – Microtubule Associated Protein 1B

mGAD1 – mice Glutamate Decarboxylase 1

mGluR – metabotropic Glutamate Receptor

miRNA – micro RNA

MN - Motoneuron

MND – Motor Neuron Disease

mRNA – messenger RNA

NES – Nuclear Export Sequence

NGS – Normal Goat Serum

NLS – Nuclear Localizing Sequence

NMDA – N-Methyl D-Aspartate

NMDAR – N-Methyl D-Aspartate Receptor

NMJs – Neuromuscular junctions

OAA – Oxaloacetic Acid

OPTN – Optineurin

PBS – Phosphate Buffer Saline

PC – Pyruvate Carboxylase

PEG – Percutaneous Endoscopic Gastrotomy

PLC/IP3/DAG – Phopholipase C/Inositol 1,4,5-triphosphate/diacylglycerol

PLP – Pyridoxal 5'-Phosphate

PLS – Primary Lateral Sclerosis

PMA – Primary Muscular Atrophy

PNS – Peripheral Nervous system

PTSD – Post Traumatic Stress Disorder

RBD – RNA Binding Domain

RBP – RNA Binding Protein

RNA – Ribonucleic Acid

RNP – Ribonuclear Particle

RRM1 – RNA Recognition Motif 1

RRM2 – RNA Recognition Motif 2

RT-PCR – Real-Time Polymerase Chain Reaction

sALS – Sporadic ALS

SeV – Sendai Virus

SN – Segmental Nerve

SNARE – Soluble N-Ethylmaleimide Sensitive Fusion Attachment Protein Receptors

SOD1 – Superoxide Dismutase 1

SQSTM1 – Sequestome 1

Syn – Synapsin

Syx – Syntaxin

TAF15 – TATA Box Binding protein associated factor 15

TARDBP – TAR DNA Binding Protein

TCA – Tricarboxylic Acid

TDP-43 – TAR DNA binding protein 43 kDa

TMD – Transmembrane Domain

tSNAREs – transmembrane Soluble N-Ethylmaleimide Sensitive Fusion Attachment Protein Receptors

UAS – Upstream Activating Sequences

UBQLN2 – Ubiquilin 2

UMN – Upper Motoneuron

VCP – Valosin Containing Protein

vGAT – vesicular GABA Transporter

vSNAREs – vesicular Soluble N-Ethylmaleimide Sensitive Fusion Attachment Protein Receptors

Wt – Wild Type

Experimental contributions

I want to thank Dr. Fabian Feiguin for supervising the project and guiding the experimental design. I wish to acknowledge Prof. Rodolfo Garcia and Dr. Raffaella Klima for most of the work done that regarded the genome wide proteomic analysis. Dr. Giulia Romano for helping and supervising the larval movements, the neuromuscular junction stainings and related quantifications, as well as for providing the material for LC-MS analysis. Dr. Corrado Guarnaccia who did the Liquid Chromatography. Federica Grilli who helped in the drug administration experiments. Dr. Monica Nizzardo and Dr. Federica Rizzo for providing us the induced pluripotent stem cells (iPSC) and Dr. Raffaella Klima who was involved in the experiments with iPSC lines. Thank You!

List of publications

Please note that some parts of this PhD thesis have been published in the following journal:

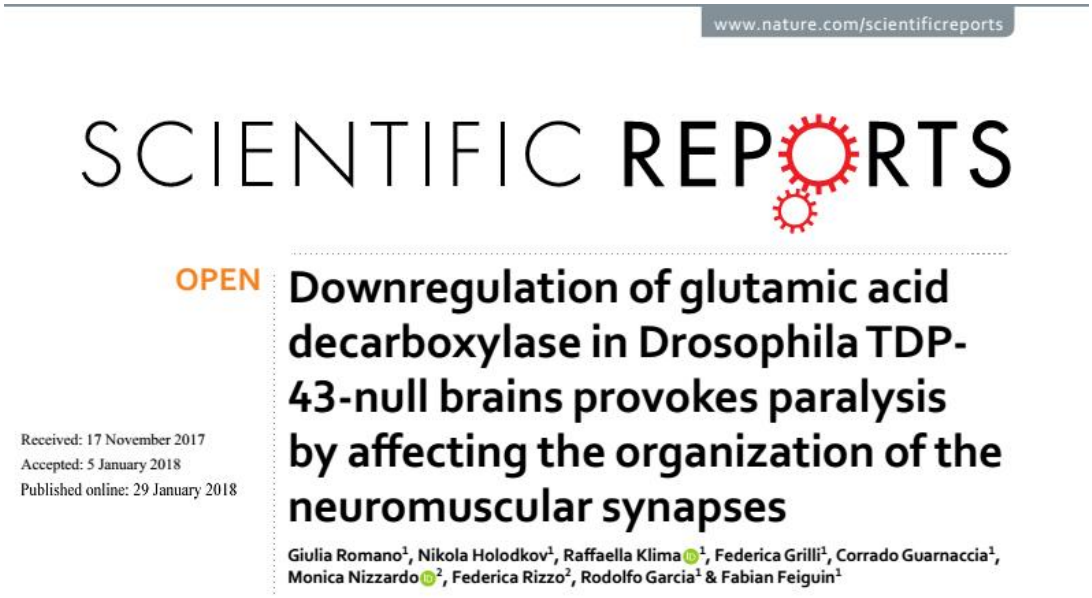
www.nature.com/scientificreports

SCIENTIFIC REPORTS

OPEN

Received: 17 November 2017
Accepted: 5 January 2018
Published online: 29 January 2018

Downregulation of glutamic acid decarboxylase in Drosophila TDP-43-null brains provokes paralysis by affecting the organization of the neuromuscular synapses

Giulia Romano[1], Nikola Holodkov[1], Raffaella Klima[1], Federica Grilli[1], Corrado Guarnaccia[1], Monica Nizzardo[2], Federica Rizzo[2], Rodolfo Garcia[1] & Fabian Feiguin[1]

INTRODUCTION

Initial remarks

"The diagnosis as well as the anatomy and physiology of the condition amyotrophic lateral sclerosis is one of the most completely understood conditions in the realm of clinical neurology". When Jean-Martin Charcot (1825-1893) said it in 1887, in his comments about "la sclérose amyotrophique", he could not have been more wrong[1].

Charcot, by many regarded the father of neurology, has enormously contributed to medicine and to medical literature. His lectures have been translated in many countries and are an essential tool of any neurologist's library[2]. A well-trained pathologist, with great eye to couple clinical observations (signs and symptoms) with anatomical evidence derived from autopsy[3], he correlated chronic progressive paralysis and contractures observed in patients, to lesions within the lateral column and the anterior horn of the spinal cord[2] (1865-1869). In 1874 he named "Sclérose Laterale Amyotrophique" for the first time[4]. Although he was not the first to discover ALS, as many predecessors of his had observed the disease in years previous to him, he was the first one in naming it and separating it from other neurological disorders[1]. Despite recent molecular and genetic discoveries have completely shaped our

understanding of ALS, many of his original clinical and pathological descriptions have remained virtually unaltered[1].

Granting Charcot with all the credentials, he failed to recognize ALS heterogenous nature and the overlapping with many other neuropathies[5]. Charcot observations were based on thorough clinical and pathological analysis, marvellous for the time, but insufficient to fully understand the complexity of the disease. Yet, he was not the only one to fall into this trap. Too many times in recent history, discoveries had led to the impression that ALS was a monogenic, homogeneous disorder. It is enough to mention the identification of the link between Superoxide Dismutase 1 (SOD1) and ALS, that inspired great excitement some 20 years ago, yet this enthusiasm now seems unjustified[1]. As Turner has correctly stated in [1], "The history of ALS is beset by misunderstandings and false beliefs. From its 19th century beginnings, the path ahead has too often been considered straightforward". Only today, thanks to advances in molecular biology and genetics, after the identification of dozens of genes correlated to ALS[6], that we are able to understand the real complexity of this disorder.

1) ALS overview

1.1) Clinical features of ALS

ALS is a progressive and fatal neurodegenerative disease of the human motor system[6]. It affects principally lower (LMN) and upper (UMN) motoneurons in the cerebral cortex, brain stem and spinal cord[7]. The impaired synaptic transmission caused by the loss of these neurons induces paralysis of voluntary and involuntary movements and subsequent muscular atrophy.

Although the signs and symptoms are of very variable nature, the clinical hallmark of ALS consists usually of a combination of LMN and UMN degeneration. Pure LMN (Progressive Muscular Atrophy – PMA) or UMN (Primary Lateral Sclerosis – PLS) are also possible, although rare. These, limb-onset manifestations, account for 70% of ALS epidemiology. In 25% of cases, bulbar-onset disease is observed, represented by speech and swallowing difficulties. Finally, 5% of patients suffer from respiratory problems at the onset[6].

UMN deterioration leads to spasticity, weakness, tendon reflexes and emotional lability. LMN loss, include fasciculation, wasting, and weakness. In most cases, the disorder begins in the arms and legs with symptoms that include foot drop, problems or inability to walk, loss of

complex hand movements or inability to lift heavier objects[8]. As the disease progresses, the patients become dependent on caregivers. In bulbar onset disease, symptoms include difficult or unclear articulation of speech due to muscle impairment (dysarthria), difficulty or discomfort in swallowing (dysphagia), hypersalivation (sialorrhea), malnutrition[8]. Tongue fasciculation is usually present. Axial decade causes head to drop and excessive outward curvature of the spine (kyphosis), pain and poor balance. Sphincter function is often spared, as are sensory functions and eye movement, the former preserved till the last stages[8].

Cognitive impairment was overlooked in the past. Today, however, it is believed that some 50% of ALS patients develop impaired neuropsychological functions[9]. It often reflects a progressive inability to understand or produce speech (dysphasia and aphasia) combined with a progressive loss of verbal and non-verbal semantic memory (semantic dementia)[10]. These cognitive modification affect "executive function, language, judgment, personality and behaviour" as explained in [10], and are associated with reduced survival.

Pain can be present and intense if sensory neurons are involved. Headaches occur quite often. Early respiratory problems give rise to

breath shortening, also at rest in advanced stages that can significantly reduce the quality of life.

The disease can induce depression and anxiety resulting in sleep deprivation and appetite loss[11]. Interestingly, some ALS patients take the situation philosophically, lowering the emotional burden in those occasions[12].

Clinical records report respiratory failure as the primary cause of death followed by pulmonary embolism and heart failure as secondary and rare[13] consequences. Studies suggest also that deaths are often related to hypertension and malnutrition[13]. A more recent study[14], performed on a cohort of 100 post-mortem ALS patients, summarized the principal causes of death and is shown in figure 1[14].

	Broncho-pneumonia	Aspiration pneumonia	Heart failures	Unknown	Pulmonary embolism	Hypoxic deaths	Digestive	Total
Site of onset								
Spinal (%)	36 (56.3)	10 (15.6)	5 (7.8)	3 (4.7)	6 (9.3)	2 (3.1)	2 (4,2)	64
Bulbar (%)	19 (52.8)	6 (16.7)	5 (13.9)	5 (13.9)	0 (0.0)	1 (2.8)	0 (0.0)	36
Total (%)	55 (55.0)	16 (16.0)	10 (10.0)	8 (8.0)	6 (6.0)	3 (3.0)	2 (2.0)	100

Fig. 1) ALS patients cause of death. The figure shows that aspiration and bronhco-pneumonia account for more than 70% of total deaths in ALS patients. It also suggest that spinal onset is predominant in ALS (figure taken from [14]).

1.2) Epidemiology of ALS

The incidence of ALS is 2-3 people per 100,000 individuals per year and more frequent in men than in women[15]. The overall lifetime risk of ALS is 1:400 in women and 1:350 in men. Higher prevalence is seen in some countries in comparison to others, indicating that geographical position plays a role[16].

Statistically, the onset of the disease is between 58 to 63 years of age for the sporadic forms and 47 to 52 for the familial ones[17]. Relentless thereafter, half of the patients die within 3 years from the first symptoms while another 20% within 5 to 10 years[17]. Early respiratory problems and bulbar involvement were associated with reduced survival[17].

1.3) Diagnosis and treatment of ALS

The more we know about ALS, the more we understand the need to formulate dynamic and evolving consensus guidelines for clinical diagnosis[18]. The first such guidelines were developed in 1994[19], by "The Consortium on Clinical Trials in ALS", that met in Airlee, Warrenton, Virginia. This group of people included clinical practitioners, Food and Drug Administration (FDA) officials, pharmaceutical companies'

representatives and patients' lawyers that met with the aim of creating a document that could provide a common groundwork for ALS diagnosis, useful to conduct clinical trials on an inclusion/exclusion base, easy accessible for health care systems at a global level. The result of this meeting was the "El Escorial Criteria"[20]. Revised many times since then, the document is intended "to improve the efficiency and consistency of trial analysis and design" and "facilitate the admission into clinical trial" sooner during the course of the disease. It also deals with ethics, patient's interests, statistical analysis approach, survival measures and more[19]. The El Escorial Criteria for diagnosis can be found on the World Federation of Neurology Research Group for Motoneuron Disease website (http://www.wfnals.org). The most updated version of the document[21] states that "ALS diagnosis is based on the exclusion of alternative causes of signs and symptoms outlined in the original diagnostic criteria" and "requires clinical progression". It needs, furthermore, the presence of at least one of the following manifestations:

- progressive UMN or LMN in at least one limb or region of the body;
- LMN deficiency evidenced by clinical examination in one body region and/or Electromyography (EMG) (in the form of neurogenic

potentials, fibrillation potentials, positive sharp waves and fasciculation potentials) in at least two body regions.

Based on the extensive data gathered in clinical trials, potential ALS patients are categorized in suspected, possible, laboratory-supported probable, probable and definite[21]. Thanks to a very limited number of false positive diagnosis in support of the El Escorial Criteria, admission for clinical trial is currently granted to all patients ranging from possible to definite[21]. As Agosta has stated in [22], "It is difficult to conceive of a less stringent criterion that would still ensure that patients are appropriately diagnosed". Consistently, a broader LMN involvement to more than one body region can be sufficient to meet the criteria for ALS diagnosis, even in the absence of UMN signs and symptoms[21], ensuring faster clinical enrolment for patients with restricted phenotype. Interestingly, even if not conceived as a staging system, the El Escorial serves very nicely in establishing the disease prognosis based on the initial diagnosis. In this sense, patients diagnosed with definitive ALS have reduced survival rates in comparison to patients diagnosed with possible ALS[23]. It is believed that ultimately, after many revisions, it seems that the El Escorial meets the present needs for a successful ALS diagnosis[22]. It must be said, however, that there are many issues still to

be addressed, overlooked by these criteria, such as the heterogeneity of ALS phenotypes and the genetic component involved[22], but in the absence of clear biomarkers for disease diagnosis and progression, The El Escorial Criteria represent a valid tool for ALS identification.

Currently, ALS is managed by treatment of symptoms and pain relief[24]. This is because it is effective, in the sense that it is correlated with longer life expectancy, especially for patients with moderate disease penetration that attend specialized and multidisciplinary ALS clinics[24]. In such institutions, patients receive "comprehensive care from a physician, physical therapist, occupational therapist, speech pathologist, dietitian, social worker, respiratory therapist, and nurse case manager", as Miller suggests in [24]. Symptomatic and palliative care, such as percutaneous endoscopic gastrostomy and non-invasive ventilation[25], are usually combined with Riluzole, an inhibitor of Glutamate release, the only FDA approved drug for ALS treatment, that prolongs survival from 3 to 6 months[26]. Many drugs are currently being tested, some of them are summarized in [27]. Still, despite intensive academic and industry efforts, it has been more than 20 years since Riluzole was first approved, and currently it is the only available drug for treatment. Reason for this lack

of success is partly the obscurity of the mechanisms that are behind ALS pathogenicity.

1.4) Genetic and environmental factors contributing to ALS

Let's talk about the genetics first: it is important to understand that in the past and present, scientists have encountered difficulties in correlating the disease with a specific set of genes. Familial ALS (fALS), where familial stands for a condition that is hereditary, accounts only for 10% of epidemiology[28]; so far, the scientific community has identified a dozen of loci that might be responsible for disease onset[6]. Most of the research in ALS is based on the characterization of these genes. However, often the same mutations can induce completely different clinical phenotypes, making the understanding of the disease even more complicated[29]. In the remaining 90% of ALS patients, no obvious genetic correlation has been found, thus referred to as sporadic ALS (sALS).

As it was mentioned at the very beginning, the identification of SOD1 mutations in fALS back in 1993[30] had inspired great excitement. It is considered that some 20% of fALS is correlated to SOD1 mutations (some 150 mutations identified to be pathogenic so far). The mutant form of

the protein escapes regulatory processes, aggregates and forms intracellular inclusions which interfere with cellular metabolism[31]. It furthermore lacks its natural ability to remove free radicals, which accumulate in the cell. Some 15 years later, SOD1 was shown to aggregate in ALS patients even in the absence of mutations[32]. Is SOD1 a cause or a consequence of ALS?[33] Similarly to SOD1, other mutant proteins have been discovered: UBQLN2, OPTN, SQSTM1, VCP and many others, suggesting that ALS is a proteinopathy[31]. Most certainly, however, one of the most important breakthroughs in the field of ALS was achieved with the identification of Transactive Response DNA Binding Protein of 43 kDa (TDP-43) protein pathology. Mutations inside TDP-43 gene (TARDBP) account for 5% of fALS. Independently of whether TARDBP gene is mutated or not, the vast majority (up to 90%) of ALS patients suffer from the neuronal aggregation of TDP-43 inside ubiquitin positive cytosolic inclusion. TDP-43, reviewed in depth later in this thesis, is a heterogeneous ribonucleoprotein located normally in the nucleus where it harbours many important cellular functions, primarily as RNA splicing factor. During stress, TDP-43 naturally shifts from the nucleus to the cytoplasm where it aggregates in stress granules through its prion like domain[34]. In ALS, however, it seems that TDP-43 is unable to leave

these structures and relocate to the nucleus. It is still a matter of debate whether it is the lack of TDP-43 function from the nucleus or the formation of TDP-43 cytosolic aggregates that causes the severe neurodegeneration described in ALS[35]. Besides TDP-43, there are others RNA binding proteins, such as FUS, TAF15, EWSR1, believed to contribute to ALS[6].

In parallel to this notion, in 2011[36] a study claimed that approximately 40% of fALS patients have an expansion of GGGGCC hexanucleotides (G_4C_2) repeats between two exons in the 5' non-coding region of C9ORF72, a gene of unknown function[36]. It is estimated that the affected individuals present hundreds or even thousands of (G_4C_2) repeats. In this direction, *in situ* hybridization studies have shown that there is an accumulation of RNA particles in the frontal cortex and spinal cord of ALS patients affected by C9ORF72 hexanucleotide repeats. It is believed that the RNA transcribed from this abnormally repeated gene are able to form RNA foci acquiring a toxic function by sequestrating healthy RNAs and or associated ribonucleoproteins[36].

Apart from the genetic origin of the disease, some studies suggested that ALS might begin consequently to the exposure to toxins of various nature present in the environment[37]. Agricultural substances and nutrition,

electro-magnetic fields, heavy metals, industrial dust or harmful vapours had been correlated with the onset of the disease. Smoking, for example, is believed to increase the probability of developing ALS, especially for those who start young[37]. Similarly, many patients have declared of having been exposed to agricultural harmful substances. Some of these are pesticides, fertilizers, herbicides, insecticides, and formaldehyde, the last believed to increase by two folds the risk of ALS[37]. In another study, low frequency radiation was proven to increase free radicals accumulation through oxidative stress[38] and was correlated with ALS. On the completely opposite direction, studies have shown that ALS is associated with increased physical activity[39], since many ALS diagnosed patient happened to be former athletes. Incongruent results were obtained in this matter, so this correlation has yet to be determined. Another study states that consumption of food rich in Glutamate can have a role in the development of the disease suggesting that increased Glutamate activity may lead to neuronal death[40]. It was also reported that the intake of Omega 3, Vitamin E and high-fiber food may have a protective effect[41].

However, since most of the evidences described above came from questionnaires that are subject to bias[42], until proper biomarkers were

available, it is difficult to assess the role played by environmental factors in ALS.

1.5) Molecular mechanism in ALS

One of the most obvious molecular mechanism disorders in ALS is related to Glutamate excitotoxicity: high levels of Glutamate - the most important excitatory neurotransmitter in the human brain - were detected in patients with ALS[43]. A reason for this could reside in the apparent downregulation of the Glutamate transporter EAAT[43], that normally removes the excess of Glutamate from the synaptic cleft. The excesses of Glutamate activates its own receptors (Glutamate Receptors), producing over-firing and neuronal degeneration, a phenomenon referred to as excitotoxicity[44].

Mitochondria are also subject of intense research in ALS[45]. These organelles have essential functions in cell respiration, energy production, calcium metabolism and apoptosis. It seems that in ALS the mitochondria are severely affected both biochemically and morphologically[46]. These modification are found in different tissues of ALS patients such as skeletal muscles, liver and/or motoneurons[47]. Interestingly, SOD1 mutant

proteins were found in aggregates at the outer membrane of the mitochondria in ALS patients[48]. The accumulation of misfolded SOD1 interferes with the processes responsible for ATP and energy production and impairs mitochondrial calcium buffering capabilities, triggers apoptosis and disrupt the axonal transport of this organelle[49]. Mitochondrial deficits affect also the transport of cellular proteins, lipids and RNA molecules[50] leading to further accumulation of these macromolecules in the degenerating motoneurons[50]. Additionally, biopsies performed in post-mortem ALS tissues have revealed the activation of oxidative stress in response to the formation of free radicals[51]. Similar evidences were obtained from patients cerebrospinal fluids, serum and urine[51]. Elucidating the molecular mechanisms underlying the pathological modifications described before is critical to uncover the molecular targets of the disease and will also help to develop efficient drugs aimed to prevent and treat ALS[51].

2) Transactive response DNA binding protein 43 kDa (TDP-43)

2.1) TDP-43, metabolic overview

During degeneration, neuronal cells suffer the aggregation of cytosolic proteins and ALS is not an exception. In 2006, Neumann and colleagues[34] discovered that TDP-43 was the most abundant protein present in the cytosolic aggregates formed in the brains of ALS patients (Fig. 2). Moreover, Neumann showed that TDP-43 appeared abnormally modified harbouring several posttranslational modifications such as ubiquitination, hyper-phosphorylation and cleavage of its C-terminal (Fig. 2). TDP-43 is a 43 kDa protein discovered in 1995 by Ou and colleagues[52]. It was initially linked to HIV infection because of its capacity to bind the TAR DNA sequences of this virus (from which TDP-43 derives the name).

TDP-43 is encoded by TARDBP gene. It localizes predominantly in the cell nucleus and is ubiquitously expressed in almost all the tissues. The molecular structure of this 414 amino acids long RNA binding protein comprises two RNA recognition motifs (RRM1 and RRM2) in the N-terminal part and a Glycine rich domain in the C-terminal[34]. Also, a nuclear localization sequence (NLS) and a nuclear export signal (NES) are both found in the N-terminal (Fig. 3).

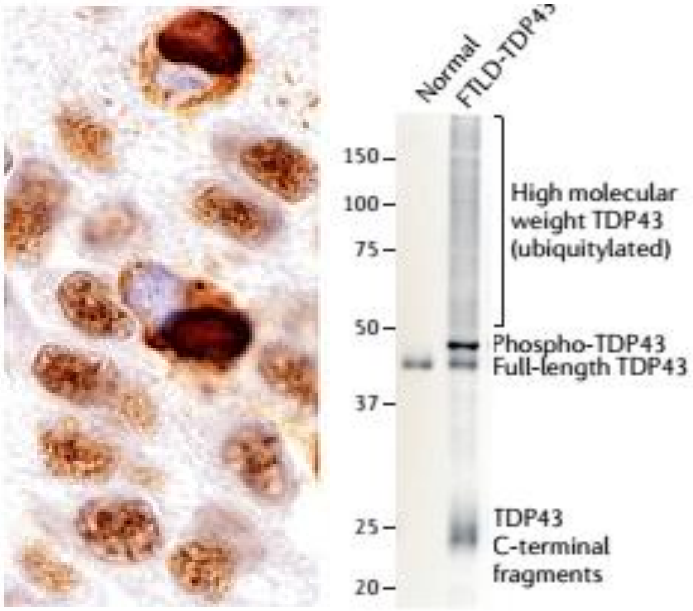

Fig. 2) TDP-43 is misregulated in motoneurons of ALS patients. On the left: Immunohistochemistry of brains derived from FTLD patients shows that TDP-43 is devoided from the nuclei and aggregated in cytosolic inclusion of affected neurons. On the right: biochemical analysis of FTLD brains reveals that TDP-43 is ubiquitinated, hyper-phosphorylated and truncated in C-terminal fragments (figure taken from [36]).

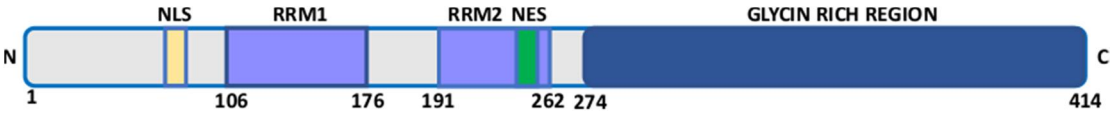

Fig. 3) Schematic representation of TDP-43 protein structure. The N-terminal of TDP-43 harbours the two RRM and the NLS/NES sequences. The C-Terminal is rich in Glycine and serves for protein-protein interactions. The total length of the protein is 414 amino acids.

2.2) TDP-43 gene and its expression

TARDBP gene is well conserved across species[53] presenting a high degree of similarity between human, mice, *Drosophila melanogaster* and *Caenorhabditis elegans*[53]. In humans, TDP-43 is located on the first chromosome at position 1p36.21 and the genomic sequence is constituted by six exons and five introns[53] that generate, at least, 10 different TDP-43 isoforms after alternative splicing[53]. Interestingly, the close examination of the databases revealed that in the mice and human genome there are multiple sequences with high homology to TARDBP, some with as much as 90% similarity. These sequences derive, most probably, from retrotransposition events that involved TDP-43 mRNA[53]. Regarding TDP-43 protein expression patterns, it is ubiquitously expressed[52] in many different tissues including brain, heart, spleen, ovary, placenta, pancreas, testis, lung and kidney[54].

2.3) TDP-43 protein structure and interactome

The first time TDP-43 was attributed the role of RNA binding protein was in 2001, when Buratti et al[54] described TDP-43 regulation of the splicing of the human cystic fibrosis transmembrane conductor regulator (CFTR)

pre-mRNA. More specifically, Buratti showed that TDP-43 RRM1 domain bounded with high affinity the TG di-nucleotidic stretches ((TG)m(T)n) present on the exon 8 – exon 9 boundary of the CTFR pre-mRNA, allowing for exon 9 skipping. Here, the phenylalanine 147 and 149 were fundamentally important for TDP-43 - CTFR interaction. In contrast, the RRM2 domain did not show to be similarly important, suggesting that the RRM1 domain is sufficient to binding RNA. A multitude of RNA molecules were later shown to be regulated by TDP-43. In contrast, the Glycine rich C-terminal serves as the docking domain for protein-protein interactions. Studies demonstrated that TDP-43 was able to interact with many other proteins, primarily heterogeneous ribonucleoproteins (hnRNP), such as hnRNP A2/B1, hnRNP A1, hnRNP C1/C2 and hnRNP A3.

According to Krecic et al[55], the presence of the two RNA binding domains (RBDs) at the N-terminal part and the Glycine rich region in the C-terminal portion, classifies TDP-43 as an RNA binding protein (RBP) that belongs to the group of hnRNPs.

2.4) TDP-43 function and localization

The best characterized role of TDP-43 is certainly related to RNA splicing through UG repeats binding[56]. However, the regulation of intronic 3'-untranslated regions (3'-UTR) and non-coding regions of long transcripts were also described[62]. High throughput sequencing of CLIP RNA derivatives showed that TDP-43 was able to bind more than 6000 RNA sequences[57], suggesting the functional importance of this protein. This last study also revealed that the great majority of these transcripts were related to synaptic activity or neuronal development including human CFTR[54], apolipoprotein 2[58], serine/arginine-rich splicing factor 2[59]. TDP-43 also affects the RNA turnover of cyclin-dependent kinase 6[59], histone deacetylase 6[60], Futsch (the Drosophila homologue of microtubule-associated protein 1B (MAP1B))[61] and low molecular weight neurofilament protein[62].

In normal conditions, TDP-43 localizes in the euchromatin zones of the nucleus, primarily in the perichromatin fibrils and nuclear speckles where transcription and splicing occur. The intracellular localization of TDP-43 is mediated by the NLS, localized before the two RRM domains and the NES, present inside the RRM2 domain, just before the Glycine rich region. However, it is possible to detect the presence of TDP-43 within

the cytoplasm in both normal and stressed cells[63]. The cytoplasmic localization of TDP-43 relates to the transport of RNA granules and to the synthesis of factors involved in neuronal plasticity[64]. Under stress conditions, TDP-43 redistributes from the nucleus to the cytoplasm where it forms part of the stress granules. These structures are able to sequester redundant mRNAs and promote neuronal survival[65]. It is also believed that TDP-43 is involved in the biogenesis and maturation of microRNA (miRNA) through the direct interaction with Drosha complex[66]. Moreover, TDP-43 may also behave as a negative transcription factor as described in the regulation of HIV DNA[52]. Finally, as described for different RNA binding proteins, TDP-43 is capable to regulate its own mRNA expression levels by interacting with specific sequences present at the 3'-UTR region of TDP-43 mRNA[67].

In conclusion, TDP-43 performs many cellular functions, primarily related to RNA biology (Fig. 4) and, therefore, it is not surprising that defects in TDP-43 metabolism lead to disease states.

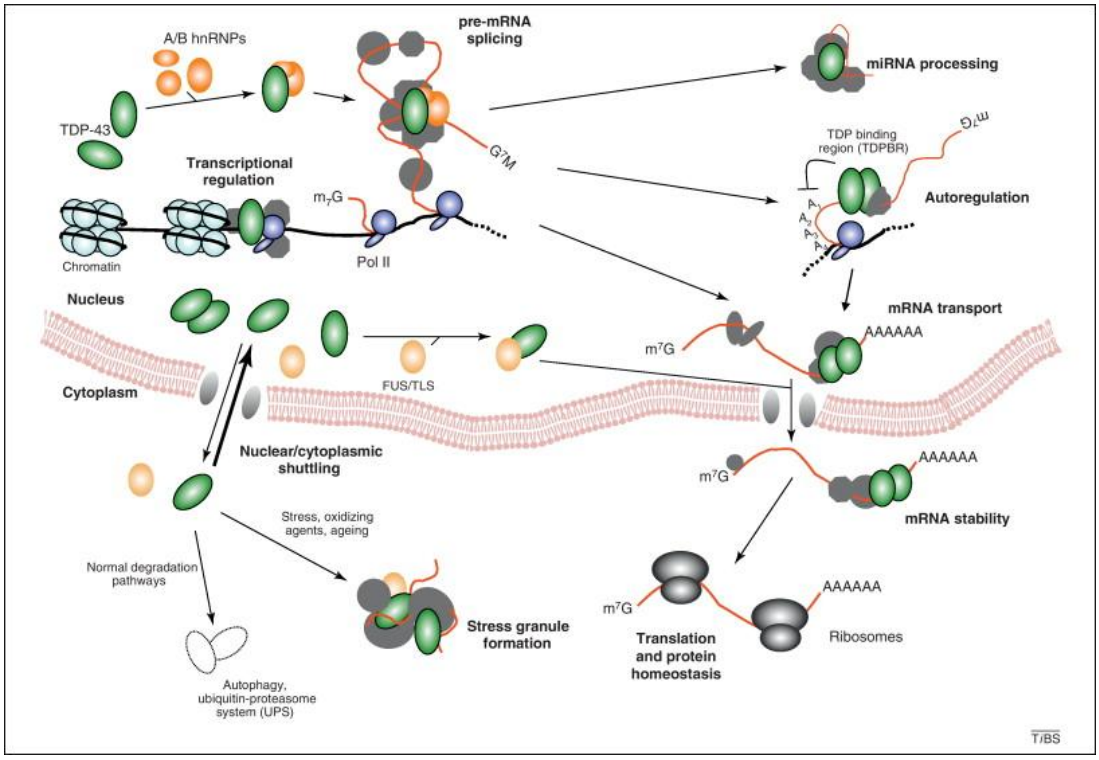

Fig. 4) TDP-43 has many important cellular functions. In the nucleus TDP-43 acts primarily in pre-mRNA splicing, miRNA processing and transcriptional regulation. Many of this functions are achieved through interactions with hnRNPs. In addition, TDP-43 is involved in mRNA transport from the nucleus to the cytoplasm, mRNA stability and stress granule formation. TDP-43 is also able to auto-regulate its own expression by regulating TDP-43 mRNA (figure taken from [68]).

2.5) Role of TDP-43 in neurodegeneration

The existence of ubiquitin positive cytosolic inclusions in post-mortem brains of individuals with ALS and FTLD was first described by by Leigh et al[69] and Okamoto et al[70] in 1991 and 1992 respectively. However, it was Neumann et al[34] in 2006 who identified that TDP-43 was the major

protein present inside these abnormally formed intracellular inclusions[34]. Immunostaining analysis performed utilizing specific antibodies raised against TDP-43 (Fig. 5) indicated that this protein was absent from the nuclei of degenerated neurons and relocated inside the characteristic ubiquitin positive inclusions suggesting that TDP-43 "may redistribute from nucleus to the cytoplasm in affected neurons". Additional observations demonstrated that TDP-43 appeared hyper-phosphorylated and ubiquitinted in affected brains. In addition, the protein seemed abnormally cleaved at its C-terminal part generating multiple degradation products. Similar modifications were observed in samples obtained from patients with sporadic forms of ALS.

After Neumann's study, the number of publications regarding TDP-43 raised dramatically (2086 hits on TDP-43 from 2006 to 2017 in comparison to 12 hits from 1995 to 2006) suggesting the rise in interest of this protein related to neurodegeneration. In agreement with this view, independent research conducted by Arai et al[71] identified TDP-43 as the main component of the ubiquitin positive inclusions present in neurons and glia sited in the temporal, frontal and parietal cortex of patients suffering of FTLD and ALS. Other anatomical areas like the hippocampus, the brain stem and the cerebellum were similarly

modified. Similar modifications in TDP-43 - ubiquitin positive and tau negative cellular aggregates - were also described in the cytoplasm and inside the neurites of the temporal cortex, hippocampus and caudate nuclei. Spinal cord motoneurons of FTLD patients with MND and ALS presented analogous modification in TDP-43.

Regarding the morphology of TDP-43 inclusions, the authors stated: "TDP-43 stained curved or bullet-shaped inclusions in the cytoplasm of glial cells in the grey matter, and anterior and lateral funiculi of lumbar spinal corda in all the ALS and FTLD-MND cases". An interesting observation is that Arai et al., study was sent to the journal revision 4 days before Neumann et al., paper was published on the 6th of October 2006, indicating that the two groups were conducting in parallel almost identical studies. Therefore, in my view, it is important to recognize Arai's work as equally pioneering as Neumann's, even if the latter is usually regarded as the discoverer of TDP-43 pathology in FTLD and ALS. Moreover, Arai's work seems to be more complete in certain segments, such as the characterization of TDP-43 localization in different regions of the brain and spinal cord.

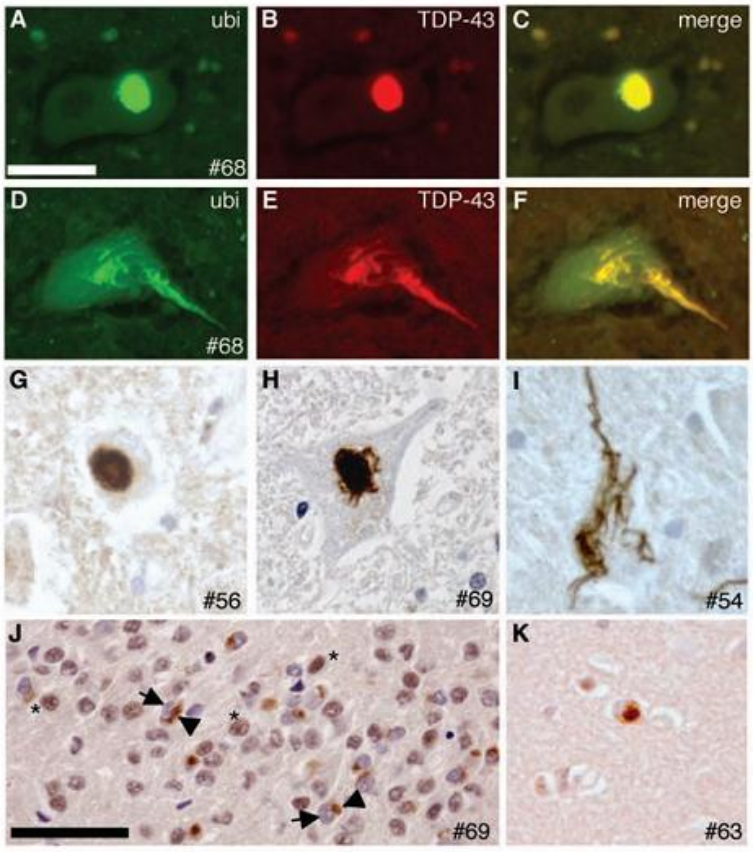

Fig. 5) TDP-43 immunoreactivity in FTLD post-mortem brains. Above: immunofluorescence studies show that TDP-43 co-localized with ubiquitin positive cytosolic inclusions in neurons derived from FTLD patients. The aggregates can either have a round or skein-like shape. Below: immunohistochemistry studies taken from ALS patients brain regions (hippocampus, frontal and temporal cortex) and at different magnifications confirm that TDP-43 pathology is widespread in FTLD brains (figure taken from [34]).

In 2007 Neumann et al[72], characterized the pathological aggregation of TDP-43 in the white matter of FTLD patients. The biochemical signature was the same as in the grey matter of FTLD and ALS patients, thus hyper-phosphorylated, ubiquitinated and cleaved in many degradation products. In addition, it was discovered that the cytoplasm of glial cells,

most probably oligodendrocytes, was also susceptible to TDP-43 aggregation. Here the abundance and the shape of the inclusions varied significantly, being rounded, comma-shaped and in certain cases extended inside cytoplasmic processes. TDP-43 aggregates in the glia (astrocytes and microglia) were not ubiquitinated and perhaps more importantly, the glial inclusions of TDP-43 in the medulla and spinal cord were found in concomitance with neuronal inclusions in the same regions.

Ahead of the demonstrations regarding the role of TDP-43 in FTLD and ALS, Mackenzie et al[73], suggested that this was not always the case. On a large cohort of post-mortem ALS brains, which included fALS with and without SOD1 mutations, sALS and ALS with dementia, the group found that TDP-43 inclusions were negative in patients carrying SOD1 mutations. Thus, in these individuals TDP-43 retained its normal nuclear localization without suffering pathological modifications. These observations were confirmed in the transgenic mouse G85R SOD1, considered to be one of the best experimental models to study ALS since 1993, indicating that the disease may arise from TDP-43 independent molecular pathways. In agreement with this idea, Amador-Ortiz et al[74], discovered TDP-43 ubiquitin positive cytosolic inclusions in patients

suffering of Hippocampal Sclerosis (HpSCL) and Alzheimer disease (AD). These studies showed that 78% and 20% of the HpSCL and AD patients respectively presented abnormal modification of TDP-43 with protein inclusions localized in the dentate fascia of the hippocampus and inside the entorhinal cortex. In some cases, the occipitotemporal lobe and the inferior temporal gyri were affected. In AD cases, the inclusions were found around the amygdala. Interestingly, this group analysed the shape of the TDP-43 positive inclusions by electron microscopy and observed that TDP-43 in FTLD and AD had mainly a granular and filamentous pattern in the cytoplasm and neuritic processes. In support to this, Higashi et al[75] observed TDP-43 positive inclusions in the amygdala, hippocampus, and dentate gyrus of patients with AD (33%). The glial and the upper layers of the cerebral cortices in these patients were also immunoreactive for TDP-43 inclusions. In addition, this group described TDP-43 inclusions in the cases of dementia with Lewy Bodies (DLB) (45% of the cases) distributed in the amygdala, hippocampus, dentate gyrus, entorhinal, occipitotemporal and inferior temporal cortices.

In summary, defects in TDP-43 metabolism has become an important research focus in neurodegeneration from 2006 onwards and TDP-43 cytosolic inclusions were documented in the brain of several neural

disorders such as ALS, FTLD, DLB and AD. Because of its recurrence, TDP-43 cytosolic inclusions seem to represent a valid marker for disease diagnosis and possibly treatment. However, we still do not know why in some ALS cases TDP-43 does not exhibit this pathological state, indicating the involvement of different molecular pathways. This is obvious in the case of SOD1-ALS mice model. Moreover, the presence of TDP-43 pathology in apparently different neuronal diseases suggests that TDP-43 may not be specific for ALS and FTLD and/or rather represents the consequence of a previously established neurodegenerative processes.

At this point, it comes naturally to redirect to Charcot's statement at the beginning of this thesis: "The diagnosis as well as the anatomy and physiology of the condition amyotrophic lateral sclerosis is one of the most completely understood conditions in the realm of clinical neurology".

Today, the best we can say is that until the molecular mechanisms of ALS are not fully elucidated, every assumption should be given very carefully.

3) Glutamate-GABA metabolism

3.1) Glutamic acid metabolism

The Glutamic acid is a ubiquitous non-essential amino acid. Glutamate, the anion of the Glutamic acid (Fig. 6), is the most abundant neurotransmitter present in the vertebrate nervous system (CNS)[76]. Since it was discovered[77], this little molecule has been related to very important cellular functions and disorders[78].

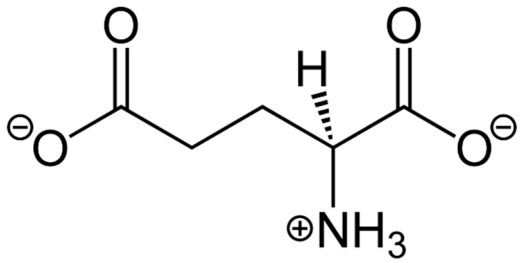

Fig 6) Chemical representation of Glutamate (figure taken from [79]).

The first to sustain the synaptic function of Glutamate was Hayashi et al., who in 1954 injected Glutamate in the brain of mice and observed that provoked strong convulsions in the animal. Today, it is known that Glutamate mediates fast excitatory responses in both the CNS and Peripheral Nervous System (PNS) and regulates diverse neurological processes such as learning, memory, long term potentiation and synaptic plasticity[76]. Glutamate resides inside presynaptic vesicles and released in a Ca^{2+} dependent manner. This process comprises N and P/Q voltage-

dependent Ca^{2+} channels[80] localized in close proximity to the Glutamate filled vesicles[80]. Once Glutamate is released, it triggers the excitatory action postsynaptic potential (EPSP) by binding to the superfamily of specific Glutamate receptors (GluRs).

Glutamate is part of the complex Glutamine-Glutamate-Gama Amino Butyric (GABA) Cycle (Fig 7)[81]. The synthesis of Glutamate starts in the astrocytes: glucose is taken up and converted in pyruvic acid by pyruvate carboxylase (PC). Pyruvate enters into the tricarboxylic cycle (TCA) and is converted to oxaloacetate (OAA) that condenses with Acetyl CoA to give rise to α-ketoglutarate. This last molecule can then be converted to Glutamate (and viceversa) by Glutamate Dehydrogenase (GDH)[81]. In the astrocytes, Glutamine Synthase (GS) converts Glutamate to Glutamine, that can now be transported to glutamatergic neurons by glutamine transporters and reconverted to Glutamate by Glutaminases[82]. Once Glutamate is released, the excess of this neurotransmitter is retaken by specific Glutamate transporters (reviewed later) and converted in glutamine by GS. Importantly, glutamine can also be transported in GABAergic cells to become transformed by GDH in Glutamate and posteriorly converted in GABA by the enzyme Glutamic Acid Decarboxylase 65 and 67 (GAD65/67)[83,81].

Regarding to the Glutamate receptors, the neurotransmitter can bind either ionotropic (iGluR) or metabotropic GluRs (mGluR). iGluRs are predominantly post-synaptic ligand gated ion channels[84]. Structurally, these channels are formed by four subunits (iGluRI, iGluRII, iGluRIII and iGluRIV) and share the same organization: an extracellular amino terminal domain (ATD), a ligand binding domain (LBD), a transmembrane (TMD) and an intracellular carboxy terminal domain (CTD). A conformational change of the TMD occurs when Glutamate binds to the LBD allowing the influx of cations, more specifically sodium, potassium and calcium inside the cell[84]. Depending on their sensitivity to Glutamate co-factor agonists, the iGluRs are classified in three different categories: thea-amino-3-hydroxy-5-methyl-4-isoxazole propionate (AMPA), Kaintate and N-methyl-D-aspartate (NMDA) iGluRs.

AMPA ($iGluR_1$ and $iGluR_4$) and Kainate ($iGluR_5$, $iGluR_7$, KA_1 and KA_2) receptors are also referred to as non-NMDA[84]. They exert fast excitatory transmission by the influx of Na^+ ions. NMDA (NR_1, NR_{2A-D}, NR_3) receptors (NMDAR) give rise to a slow electrical transmission carried out by Ca^{2+} entry[84]. It is also common that NMDARs need glycine in combination with NMDA and Glutamate for their activation. In addition to the binding of the ligands, NMDARs require a partial membrane depolarization to

overcome the voltage sensitive block that is created by Mg^{2+} ions, normally present in the inner part of the channel[84].

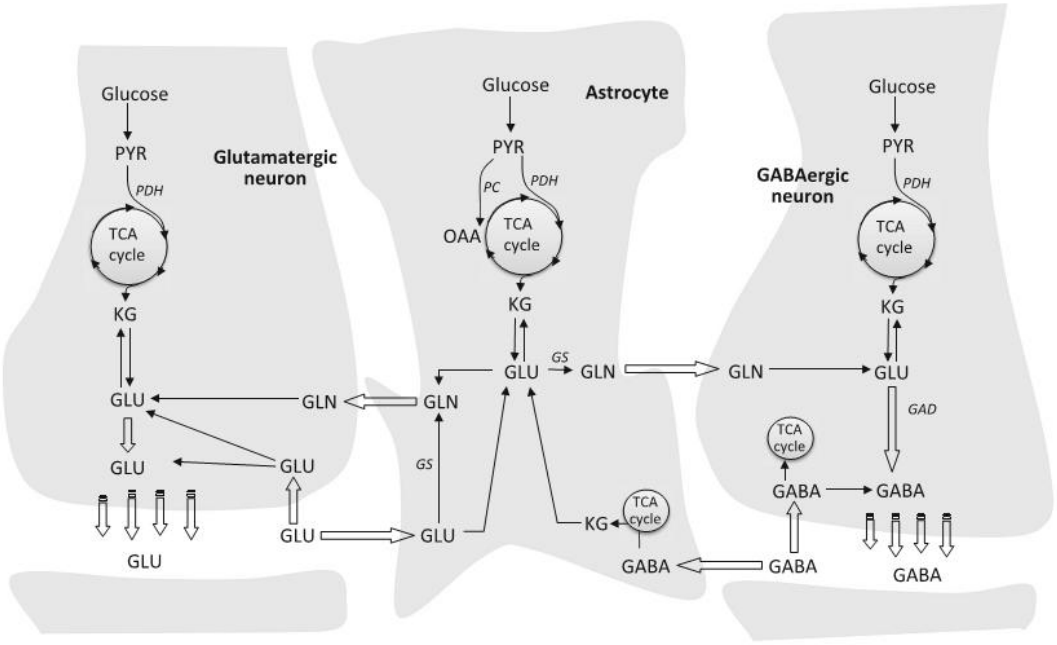

Fig. 7) Glutamine-Glutamate-GABA cycle (taken from [81]). Detailed explanation in the text.

iGluRs are believed to have many more functions than just electrical transmission, such as pre-synaptic modulation and signal transduction, usually mediated by the interaction of their carboxy terminal with a wide variety of intracellular proteins[84].

In contrast, the mGluRs are G protein-linked metabotropic receptors constituted by an extracellular amino-terminal (ATD) where the ligand binds, a cysteine rich domain (CRD) crucial for protein dimerization as well as activation and a seven alpha helix transmembrane domain (TMD) followed by the intracellular carboxy-terminal (CTD)[85]. Apart for the

TMD, which is common to all the G protein coupled receptors (GPCR), the mGluRs share little homology with the other GPCR known. In addition, the mGluR family is formed by 12 members, some isoforms derived from differential splicing[85], subdivided as follows in three categories based on the agonists molecule required for their activation: group I mGluRs ($mGluR_1$ and m $GluR_5$) are coupled with Gq proteins and activate Phopholipase C/Inositol 1,4,5-triphosphate/diacylglycerol (PLC/IP3/DAG) pathway. Groups II ($mGluR_2$ and $mGluR_3$) and III ($mGluR_4$, $mGluR_6$, $mGluR_7$ and $mGluR_8$) are coupled with Gi proteins and act on lowering cAMP levels[86]. Some mGluRs have long proline rich domains, named Homer1, that mediates their interactions with NMDARs and many other proteins[87]. Besides the CNS and PNS, the mGluRs were also found in various other tissues where they regulate subcellular homeostasis[88]. The mGluRs belonging to the group II and III are usually presynaptic and predominantly localized in the nervous system where they modulate the opening of ion channels. Group I mGluRs instead are predominantly localized in post-synaptic structures and found in the majority of tissues[85]. Figure 8 summarizes the GluRs classification.

Glutamate Receptors (GluRs)					
Ionotropic (iGluRs)			Metabotropic (mGluRs)		
NMDA	AMPA	Kainate	Group I	Group II	Group III
NR1 NR2 - A, B, C, D NR3 - A, B	GluR1 GluR2 GluR3 GluR4	KA1 KA2 GluR5 GluR6 GluR7	mGluR1 mGluR5	mGluR2 mGluR3	mGluR4 mGluR6 mGluR7 mGluR8
Fast Excitatory			Slow Excitatory	Slow Inhibitory	

Fig. 8) The GluRs classification. Detailed explanation in the text.

Once Glutamate has bounded to the GluR and exerted its functions, it must be taken away from the synaptic cleft to allow the recovery of the system. Glutamate cleaning is mediated by a series of proteins, called excitatory amino acid transporters (EAAT), that are expressed in postsynaptic cells and supporting tissues such as the glia. So far, five different EAATs have been encountered in mammals: glial Glutamate and Aspartate transporter (GLAST or EAAT1) and glial Glutamate transporter (GLT-1 or EAAT2)[89], both found in the glial tissue and three more in the nervous system, the excitatory amino acid transporter 3-5 (EAAT3, EAAT4 and EAAT5)[92]. All of the transporters are Na+, H+ and probably Cl- co-transport and K+ counter-transport dependent[89].

Prolonged stimulation by Glutamate-GluR interaction is called excitotoxicity and is at the origin of many neurodegenerative diseases. Since a long time, Glutamate metabolism has been linked to ALS, AD, Parkinson, Huntington's disease and many others[90]. In ALS, several

studies have addressed the role of AMPA receptors[91]. A recent study[92], demonstrated a failure in ADAR2 mediated mRNA editing of the GluR2 at the Glutamine/Arginine (Q/R) position in motoneurons of ALS patients. The lack of conversion from Adenosine to Inosine (A to I editing) makes the AMPA channel highly permeable to Ca^{2+}, which in turn causes excitotoxicity and neuronal death[92]. The role of NMDAR and Kainate receptors, have been somehow neglected. Nonetheless, a study has shown NMDA/Ca^{2+}-mediated excitotoxicity in the heavy neurofilament aggregated ALS mouse model[93]. Importantly treatment of excitotoxicity by GluRs antagonists has resulted in neuroprotection[94], indeed the only FDA approved drug Riluzole, is a sodium channel antagonist and inhibitor of Glutamate release. AMPA antagonist GYKI 52466 was beneficial in SOD deficient cultured mouse neurons[94]. NMDARs mediated Ca^{2+} influx was blocked by NMDARs inhibitors MK-801 (dizolcipine), Memantine, Cerestat, Dextromethorphan and its metabolite Dextrorphan, all of which provided benefits after locally induced ischaemia[94].

Similarly, mGluRs overstimulation leads to neuronal disorders. When the group I of mGluR agonists are injected locally in the brain this results in epileptic manifestations[95] and leads to cell death in combination with cerebral ischemia. On the other hand, mGluR group I antagonist

treatments are neuroprotective. In contrast, the treatment with mGluR group II agonists is neuroprotective after focally induced brain lesions[96]. Activation of these receptors at the level of astrocytes induce neurotrophic factors release which prevents NMDA excitotoxicity induced apoptosis[97].

Finally, EAATs impairment leads to excitotoxicity. Rothstein et al.[98], have shown that loss of motoneurons was correlated with a reduction in the expression of GLT-1. In support of this idea, Glutamate transporter inhibitors caused degeneration of motoneurons[98].

3.2) GABA and related pathways

GABA is the most important inhibitory neurotransmitter in the brain of mammals[99]. In humans, GABA (Fig. 9) is synthetized from Glutamate by GAD65 and GAD67 and shuttled in synaptic vesicles by Vesicular GABA transporter (vGAT). It can also remain cytosolic[99] or leak from vesicles, ensuring a dynamic equilibrium of GABA cellular pools. When appropriate, GABA is released by Ca^{2+} dependent exocytosis[100] in the synaptic cleft where it binds ionotropic ($GABAR_A$ and $GABAR_C$) and metabotropic ($GABAR_B$) receptors causing the hyperpolarization and/or the activation of different cellular cascades. Depending on the type and

function of the GABAergic neurons releasing GABA, this neurotransmitter can act on a restricted number of neurons or in entire neuronal circuitries [99].

Inhibition is crucial in maintaining neuronal network homeostasis and inhibitory cells are part of almost every neuronal circuitry. The primary role of GABA and GABAergic cells is to control that excitatory neurons within a neuronal network were not stimulated very often[99]. It should also be noted that GABAergic neurons are not merely limited to excitotoxicity prevention but have a wide range of important cellular functions related to the fine tuning of the brain electrical activity[99] such as locomotor activity, reproduction, learning and circadian rhythms[99].

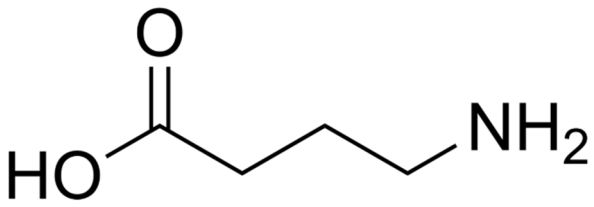

Fig. 9) GABA molecular structure (figure taken from [101]).

Ionotropic GABA receptors ($GABAR_A$ and $GABAR_C$) are Cl^- and HCO^{3-} selective fast hyperpolarizing channels. $GABAR_A$ is the best known, made from α, β, γ, δ and ε subunits organized in a heteropentamer[102]. Additional diversity within the subunits allow for more heterogeneity that is correlated with slightly different functions and tissue localization.

$GABAR_C$ is found in the CNS and vertebrate retina, it has a homopentameric structure and can partner with $GABAR_A$[102]. Its role is far from clear.

The metabotropic $GABAR_B$ induce slow transmission currents and mediates several other neuronal effects by activating cellular effectors such as adenyl cyclases, voltage-dependent Ca^{2+} channels or inwardly rectifying potassium channels[102]. This receptor is found both pre and post-synaptically.

The binding of GABA results in the release of the G associated protein subunits, which then diffuse and activate various intracellular signal cascades and, ultimately, lead to either the activation of post-synaptic K+ channels or the inhibition of pre-synaptic Ca^{2+} channels[102].

Disorders in the regulation of GABA metabolism have been linked to many neurodegenerative diseases, such as epilepsy, Parkinson's disease, schizophrenia, anxiety disorders, autism, bi-polar disorder and PTSD (post-traumatic stress disorder)[103].

3.3) Glutamic acid decarboxylase (GAD)

GAD is the enzyme that catalyses the α-decarboxylation of L-Glutamate into GABA[104]. In humans, the enzyme is expressed in two isoforms, GAD67 (Fig. 10) and GAD65[104]. The isoforms are encoded by two genes (GAD1 and GAD2) located in different chromosomes (chromosome 2 and 10 respectively). GAD67 and GAD65 are expressed in the brain, in pancreatic insulin producing B-cells, the oviduct and testis[105]. Additional transcripts of the enzyme are detected in the brain and come, most probably, from alternative splicing.

GAD67 and GAD65, that weigh 67 and 65 kDa respectively, are highly divergent in the N-terminal part (just 23% of identity). This domain is involved in the intracellular localization, membrane association and homo/hetero-dimerization. On the contrary, they are highly similar in the C-terminal part (73% of identity), a domain related to the catalytic activity of the enzyme[103] and pyridoxal 5'-phosphate (PLP) binding site[105]. Both GAD67 and GAD65 need to homo/heterodimerize, auto-phosphorylate and bind PLP to become active[103]. Structural studies have shown that the active site is formed by a flexible catalytic loop domain that goes from His 422 to Tyr 433[103].

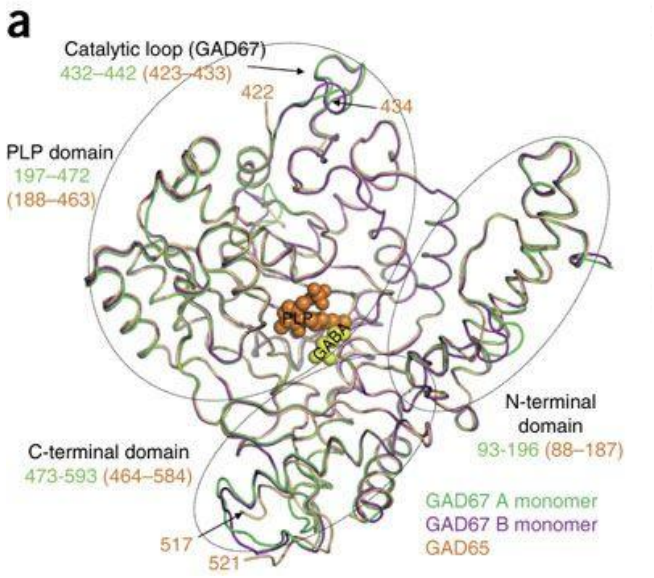

Fig. 10) GAD67 protein structure (figure taken from [106]). GAD67 needs to homo/heterodimerize, auto-phosphorylate and bind PLP to become catalytically active. The active site and PLP binding region of the enzyme are found close to the C-terminal part of the protein. In contrast, the N-terminal domain is involved in localization, membrane association and dimerization of the protein.

In the adult rat brains, GAD67 and GAD65 mRNAs are usually co-expressed in the majority of neurons, but at different concentrations depending on the brain region. As Pinal et al.[105] have observed, GAD65 is predominant in “the pyramidal layer of the olfactory tubercle, the superior colliculi, the lateral nuclei of the hypothalamus and several regions of the amygdala” whereas GAD67 is more abundant in “the granular layer of the olfactory bulb, the inferior colliculi, cerebellar cortex, neocortex and globus pallidus”. Also, GAD67 is more abundant during early development and after neuronal injury, possibly due to the

role of GABA as a trophic factor, whereas GAD65 is expressed later in development and is more important in synaptogenesis[105].

The enzymes can be found in soluble fractions or associated to membranes. The subcellular localization seems to depend on the post-translational modification of their N-terminal part by phosphorylation and palmitoylation; but the exact mechanisms are still unknown[107]. Usually, GAD65 is membrane associated and localizes in the nerve terminals whilst GAD67 is found in the cell body and soluble fractions[107]. The different spatial and temporal expression patterns, would suggest a different function for the two isoforms. Accordingly, GAD67 accounts for up to 90% of GABA synthesis and is important for the maintenance of the vesicular and cytosolic GABA pools present in the mouse brains. In contrast, GAD65 is required for the maintenance of the vesicular synaptic pools after prolonged stimulation[104]. GAD67 is constitutively active whereas GAD65 predominantly appears as inactive, with the possibility of becoming rapidly activated upon the binding of PLP. Moreover, mice knockout for GAD67 (mGAD1) are lethal at birth in contrast to GAD65[104].

The gene GAD67 has at least two promoters that can be alternatively used at different developmental stages. In addition, GAD67 mRNA undergoes alternative splicing during the brain and spinal cord

development producing two shorter and inactive proteins called GAD25 and GAD44[105] after their respective molecular weights. These transcripts contain a start/stop codons inside an additional exon, that results in the translation of two different proteins. The truncated proteins are expressed in neuronal progenitor cells at day 13 of embryonic development and, consequently, GABA is not detected at that time[105]. By the day 17, some neurons start to transiently express the full GAD67 protein resulting in GABA immunoreactivity[105]. Here, GABA is distributed in a diffuse manner throughout the neuronal cells. The early synthesis of GABA plays a trophic, rather than signalling role in neurotransmission. As the development of the brain progresses, GABA starts to localize in synaptic vesicles. These modifications coincide with the expression of GAD65 in late embryos and early postnatal life. At this point, the first mature synapses starts to form[105].

Importantly, as mentioned, GADs activation is achieved by the binding of the PLP co-factor to the GAD67 and GAD65 specific domains. These interactions depend on the levels of ATP and phosphate. These conditions are reached when the neuronal firing is intense, promoting the activation of GADs and the increased production of GABA during neuronal hyperpolarization[105]. It has also been found that GAD67 activity

is compromised during neurodegeneration. These findings were evident in patients suffering from Parkinson's disease, who presented increased levels of GAD67 and GABA. In addition, the decrease in the sensory inputs after spinal cord transection in cats and rats resulted in increased levels of GAD67 mRNA[105]. In both circumstances, GAD67 increased activity was correlated with GABA's trophic function and none of these changes were found for GAD65.

Finally, many authors have found GADs autoantibodies in the serum of patients suffering from epilepsy, stiff person syndrome, cerebellar ataxia, limbic encephalitis, myoclonus and diabetes mellitus type 1, suggesting the implication of GADs in autoimmunity and related disorders[108].

4) *Drosophila melanogaster* in the study of ALS, TDP-43 and Glutamate-GABA metabolism

4.1) *Drosophila melanogaster*

Drosophila melanogaster has been employed for more than 100 years in research. The first to make intensive use of this model system was Thomas Hunt Morgan (1866-1945). Inspired by Mendel's theories, Morgan used the fruit fly to speculate about genes and their function, thus becoming one of the pioneers of genetics[109]. In 1933, he was granted a Nobel Prize in Physiology and Medicine for his discoveries about chromosomes and heredity. Soon after, Hermann Muller (1890-1967) won a Nobel Prize in Physiology and Medicine for discovering that genetic mutations can be induced by x-ray irradiation. He, once again, took advantage of the fruit fly. There has been a well-rewarded history of scientific discoveries when Drosophila was employed. Many are the reasons why this model system is so advantageous in scientific research, some of them summarized in [109]. Briefly, the rapid life cycle, the cheap cost of maintenance and the ease of use are some worth mentioning. However, the most important characteristic of this animal, that makes it an ideal model system in so many different fields, is certainly its genetics: compared to humans, the impressively high DNA sequence homology

that is reflected in so many well conserved cellular and physiological pathways between the two species. Yet even more important might be the ease of genetic manipulation.

4.2) Drosophila's life cycle

Drosophila melanogaster is a dark bellied insect and dew eater with African origins belonging to Dipteria species. These sexually dimorphic animals allow easy recognition between male and female. The males are smaller, with black bristles on the forelegs called sex combs and a crown-like reproductive organ situated on the end of the five-segmented abdomen, opposite to the black dorso. Females are bigger, have a seven-segmented abdomen that ends with a less evident reproductive organ. In laboratory conditions, flies are usually kept on a 25% cornmeal medium in 10 cm long plastic tubes in chambers at 25ºC and 60% of humidity. In this environment, fecundated females can lay 0.5 mm long eggs (embryos) at a constant rate. The eggs will hatch and start growing into first instar larvae within 24 h after egg lay (AEL), second instar larvae within 48 h and third instar larvae within 72 h AEL (this last stage is divided in early and late and lasts 48 h). At approximately 120 h AEL, the larvae will enter into a process of metamorphosis that includes the

search for a dry place followed by transformation in pre-pupal and pupal stage. 120 h later, the adult fly will break and exit the pupal shall. From the time the embryos had been laid, it takes just 10 days for the adult fly to born (Fig 11). An adult fly lives typically 60 days.

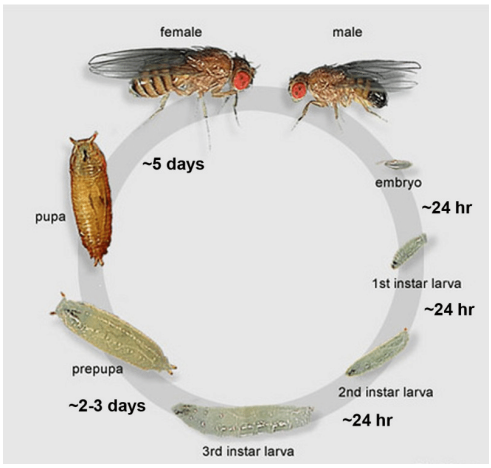

Fig. 11) Drosophila life cycle (figure taken from [110]). Once laid, the embryo will start growing and differentiating in first, second and third instar larvae, will enter the pre-pupal and pupal stage and undergo metamorphosis, after which the adult fly will hatch the pupal shell. From the time the embryo has been laid, it takes only 10 days (at 25 °C) for an adult fly to be born.

4.3) Drosophila's genetics

Drosophila has four pairs of chromosomes, three pairs of autosomes and one pair of sex chromosome. Genome sequencing revealed that the fly's genome is 180 Mb long and contains approximately 13.600 genes. It has been showed, moreover, that there is high sequence similarity with many evolutionary complex species, such humans, especially regarding

genes involved in important molecular pathways such as gene expression, cell cycle and fundamental and well known metabolic processes.

The ease of genetic manipulation makes Drosophila an ideal model system. Here I will summarize the most widely used genetic tools:

1. Balancer chromosomes, first developed by Herman Muller, are multiply inverted stretches of nucleotides that harbour at least one phenotypic marker that expresses in a dominant manner. This genetic tool prevents the process of meiotic recombination between the homologous chromosomes, assuring the integrity of the genetic construct inserted in the genome (note that Drosophila males do not undergo meiotic recombination) and helps in following the insert through fly generations.

   There are several balancers designed for chromosomes X, II and III (recombination does not occur on the IV chromosome). The most widely used are the balancer CyO of the II chromosome, that expresses curly wings, TM3SB and TM6B of the III chromosome, that expresses short or thick bristles and tubby larvae/pupae respectively.

2. P-elements are transposons specific for Drosophila. These elements can be manipulated to jump and create deletions inside genes of interest in the genome of the fruit fly. They can be autonomous or non-autonomous, depending on the presence of the transposase gene. When creating gene deletions, a combination of an autonomous but immobile transposon[111] and several non-autonomous mobile elements is used. A second use of this tool is to create transgenic flies[111]. In this case, a plasmid containing the gene of interest and the p-element sequence is created and then injected in pre-blastoderm embryos in addition to the plasmid containing the gene for the transposase. The p-element will jump randomly across the fly genome allowing the insertion of the desired gene. Recently, a site-specific transformation system has been created that allows the insertion of the p-element site-specifically[112]. The successful integration of the p-element is validated by PCR.

3. The GAL4-UAS expression system, developed by Brand and Perrimon in 1993[113], allows tissue specific gene expression. The system takes advantage of the *S. cereviseae* GAL4 transcription factor, a 881 amino acids long protein that does not have a particularly toxic effect on flies

even at high expression levels. The GAL4 binds to 17 bp long cys-regulatory enhancer elements called Upstream Activating Sequences (UAS) promoting the assembly of the transcriptional machinery and, consequently, gene expression. For the system to work, the sequence for the GAL4 must be inserted downstream a tissue specific promoter, creating a so-called “driver” (e.g. Actin-GAL4, Elav-GAL4, Repo-GAL4,…), and the UAS sequence must be inserted upstream of the gene of interest. Usually, two different Drosophila stocks are created, one harbouring the GAL4 and the other harbouring the UAS sequence. When these stocks are crossed together, the progeny will express a tissue specific GAL4, that will bind and overexpress the gene of interest only in that tissue. This system can be used also to silence genes of interest, when a target gene RNAi is inserted downstream of the UAS sites.

4.4) Neural development in Drosophila

Drosophila’s nervous system has been intensively studied and incredibly helpful in understanding the processes of neurodevelopment and neurodegeneration. The nervous system in Drosophila is of ganglionic type. The CNS is made of the central brain and the ventral nerve chord,

while the PNS consists of nerve fibers that extend from the CNS. During development, the neurons and glial cell bodies form the outer layer that surrounds the inner neuropile, a region where axons and branches extend into and create bundles[114]. These bundles can extend for long distances and create neural pathways called commissures[115].

Drosophila neurogenesis starts early in embryonic development, when the ectoderm is subdivided into the epidermal ectoderm and the neuroectoderm[116]. A subset of neuroectodermal cells will give rise to neuroblasts (NB), stem-like cells from which neurons and glia will later form[116]. Drosophila CNS begins as a cluster of ~ 100 NBs as early as stage 9 of embryonic development[117]. NBs will start dividing in a stem-like fashion, each giving rise to a ganglion mother cell (GMC) and a NB. The GMC will divide into two primary neurons which will start extending their first axons towards the neuropile[117]. During larval development, the NBs will divide again, giving rise to secondary neurons. All neurons that derive from a specific NB belong to the same "lineage" (Fig. 12). Some NB lineages will give rise to Raw Prawn (RP) neurons – Drosophila motoneurons[119]. There are 5 well characterized RPs (RP1-5). Since it is inherent to the experimental work in this thesis, RP3 will be discussed in more detail: the cell body of RP3 starts migrating towards the ventral

midline of the ventral nerve chord at stage 12 and extending its first growth cones at stage 13[119].

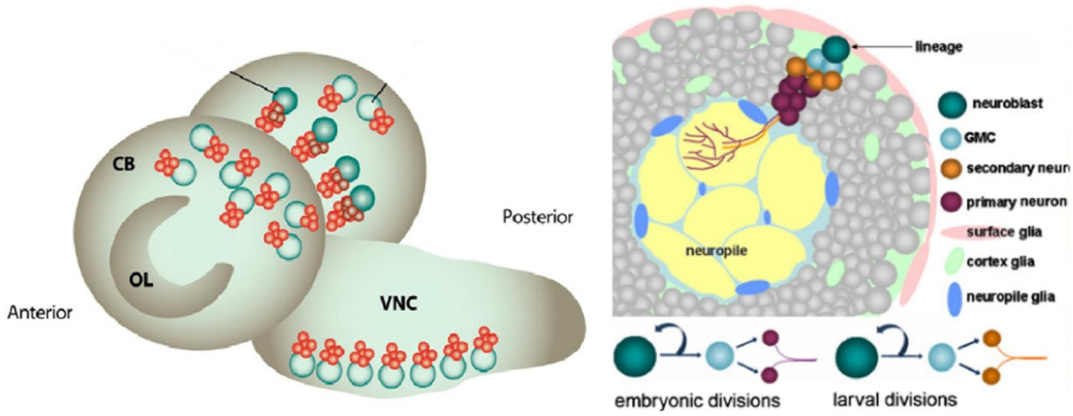

Fig. 12) Drosophila larval CNS. The CNS of a developing larvae is made of the central brain (CB) that includes two optic lobes (OL), and the ventral nerve chord (VNC). The brain begins as a cluster of ~ 100 NBs. NBs will start dividing in a stem-like fashion giving rise to GMC that will later differentiate into neurons and glial cells. Soon after, the neurons will extend their axons towards the neuropile and into commissures (figure taken from [118] and [117]).

RP3 will extend a prominent contralateral axon which will enter the Intersegmental Nerve (ISN), exit the CNS and join the Segmental Nerve (SN) in the PNS, ultimately ending to make close contact with muscles at stage 14[119]. RP3 will continue extending its processes, until it reaches its target muscles, ventral muscles 6 and 7, at stage 16 (Fig. 13). Coincidently, this is also the time when the first muscular movements become apparent. Detailed information about development of Drosophila growth cones and muscle innervation are found in [119].

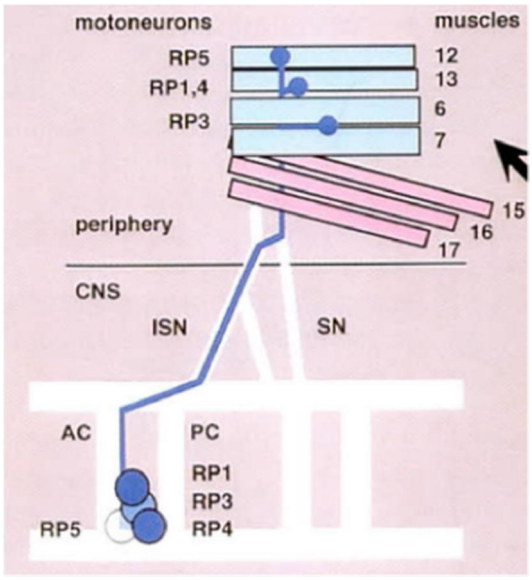

Fig. 13) The RP lineages and the innervation of muscles. RP3 migrates towards the VNC and starts extending a prominent contralateral axon that will exit the CNS following the ISN and enter the SN in the PNS, ultimately innervating muscle 6 and 7 (figure taken from [119]).

4.5) Drosophila's neuromuscular junctions

The Drosophila neuromuscular junction (NMJ) is a powerful platform for the study of synaptic development and neurotransmission[120]. The NMJ is the place where motoneurons make contact with their target muscles. Drosophila offers the possibility to study this interaction on a single cell resolution. Almost all the studies are performed on larval abdominal segments which present a simple and accessible organization. Each muscle fiber is multinuclear, formed by the fusion of several myoblast and organized in A1 to A7 segments, with about 30 muscle fibers per segment (A1 differs in this organization)[121] (Fig. 14).

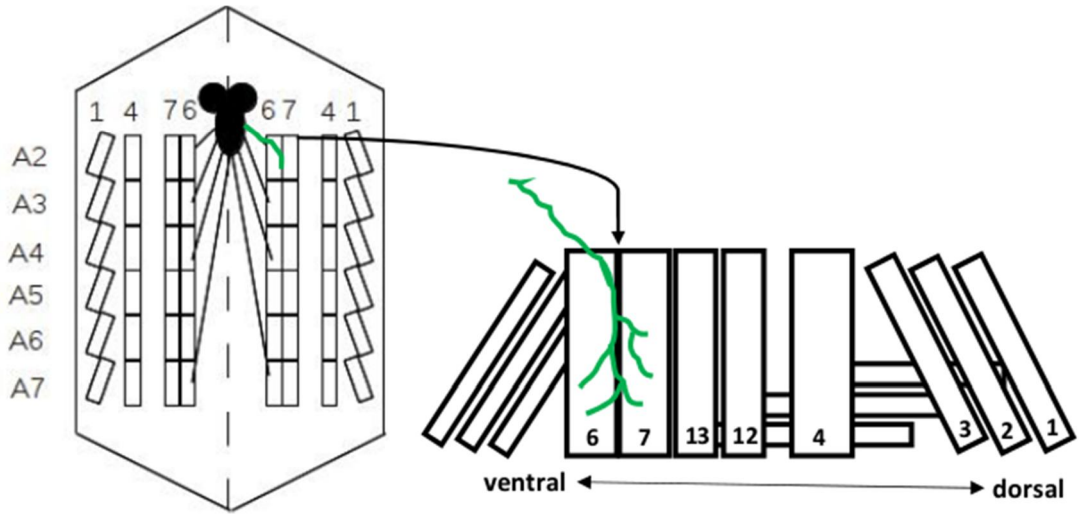

Fig. 14) Drosophila larvae neuro-muscular structure. On the left: Schematic representation of third instar larva muscle structure and its innervation pattern. On the right: schematic magnification of second abdominal segment in third instar larva, with special focus on the motoneuron laying on the muscle 6 and 7.

Each motoneuron interacts with two or more muscle fibers[121]. Neuromuscular development starts as soon as stage 14 of embryonic development, when the specialized processes called myopodia extend from the muscle fibers to make their first contact with motoneuron's growth cones[122]. When this interaction has occurred, GluRs start to cluster in the post-synaptic areas of the muscles, followed by the maturation of pre-synaptic boutons, pre-synaptic vesicles and the formation of the active zones at stage 16 of development[123]. Initially, these structures are very primitive and comprise few boutons with no branches. During development, consequently to the spreading of branches and boutons, the motoneurons start to expand on the surfaces

of muscles. At late 3rd instar larval stage, these structures increase in their volume and facilitate the recognition of the neuromuscular networks.

4.6) Neuron-glia interaction in Drosophila

The vast majority of cells in the human brain (90%) are glial cells[124]. The glia has essential functions in regulating the brain development and homeostasis. During development the glia regulates neural stem cell proliferation, provides trophic factors for growing neurons, guides axon pathfinding, ensheaths axons, promotes synaptic formation and maturation and eliminates neuronal waste[124]. In the mature nervous system, the glia maintains ionic equilibrium, regulates neurotransmitter re-uptake from the synaptic cleft and modulates synaptic activity by associating with synaptic terminals[124]. In addition, glial cells are the major immune cells in the CNS[124]. Despite all these important roles, we know very little about the glia, and this is partly because it is very challenging to study this tissue on a single cell resolution.

Drosophila's glia shares the majority of these functions with its human counterpart. Glial cells in Drosophila are classified as follows: in the CNS,

I) surface glia, that covers the entire surface of the brain, and is further subdivided in perineurial (outer) and subperineurial (inner) layer glia; II) cortex glia, that ensheaths neuronal and NBs cell bodies; III) neuropile glia, that is located between the cortex and the neuropile, and is further subdivided in ensheathing glia (remains at the neuropile surface) and astrocyte-like or reticular glia (surrounds nerve fibers inside the neuropile)[125]. In the PNS, we recognize I) perineurial and II) subperineurial glia, that form the septate junctions seal; III) wrapping glia, that surrounds the individual axons[125].

Drosophila's PNS glial cells derive from NBs lineages, nearly all brain NBs. These cells migrate out of the CNS along the extending axonal tracts of motoneurons, following the ISN and SN. As the development goes on, glial cells grow in size and wrap around axons and axon fascicles[126].

Drosophila's genetic toolbox has allowed the study of the lack-of-glia effects on the organization of the CNS and PNS. The lack of gene *gcm*, the master regulator of glial development, was associated with severe defects in axon guidance, nerve ensheathment and fasciculation[126].

Gmc$^{-/-}$ embryos have aberrant CNS longitudinal nerve tracts including complete disorganization of the ISN and SN. The absence of glial wrapping onto individual axons results in their morphological deficits,

degeneration and problems in signal conducatance[126]. These are just some of the deficits caused by the lack-of-glia, suggesting the importance of this tissue in promoting neuronal homeostasis.

4.7) Neurotransmission in Drosophila

Neurotransmission is made possible by a complex network of functionally specialized synaptic proteins. The evolutionally conserved family of Synapsins govern the release of presynaptic vesicles filled with neurotransmitters[127]. These proteins called SNAREs (Soluble N-Ethylmaleimide sensitive fusion attachment protein receptors) can be found on both pre-synaptic and vesicular membranes. Vesicle release is dependent on the phosphorylation status of SNAREs, which is governed by intracellular signal cascades, usually an arriving action potential that leads to a rise of presynaptic Ca^{2+} and activation of Ca^{2+}/Calmodulin dependent kinases. The interaction between vesicular SNAREs (vSNARES – synaptobrevin, synaptogamin), and pre-synaptic membrane SNAREs (tSNAREs – syntaxin, SNAP25) will lead to vesicle-membrane fusion, neurotransmitter exocytosis and vesicle recycling[128]. An important pre-synaptic protein in Drosophila is Bruchpilot, with homology to vertebrate CAST (Cytoskeletal matrix associated with the active zone structural

protein), involved in the maturation of T-Bars, structures that promotes vesicle scaffolding[129].

Neurotransmitter release occurs in the active zones of the synaptic cleft, with consequent binding to the post-synaptic receptors and signal propagation. First thing to mention is that the fruit fly uses Glutamate (therefore glutamatergic synapses) in both the brain and the NMJs, which contrasts with mammals that use Acetylcholine (Ach) and Cholinergic Receptor (AchR) to communicate at the level of NMJ and Glutamate-GluR only in the brain (although some studies suggest the existence of glutamatergic synapses at the NMJ in humans as well[130]). Most of the invertebrates use glutamatergic synapses at the NMJ, so mammals are an oddity in evolution.

Like in the mammals, Drosophila's GluRs can either be ionotropic or metabotropic. iGluRs in Drosophila are subdivided in 1) NMDA dependent, 2) NMDA non-dependent and 3) Glutamate-gated chloride channels. The first group of NMDA-like proteins (dNR1/NMDAR-I and dNR2/NMDAR-II) are similar to human's NMDARs[131], activated by Glutamate and NMDA, modulated by Glycine and with a Mg^{2+} voltage sensitive block. They are mainly spread in the fly's brain where they modulate learning processes.

The best studied iGluRs in Drosophila, however, are certainly the NMDA non-dependent. These receptors are found in the embryonic and larval body muscles. Depending on the type of electrical transmission and the subunits that form the protein complex, non-NMDA receptors are further subdivided in type A (excitatory, GluRIIA + GluRIIC/GluRIII + GluRIID + GluRIIE + the accessory subunit Neto) and type B (excitatory, GluRIIB + GluRIIC/GluRIII + GluRIID + GluRIIE + the accessory subunit Neto)[132]. Despite the structural similarity to human receptors, Drosophila's non-NMDA GluRs are activated by Glutamate and Quisqualate but not Glycine, GABA, Acetylcholine, NMDA, or Kainate[132], therefore they are not to be considered AMPA or Kainate receptors.

The Glutamate-gated Chloride channels type H, are inhibitory channels but their functions were not clearly elucidated yet.

Only two mGluR-like proteins have been encountered in the fly: dmGluRA and dmXR. The former is similar to human mGluR group II, found predominantly in the brain where it regulates learning[133] or at pre-synaptic terminals, where its function is unknown. DmXR has not yet been well characterized[133]. Detailed information on Drosophila GluRs can be found in [133].

The clustering and recycling of GluRs is promoted by Disc-Large, a scaffolding protein of the post-synaptic membranes that belongs to the evolutionally conserved family of Membrane Associated Guanylate Kinases (MAGUK), widely expressed in neurons and glia of vertebrates. Disc Large 1 is the exclusive ortholog in Drosophila[134].

4.8) Drosophila GAD1

The two GAD ortholog genes in Drosophila, GAD1 and GAD2[135], generate two different proteins. Drosophila GAD1 has a mass of 57 kDa and a length of 510 amino acids. This protein shares 53% of total identity with its mammalian counterpart that increases to reach the 70% of identity in the C-terminal, the PLP binding domain. Biochemical analysis revealed that dGAD1 catalyses the production of GABA from Glutamate with an efficiency and kinetics similar to the mammalian GAD[136]. dGAD1 is widespread in the nervous system from the early stages of embryogenesis till late adulthood. dGAD2, instead, shares 42% of identity and encodes a 58 kDa protein[137]. dGAD2 heterozygous flies showed, however, normal levels of GABA. Moreover, it seems that dGAD2 is expressed just in the glia indicating that dGAD1 is the more important for the GABA metabolism in neurons[137].

Insects homozygous mutants for dGAD1 enzymatic activity display severe locomotive and behavioural defects and die at embryonic or first instar larvae stages[136]. The pan-neuronal overexpression of dGAD1 rescues completely these phenotypes indicating that the protein is essential in the neurons for survival[136]. dGAD1 is present in the cell bodies, axons and synaptic boutons of third instar larvae, in both the CNS and the PNS (Fig. 15)[136].

In the NMJ, dGAD1 is required to regulate the levels of Glutamate and ensure the proper GluRs receptor field organization. Featherstone et al.,[136] observed that, despite the high concentration of dGAD1 in the motoneurons synaptic terminals, there was no GABA immunoreactivity and the injection of GABA was not producing any transmission event indicating that GABA may not have synaptic functions in flies NMJs. In contrast, Glutamate was required. Thus, the neurotransmission in dGAD1 mutants was highly impaired. The phenotype was a consequence of a 4-5 fold reduction in the number of post-synaptic GluRs compared to wild type[136]. These studies demonstrated that pre-synaptic dGAD1 is required to orchestrate the organization of GluRs in the post-synaptic membrane of the flies NMJs. These findings go along with the theory that indicates that the communication between pre-synaptic and post-

synaptic networks is dictated by the release of pre-synaptic signalling molecules[136].

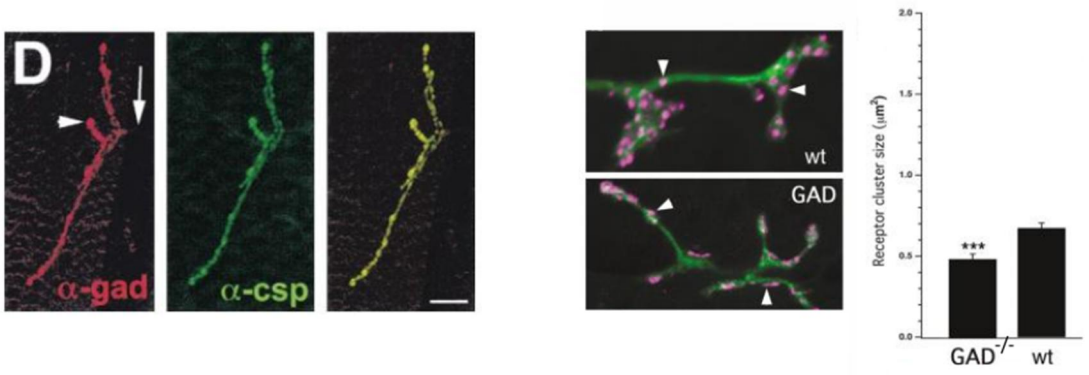

Fig. 15) GAD1 localization and the effects of GAD1 genetic manipulation on the GluRs field at Drosophila's NMJs (figures taken from [136, 138]). On the left: GAD1 naturally localizes in the motoneurons pre-synaptic terminal in wild type larvae. On the right: GAD1 mutant larvae have reduced GluRs field in the NMJs.

In the NMJs of vertebrates, Agrin and Neuroregulins are secreted by the pre-synaptic neurons to initiate the expression and clustering of AChR on the muscle surface. In Drosophila, it seems that the concentration of Glutamate is critical to accomplish the analogous processes.

Two years later, Featherstone et al.[138], observed that "the size of the postsynaptic Glutamate response was inversely correlated with the presynaptic levels of Glutamate". In this study, the group concluded that the downregulation of GluRs in dGAD1 mutants was mediated by an excess of Glutamate in the synaptic cleft, released by a non-vesicular mechanism. They proposed that Glutamate (thus the dGAD1 by-product)

would have two distinct functions in the NMJs of flies: the first one is related to its well-known role in the propagation of action potentials mediated by the vesicular release of Glutamate. The second one, relates to the slow and constant non-vesicular release of the neurotransmitter and is intended for the expression and clustering of GluRs at the post-synaptic membranes[138].

4.9) Drosophila in the study of ALS and TDP-43

In recent years great efforts has been invested in the study of ALS using the fruit fly. Many models have been created with the aim of simulating the disease in this animal. Manipulation of the main genes thought to be involved in the appearance of ALS, such as C9ORF72, SOD1 and TDP-43 have been performed in the fly[139,140,141].

In 2009, Feiguin et al.[142], generated a deletion of the gene TBPH, the homolog of TDP-43 in the fruit fly. Protein alignment has shown 59% of identity in the RRM region between these two orthologs suggesting high structural and functional conservation[56]. TBPH deletion completely abolished the endogenous expression of the protein (TBPH null flies) (Fig 16). Flies lacking TBPH had reduced life span and strong locomotor impairments due to structural defects at the level of NMJs (Fig 16)[142]. In

addition, it was discovered that TBPH silencing in neurons provoked clustering deficits of pre-synaptic proteins Syntaxin, Synapsin and Cystein String Protein (csp) and post-synaptic proteins Disc Large and the GluRIIA (Fig. 17) at the level of larval NMJs. On the contrary, the pre-synaptic protein Bruchpilot was not affected (Fig. 17). Similarly, silencing of TBPH in the glia provoked life span reduction and locomotion problems, accompanied with GluRIIA clustering alterations and also the retraction of glial wrapping around motoneurons. These data indicated that TBPH promoted the assembly of proteins at the synaptic terminals in both neurons and muscles, acting from different tissues, and thus had a pivotal role in the structural and functional complexity of the Drosophila's NMJs. These proteins were also downregulated at protein level, indicating that it was not a problem of transport or localization but rather of gene expression.

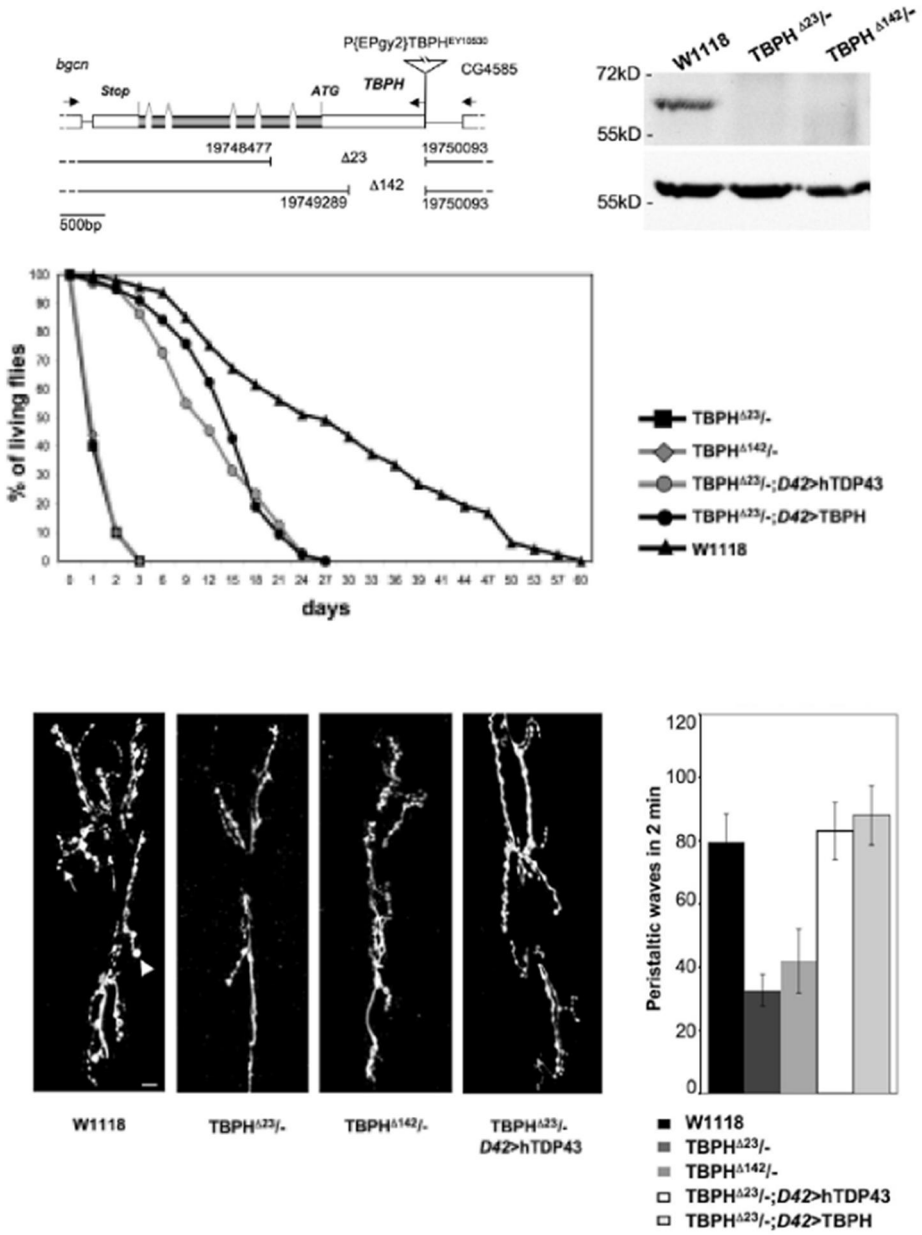

Fig. 16) Loss of TBPH expression in Drosophila is associated with reduced life expectancy, locomotion impairment and neuro-muscular junctions deficits (figure taken from [142]). In 2009, Feiguin has abolished the expression of endogenous TBPH by creating two different deletions models ($TBPH^{\Delta 23/\Delta 23}$, $TBPH^{\Delta 142/\Delta 142}$) inside the promoter region of Drosophila TBPH gene.

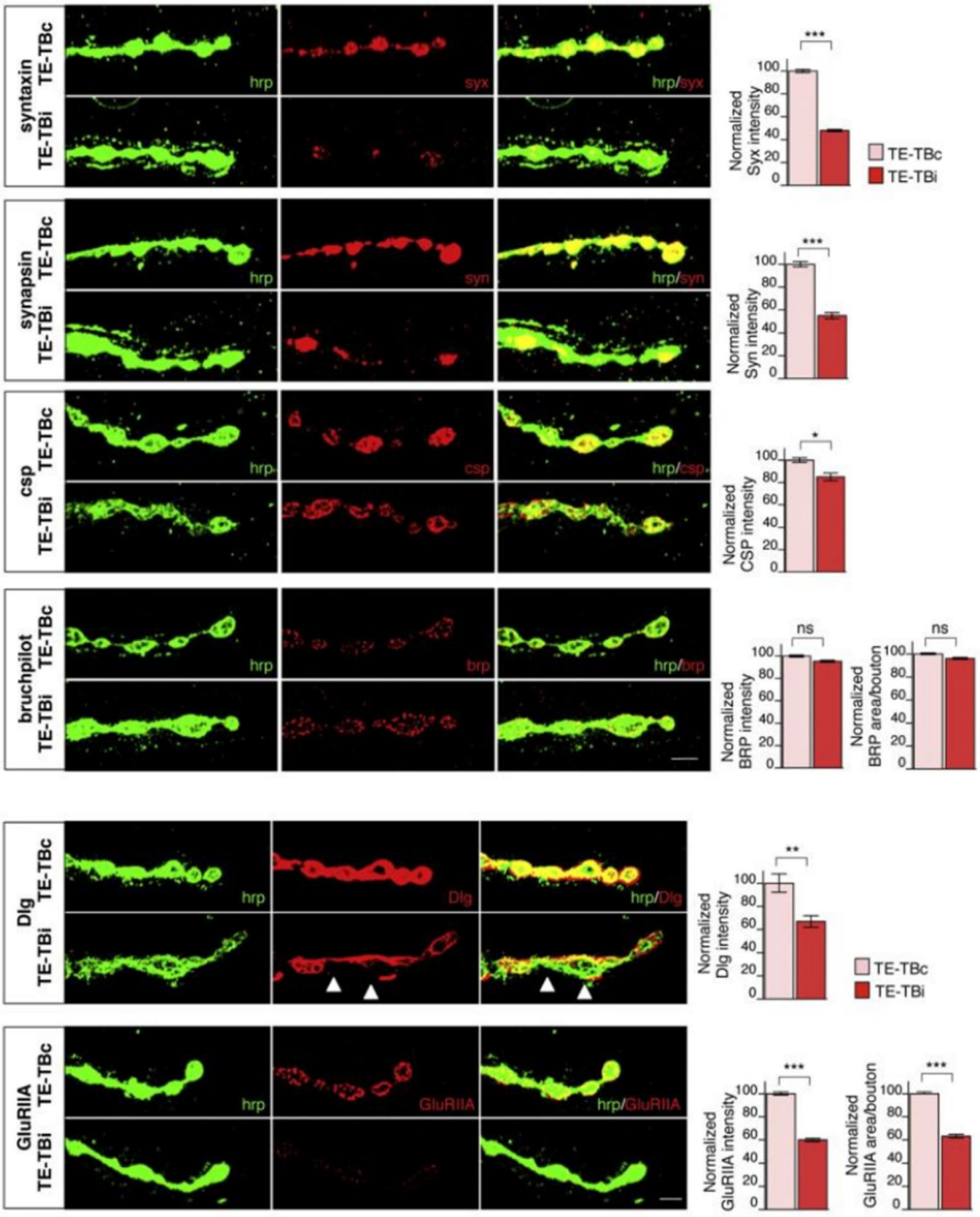

Fig. 17) Reduced expression of TBPH in Drosophila neurons (TE-TBi) is associated with reduced clusterization of Syx, Syn, Csp on the pre-synaptic membrane, Dlg and GluRIIA on the post-synaptic membrane, at the Drosophila larval NMJs. Hrp is a glycoprotein of neuronal membranes (figure taken from [143]).

AIM OF THESIS

In this PhD thesis, my aims were to investigate the proteins that intermediate the role of TDP-43 in the organization of the synapses using a TDP-ALS fly model. More specifically, the questions addressed were the following:

- To investigate which proteins are directly or indirectly regulated by TDP-43 by performing TBPH null wide screen proteomic analysis

- To understand the role of these proteins in neuronal and non-neuronal tissues by genetically manipulating their expression

- To study how these proteins influence synaptic communication by measuring their activity

- To investigate if these molecular pathways are conserved in humans and ALS patients

RESULTS

5) Proteomic alterations in TBPH null flies

5.1) The enzyme GAD1 is downregulated in TBPH null brains

In the first part of this study, we performed a genome wide high throughput proteomic analysis aiming to identify all the molecules that were translationally misregulated in TBPH mutant flies compared to wild type controls. To do so, we carried out a two-dimensional gel electrophoresis between 1-day old Drosophila adult heads from wild type (w^{1118}) as well as TBPH null alleles ($TBPH^{\Delta 23/\Delta 23}$ and $TBPH^{\Delta 142/\Delta 142}$) and analysed statistical differences in spot intensities after normalization. We fixed a 1.5 threshold and obtained a total number of 35 modified spots out of 1383 examined (Fig. 18). We then selected the spots that were similarly modified in both mutants ($TBPH^{\Delta 23/\Delta 23}$ and $TBPH^{\Delta 142/\Delta 142}$) for a total number of 7 spots, 5 downregulated and 2 upregulated. The proteins corresponding to these spots were extracted and sent to MALDI-TOF mass spectrometry analysis for identification. Among the downregulated proteins, GAD1 (cg14994, FBgn0004516) was the most prominent (Fig. 19). GAD1 is an evolutionary conserved enzyme that converts Glutamate to GABA. Since these fundamentally important neurotransmitters promote synaptic communication, GAD1

downregulation could explain TBPH null neurodegeneration, especially related to the loss of synaptic stability that these mutants exhibit.

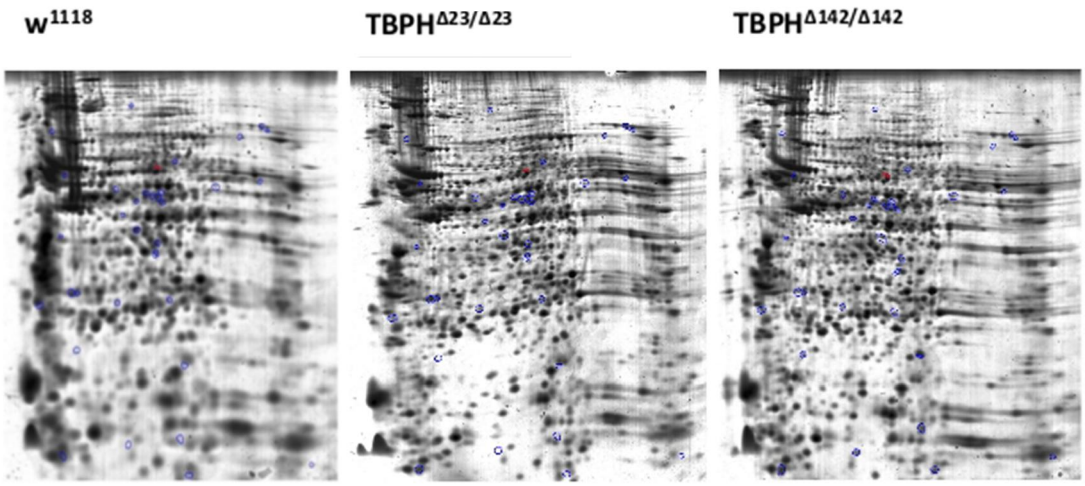

Fig. 18) Genome wide proteomic analysis of TBPH null adult flies heads. 2D gel electrophoretic analysis of TBPH null adult heads showed several spots whose intensities were altered (highlighted in blue) in respect to wild type. GAD1 protein (corresponding to spot 701) was one of the spots that resulted downregulated (shown in red). Genotypes: w^{1118}, $TBPH^{\Delta 23/\Delta 23}$ and $TBPH^{\Delta 142/\Delta 142}$. n=100 per genotype (technical procedures for 2D gel analysis are explained in the text and in more detail in the Material and Methods section). Courtesy of Dr. Raffaella Klima and Prof. Rodolfo Garcia.

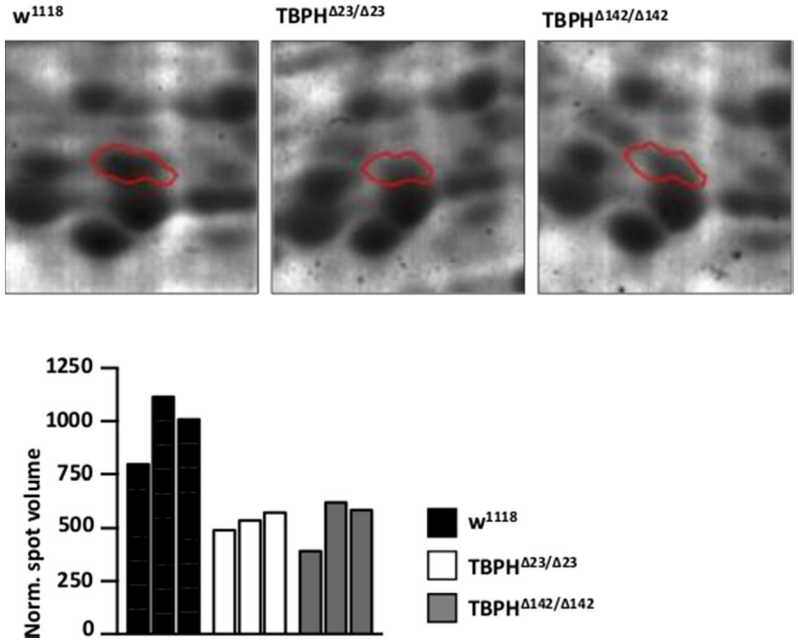

Fig. 19) Magnification and quantification of the downregulated spot 701 in 2D gel electrophoresis of TBPH null adult flies heads. The enzyme GAD1 is one of the proteins downregulated in both $TBPH^{\Delta 23/\Delta 23}$ and $TBPH^{\Delta 142/\Delta 142}$ in comparison to w^{1118}. Beneath are the intensity quantification for GAD1 protein after normalization, total n was 100 per genotype (the quantification of spots intensities is explained in the text and in more detail in the Material and Methods section). Courtesy of Dr. Raffaella Klima and Prof. Rodolfo Garcia.

Next, we decided to confirm this result by western blot. Unfortunately, the only available antibody that recognizes Drosophila GAD[136], was not provided to us. For this reason, we used a fly ($GAD1^{MIMIC}$/Tm3sb) that carried an endogenously tagged GAD1 gene. In brief, a MIMIC cassette comprehending a triple flag tag was inserted in the middle of the coding region of GAD1 gene (w;Mi{MIC}$GAD1^{MI09277}$/+). The protein encoded by this gene was supposed to weight approximately 95 kDa, that is the combined mass of GAD1 protein (57.8 kDa) and the MIMIC cassette

(EGFP-FlAsH-StrepII-TEV-3xFlag-tag insertion) (35kDa). We have then constructed a fly carrying this construct in a TBPH$^{\Delta 23}$ background (TBPH$^{\Delta 23}$/yGFP; GAD1^{MIMIC}/Tm6b) and crossed to TBPH$^{\Delta 23}$/yGFP to obtain a fly expressing the tagged GAD1 in a TBPH null background (TBPH $^{\Delta 23}$/$^{\Delta 23}$; GAD1^{MIMIC}/+). This fly was compared to TBPH $^{+/+}$; GAD1^{MIMIC}/+. The brains of third instar larvae were lysed and labelled with anti-flag M5 in western blot. The data clearly indicated that of GAD1^{MIMIC} was downregulated in TBPH mutant larvae in comparison to the controls, confirming the proteomic findings (Fig. 20).

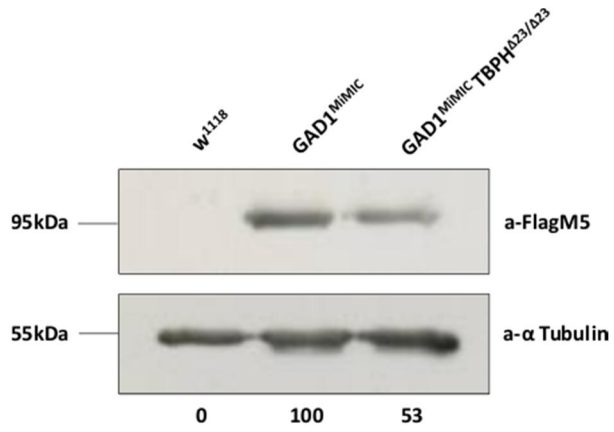

Fig. 20) GAD1^{MIMIC} protein levels in TBPH null larvae. Western blot showed that GAD1^{MIMIC} is downregulated in TBPH null third instar larval brains in respect to controls. The antibody against GAD1 was not available to us, therefore we visualized GAD1^{MIMIC} (MIMIC being a tag insertion in the middle of the GAD1 allele). The samples were run on polyacrylamide gels, transferred and labelled with a-Flag M5 and a-Tubulin primary antibodies. Data were normalized, n=20 per genotype. Beneath is the normalized quantification of bands' intensity (a-FlagM5/a-Tubulin) that was done in ImageJ (more in detail in the Material and Methods section). Courtesy of Dr. Giulia Romano.

To test GAD1 mRNA levels, we performed a real time PCR (RT-PCR) against GAD1 mRNA in TBPH null third instar larvae (Fig. 21). The data indicated that GAD1 mRNA is downregulated in $TBPH^{\Delta 23/\Delta 23}$ and $TBPH^{\Delta 142/\Delta 142}$ compared to w^{1118}. In summary, these results demonstrated that GAD1 was downregulated in TBPH mutants at both the transcriptional and translational level. These results were extremely interesting given the function of TBPH as a RNA binding protein and regulator of RNA metabolism. Naturally, one would assume that TBPH could directly bind and positively regulate GAD1 pre-mRNA (or mRNA) and that GAD1 mRNA downregulation in TBPH null flies was due to the obstruction of this TDP-dependent regulatory step. Thus, we performed immunoprecipitation studies to test TBPH-GAD1 mRNA interaction. However, despite intensive efforts, we were not able to observe any direct binding between the two (data not shown), indicating that GAD1 mRNA was processed by different molecules.

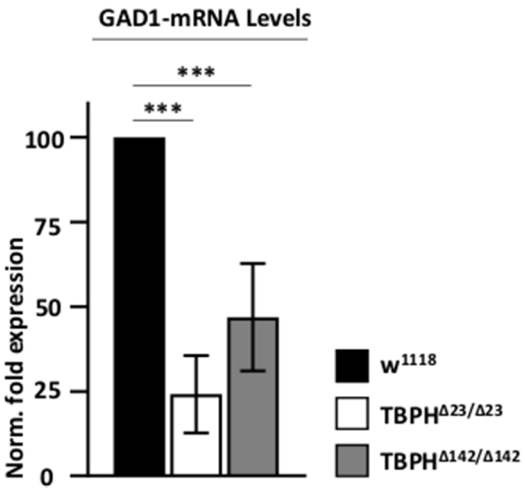

Fig. 21) mRNA levels of GAD1 in TBPH null larvae. RT-PCR demonstrated that GAD1 mRNA is downregulated in TBPH null third instar larval brains (both $TBPH^{\Delta 23/\Delta 23}$ and $TBPH^{\Delta 142/\Delta 142}$) in comparison to wild type (w^{1118}). mRNA levels were normalized on Rpl11, a housekeeping gene. Quantification was done in GraphPad Prism 7.0, ***$p < 0.001$ calculated by one-way ANOVA. Error bars SEM. n=20. Courtesy of Dr. Giulia Romano.

6) The role of GAD1 in neurons

6.1) The reintroduction of GAD1 in neurons rescues the TBPH null motility defects

In our previous experiments we assessed that GAD1 was downregulated in TBPH mutants. To establish whether this enzyme played a role in TBPH null flies motility phenotypes, we reintroduced GAD1 in neurons of TBPH mutant flies taking advantage of the GAL4-UAS expression system. To do so, we used a fly that was carrying GAD1 gene placed under UAS control (uasGAD1), allowing the transgene to be expressed in a controlled and tissue specific manner. We therefore discarded the fly carrying $GAD1^{MIMIC}$, a mutated form of the endogenous gene, used earlier to quantify the expression of the endogenous protein. We specifically utilized Elav-GAL4, a pan-neuronal driver and D42-GAL4 a driver specific for motoneurons and measured the locomotion performance of third instar larvae and adult flies. Our data showed that GAD1 reintroduction in neurons and motoneurons significantly rescued the locomotion impairments of TBPH null larvae (Fig. 22). This rescue was observed only at larval stage but not in the adult flies (data not shown), indicating that the adult developmental stage involved more complex degeneration pathways that were not limited to GAD1 downregulation. In parallel, the

reintroduction of exogenous TBPH yielded a stronger recovery of these genetics backgrounds, in both larvae and adult flies (not shown), suggesting that GAD1 could only partially replace TBPH. In summary, these results indicated that GAD1 downregulation played a role in TBPH null motility defects and its reintroduction rescued, although only partially, the locomotion phenotypes.

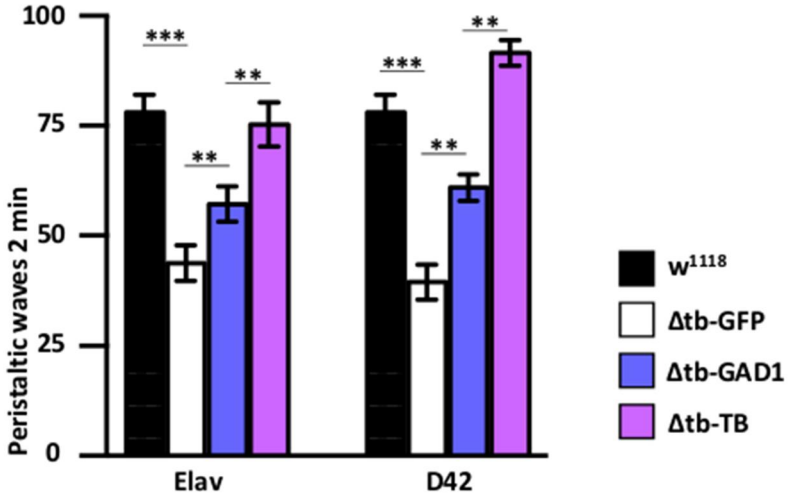

Fig. 22) GAD1 overexpression in pan-neuronal tissues in TBPH null larvae. GAD1 reintroduction (Δtb-GAD1) in neurons by Elav-GAL4 and D42-GAL4 drivers have significantly recovered the motility defects of TBPH null third instar larvae compared to the negative control (Δtb-GFP). Recovery was calculated measuring the number of larval waves the animals were performing in 2 min. Genotypes: w^{1118}, Δtb-GFP (on the left: Elav-GAL4, $TBPH^{\Delta 23/\Delta 23}$; uasGFP/+ and on the right: $TBPH^{\Delta 23/\Delta 23}$; uasGFP/D42-GAL4,) Δtb-GAD1 (on the left: Elav-GAL4, $TBPH^{\Delta 23/\Delta 23}$; uasGAD1/+ and on the right: $TBPH^{\Delta 23/\Delta 23}$; uasGAD1/D42-GAL4) and Δtb-TB (on the left: Elav-GAL4, $TBPH^{\Delta 23/\Delta 23}$; uasTBPH/+ and on the right: $TBPH^{\Delta 23/\Delta 23}$; uasTBPH/D42-GAL4), Quantification was done in GraphPad Prism 7.0, **p < 0.01, ***p <

0.001 calculated by one-way ANOVA. Error bars SEM. Total number of tested animals per genotype was 25.

6.2) The reintroduction of GAD1 does not rescue motoneurons terminal growth

We have established that GAD1 rescued TBPH null motility defects and suspected that the role played by GAD1 was related to the regulation of synaptic homeostasis. Accordingly, we have previously discovered that the neuronal growth depends strictly on the stability of the synaptic communications and that both, the neuronal branching and the shape of the synaptic boutons were highly compromised in TBPH null flies. Therefore, we first decided to investigate whether GAD1 was able to recover the morphological integrity of motoneurons. For these experiments, we dissected and labelled third instar larvae against HRP, an antigenic glycoprotein present in neuronal membranes[144]. Next, we measured the number of branches and the number of spherically shaped synaptic boutons that motoneurons can extend on the surface of muscles 6 and 7 in the second abdominal segment. We noticed that none of these parameters were ameliorating upon GAD1 reintroduction (Fig. 23). Although disappointing, these results were not surprising as

previous studies have shown that TBPH regulates the organization of microtubules by directly binding and regulating Futsch mRNA[61], the Drosophila microtubule associated protein. Thus, it seemed that GAD1 reintroduction was not able to replace TBPH functions that are related to the morphological structure of the pre-synaptic terminal suggesting that GAD1 rescue of TBPH null locomotion impairment was independent of the pre-synaptic morphological growth.

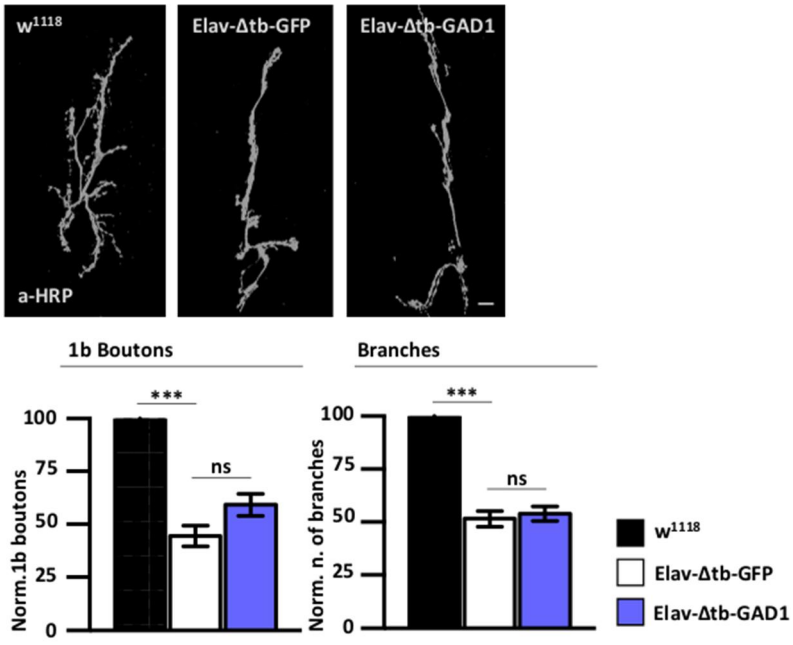

Fig. 23) Motoneuron branching and synaptic boutons shape integrity in TBPH null larvae upon GAD1 overexpression in neurons (Elav-Δtb-GAD1). This figure indicates that GAD1 reintroduction did not ameliorate neuronal branching or boutons shape integrity of TBPH null larvae in comparison to the negative control (Elav-Δtb-GFP). Above: confocal microscopy acquisition of the motoneuron laying on the muscles 6/7 of the second abdominal segment of third instar larvae. The nerve cell was stained with anti-HRP, a glycoprotein of outer neuronal membranes. Below: quantification of 1b boutons and synaptic branches

ramification of the motoneurons. Genotypes: w^{1118}, Elav-Δtb-GFP (Elav-GAL4, $TBPH^{\Delta 23/\Delta 23}$; uasGFP/+) and Elav-Δtb-GAD1 (Elav-GAL4, $TBPH^{\Delta 23/\Delta 23}$; uasGAD1/+). Quantification was done in GraphPad Prism 7.0, ***p < 0.001 calculated by one-way ANOVA. Error bars SEM. Scale bar: 10 μm. 15 larvae examined per genotype.

6.3) The reintroduction of GAD1 in neurons rescues the pre-synaptic protein Syntaxin and the post-synaptic proteins Disc Large and GluRIIA

GAD1 reintroduction was not recovering the morphological integrity of motoneurons. However, these evidences were not ruling out the possibility that GAD1 could ameliorate the synaptic communication between the motoneurons and the muscle. We knew from previous studies[143] that several pre-synaptic and post-synaptic proteins were downregulated in TBPH mutants. The pre-synaptic protein Syntaxin and the post-synaptic Disc Large and GluRIIA proteins are few examples. To investigate if their distribution was rescued by GAD1 reintroduction, we performed a series of dissections and labelled third instar larvae NMJs against Syntaxin, Disc Large and GluRIIA. As an internal control we used the pre-synaptic protein Bruchpilot, shown to be unaffected in TBPH null flies[143].

Our data indicated that GAD1 reintroduction significantly rescued the distribution of Syntaxin (Fig. 25) on the pre-synaptic membranes and the distribution of Disc Large (Fig. 26) and GluRIIA (Fig. 27) on the post-synaptic terminals. Bruchpilot, instead, remained unaltered (Fig. 24) confirming the reliability of this internal control. As these proteins tightly regulate synaptic communication, these results could indicate that GAD1 rescue of TBPH null motility defects was driven by an enhancement in synaptic communication between neurons and muscles. In addition to the evident rescue of post-synaptic proteins Disc Large and GluRIIA, it was surprising to observe that Syntaxin, a pre-synaptic protein that is naturally directly bounded and regulated by TBPH[61], was also partially rescued by GAD1 reintroduction in neurons.

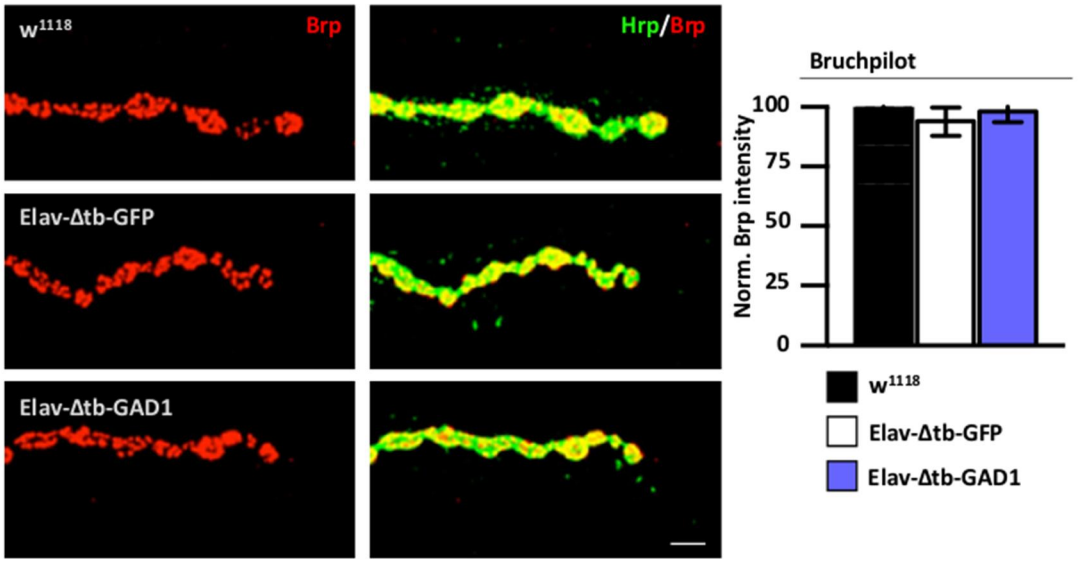

Fig. 24) Distribution of pre-synaptic protein Bruchpilot in the NMJ of TBPH null larvae upon GAD1 overexpression in neurons (Elav-Δtb-GAD1). Bruchpilot distribution was not affected in TBPH null flies. We used this protein as an internal control. Our quantification showed that Bruchpilot distribution remained unchanged in the tested samples. On the left: confocal microscopy acquisition of the motoneuron laying on the muscles 6/7 of the second abdominal segment of third instar larvae. The nerve cell was stained with anti-HRP (green, merged to Brp) and anti-Brp (red). On the right: quantification of Brp/Hrp intensity. Genotypes: w^{1118}, Elav-Δtb-GFP (Elav-GAL4, $TBPH^{\Delta 23/\Delta 23}$; uasGFP/+) and Elav-Δtb-GAD1 (Elav-GAL4, $TBPH^{\Delta 23/\Delta 23}$; uasGAD1/+). Quantification was done in GraphPad Prism 7.0, ns = non-significative (not shown), calculated by one-way ANOVA. Error bars SEM. Scale bar: 5 µm. n>200 boutons per genotype.

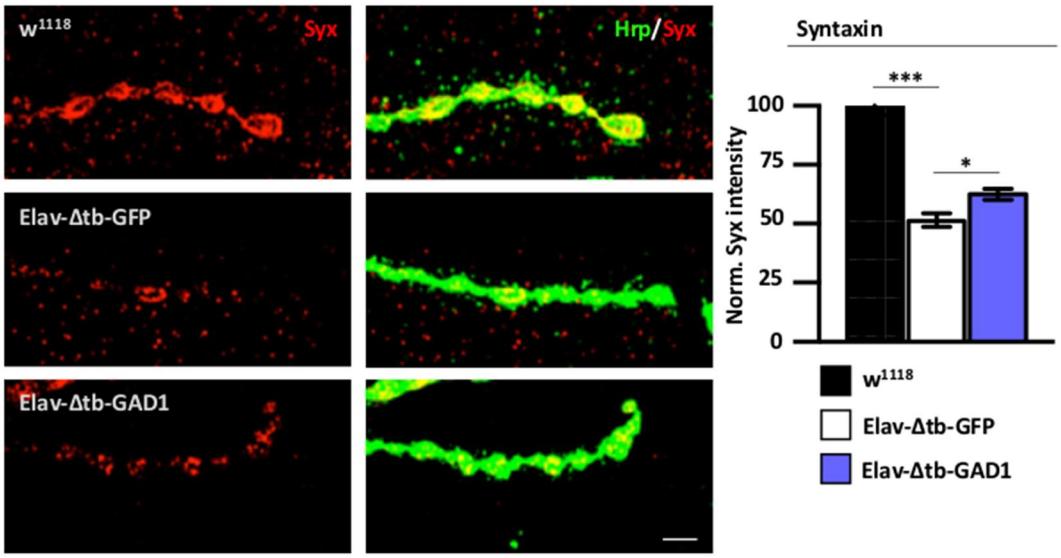

Fig. 25) Distribution of pre-synaptic protein Syntaxin in the NMJ of TBPH null larvae upon GAD1 overexpression in neurons. Syntaxin was previously described to be downregulated in TBPH null flies. GAD1 reintroduction in neurons (Elav-Δtb-GAD1) rescued significantly the distribution of Syntaxin in comparison to the negative control (Elav-Δtb-GFP). On the left: confocal microscopy acquisition of the motoneuron laying on the muscles 6/7 of the second abdominal segment of third instar larvae. The nerve cell was stained with anti-HRP (green, merged to Syx) and anti-Syx (red). On the right: quantification of Syx/Hrp intensity. Genotypes: w^{1118}, Elav-Δtb-GFP (Elav-GAL4, $TBPH^{\Delta 23/\Delta 23}$; uasGFP/+) and Elav-Δtb-GAD1 (Elav-GAL4, $TBPH^{\Delta 23/\Delta 23}$; uasGAD1/+). Quantification was done in GraphPad Prism 7.0, *$p < 0.05$, ***$p < 0.001$ calculated by one-way ANOVA. Error bars SEM. Scale bar: 5 µm. n>200 boutons per genotype.

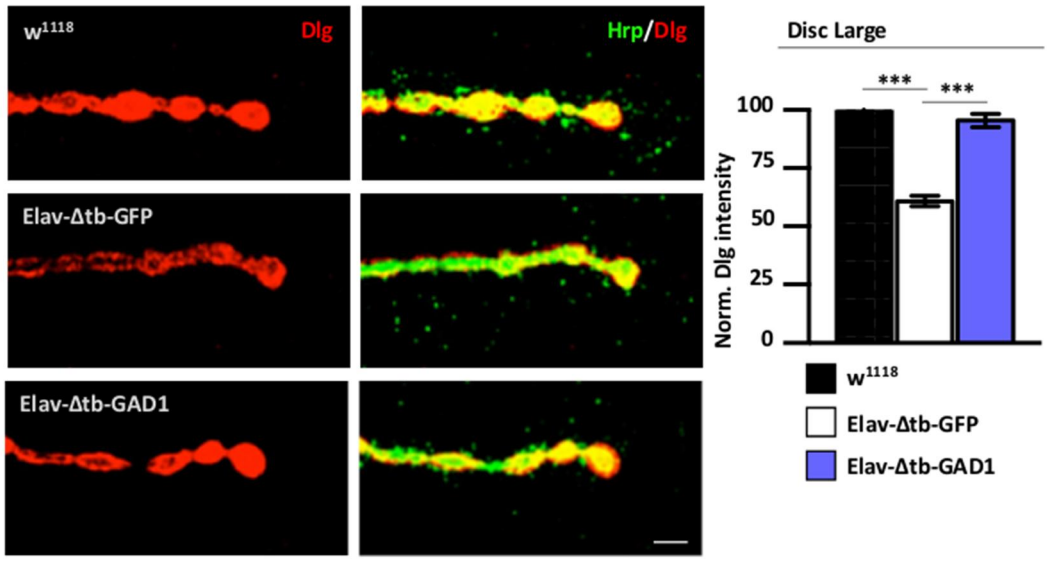

Fig. 26) Distribution of post-synaptic protein Disc Large in the NMJ of TBPH null larvae upon GAD1 overexpression in neurons. Disc Large was previously described to be downregulated in TBPH null flies. GAD1 reintroduction in neurons (Elav-Δtb-GAD1) rescued significantly (to wild type level) the distribution of Disc Large in comparison to the negative control (Elav-Δtb-GFP). On the left: confocal microscopy acquisition of the motoneuron laying on the muscles 6/7 of the second abdominal segment of third instar larvae. The nerve cell was stained with anti-HRP (green, merged to Dlg) and anti-Dlg (red). On the right: quantification of Dlg/Hrp intensity. Genotypes: w^{1118}, Elav-Δtb-GFP (Elav-GAL4, $TBPH^{\Delta 23/\Delta 23}$; uasGFP/+) and Elav-Δtb-GAD1 (Elav-GAL4, $TBPH^{\Delta 23/\Delta 23}$; uasGAD1/+). Quantification was done in GraphPad Prism 7.0, ***$p < 0.001$ calculated by one-way ANOVA. Error bars SEM. Scale bar: 5 µm. n>200 boutons per genotype.

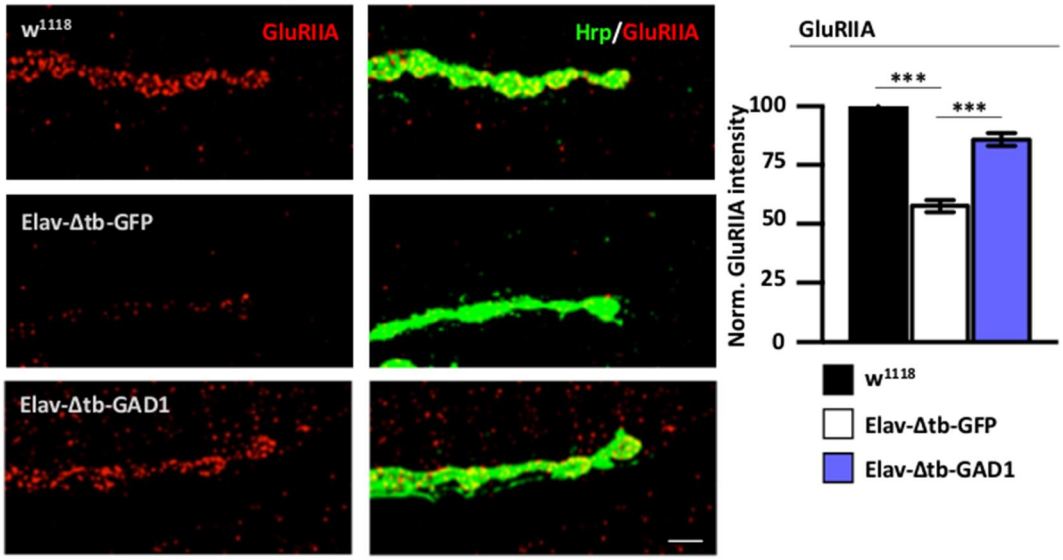

Fig. 27) Distribution of post-synaptic protein GluRIIA in the NMJ of TBPH null larvae upon GAD1 overexpression in neurons. GluRIIA was previously described to be downregulated in TBPH null flies. GAD1 reintroduction in neurons (Elav-Δtb-GAD1) rescued significantly (to wild type level) the distribution of GluRIIA in comparison to the negative control (Elav-Δtb-GFP). On the left: confocal microscopy acquisition of the motoneuron laying on the muscles 6/7 of the second abdominal segment of third instar larvae. The nerve cell was stained with anti-HRP (green, merged to GluRIIA) and anti-GluRIIA (red). On the right: quantification of GluRIIA/Hrp intensity. Genotypes: w^{1118}, Elav-Δtb-GFP (Elav-GAL4, $TBPH^{\Delta 23/\Delta 23}$; uasGFP/+) and Elav-Δtb-GAD1 (Elav-GAL4, $TBPH^{\Delta 23/\Delta 23}$; uasGAD1/+). Quantification was done in GraphPad Prism 7.0, ***$p < 0.001$ calculated by one-way ANOVA. Error bars SEM. Scale bar: 5 µm. n>200 boutons per genotype.

6.4) GAD1 silencing in neurons induces motility problems by regulating Disc Large and GluRIIA clustering

We have previously suggested that GAD1 rescue of TBPH null motility problems was, most probably, related to the recovery of the distribution of pre-synaptic and post-synaptic proteins Syntaxin, Disc Large and GluRIIA. Still, we wanted to confirm that this recovery was specific to GAD1 metabolism. Thus, we silenced GAD1 in a $TBPH^{+/+}$ background by using Elav-GAL4 and D42-GAL4. In this regard, we noticed strong locomotion impairments (Fig. 28) confirming the precious contribution of GAD1 to the control of locomotion behaviours in flies. Subsequently, we performed NMJ dissections in third instar larvae to investigate motoneurons morphological integrity. Thus, we did not find alterations in the neuronal growth upon GAD1 silencing (Fig. 29) indicating that GAD1 did not promote neuronal branching or the regular shape of the synaptic boutons, which was in agreement with our previous results. Finally, we stained the NMJs for Bruchpilot, our internal control, Syntaxin, Disc Large and GluRIIA. As expected, GAD1 silencing in Elav-GAL4 affected the distribution of Disc Large (Fig. 32) and GluRIIA (Fig. 33). These results confirmed our hypothesis by which GAD1 promoted Disc Large and GluRIIA clustering. Syntaxin distribution, instead, was

unaltered (Fig. 31). We feel to speculate that Syntaxin was not directly influenced by GAD1 and that its recovery in our rescue experiments was due to a general beneficial status of the recovered system. Bruchpilot was not changing either (Fig. 30). Collectively these results suggested that GAD1 had an important role in TBPH null motility problems. It contributed to locomotion homeostasis and promoted the synaptic stability by regulating the clustering of Disc Large and GluRIIA at the post-synaptic membrane.

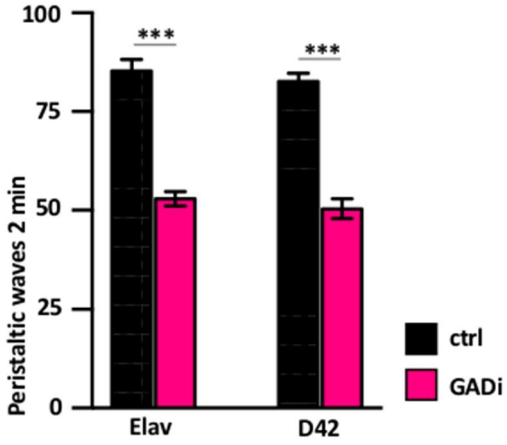

Fig. 28) Motility assays upon GAD1 silencing in pan-neuronal tissues. GAD1 suppression (GADi) with Elav-GAL4 and D42-GAL4 drivers induced strong motility problems in comparison to controls (ctrl). The phenotype was calculated by measuring the number of peristaltic movements third instar larvae were able to perform in 2 min. Genotypes: ctrl (on the left: uasLACZ/Elav-GAL4 and on the right: uasLACZ/+; +/D42-GAL4), GADi (on the left: Elav-GAL4/+; uasGAD1-RNAi and on the right: D42-GAL4/uasGAD1-RNAi). Quantification was done in GraphPad Prism 7.0, ***$p < 0.001$ calculated by T-Test. Error bars SEM. Total n per genotype was 20.

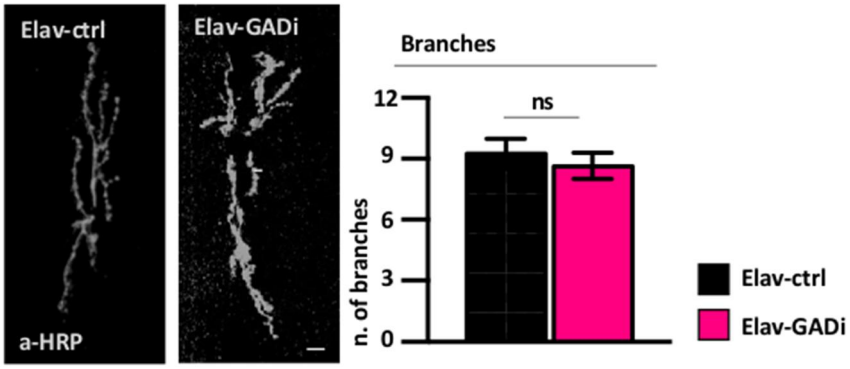

Fig. 29) Branching of motoneurons upon GAD1 suppression in neurons. Silencing of GAD1 in neurons by Elav-GAL4 driver (Elav-GADi) did not affect the structural ramification of the motoneuron over the muscles. On the left: confocal microscopy acquisition of the motoneuron laying on the muscles 6/7 of the second abdominal segment of third instar larvae. On the right: quantification of synaptic branches ramification. The motoneuron was labelled anti-HRP. Genotypes: Elav-ctrl (uasLACZ/Elav-GAL4), Elav-GADi (Elav-GAL4/+; uasGAD1-RNAi). Quantification was done in GraphPad Prism 7.0, ns = non-significative, calculated by T-Test. Error bars SEM. Scale bar: 10 µm. Number of investigated larvae per genotype was 15.

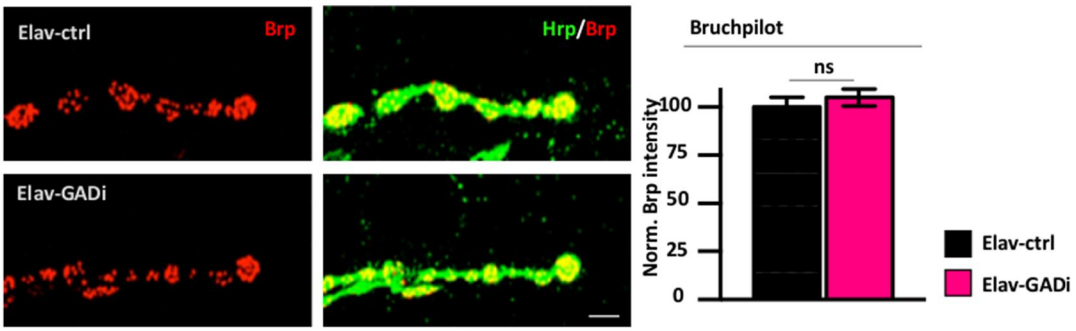

Fig. 30) Bruchpilot distribution in the NMJ upon GAD1 silencing in neurons. GAD1 suppression in neurons (Elav-GADi) did not influence Bruchpilot distribution in neurons. Bruchpilot was used as an internal control. On the left: confocal microscopy acquisition of the motoneuron laying on the muscles 6/7 of the second abdominal segment of third instar larvae. The nerve cell was stained with anti-HRP (green, merged to Brp) and anti-Brp (red). On the right: quantification of Brp/Hrp intensity. Genotypes: Elav-ctrl (uasLACZ/Elav-GAL4), Elav-GADi (Elav-GAL4/+; uasGAD1-RNAi). Quantification was done in GraphPad Prism 7.0, ns = non-significative, calculated by T-Test. Error bars SEM. Scale bar: 5 µm. Number of examined synaptic boutons per genotype was <200.

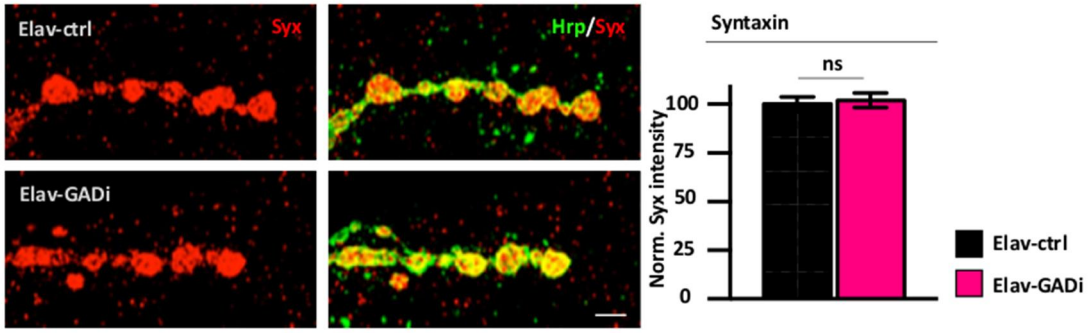

Fig. 31) Distribution of pre-synaptic protein Syntaxin in the NMJ upon GAD1 silencing in neurons. Syntaxin was not affected by GAD1 silencing in neurons (Elav-GADi). On the left: confocal microscopy acquisition of the motoneuron laying on the muscles 6/7 of the second abdominal segment of third instar larvae. The nerve cell was stained with anti-HRP (green, merged to Syx) and anti-Syx (red). On the right: quantification of Syx/Hrp intensity. Genotypes: Elav-ctrl (uasLACZ/Elav-GAL4), Elav-GADi (Elav-GAL4/+; uasGAD-RNAi). Quantification was done in GraphPad Prism 7.0, ns = non-significative, calculated by T-Test. Error bars SEM. Scale bar: 5 µm. Number of examined synaptic boutons per genotype was <200.

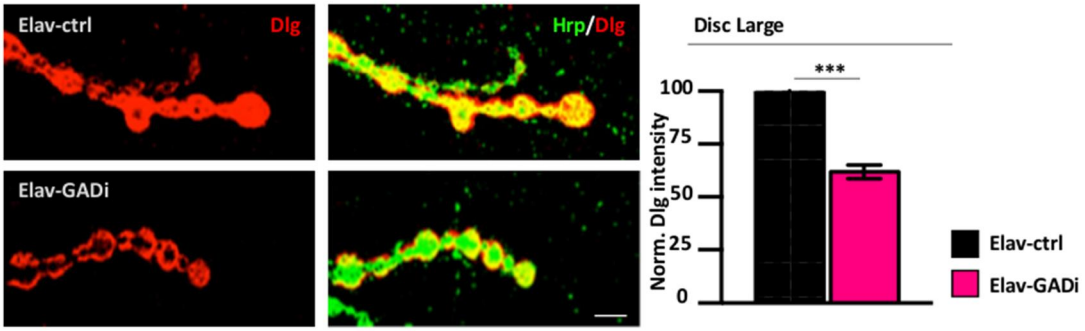

Fig. 32) Distribution of post-synaptic protein Disc Large in the NMJ upon GAD1 silencing in neurons. Disc Large was severely affected by GAD1 silencing in neurons (Elav-GADi) in comparison to the control (Elav-ctrl). On the left: confocal microscopy acquisition of the motoneuron laying on the muscles 6/7 of the second abdominal segment of third instar larvae. The nerve cell was stained with anti-HRP (green, merged to Dlg) and anti-Dlg (red). On the right: quantification of Dlg/Hrp intensity. Genotypes: Elav-ctrl (uasLACZ/Elav-GAL4), Elav-GADi (Elav-GAL4/+; uasGAD-RNAi). Quantification was done in GraphPad Prism 7.0, ***$p < 0.001$ calculated by T-Test. Error bars SEM. Scale bar: 5 µm. Number of examined synaptic boutons per genotype was <200.

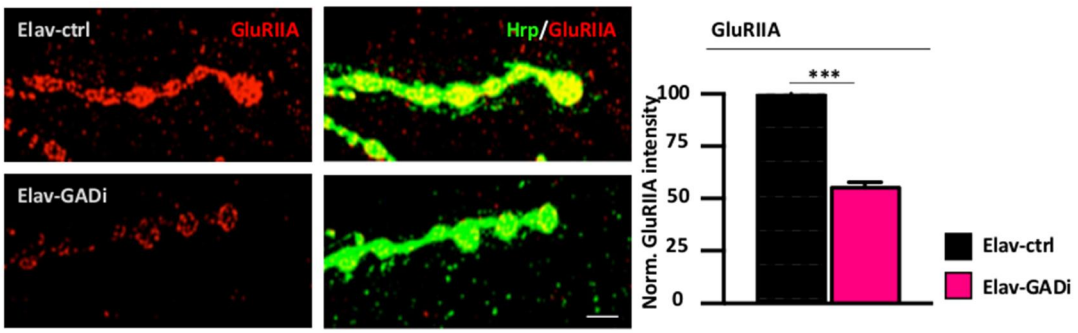

Fig. 33) Distribution of post-synaptic protein GluRIIA in the NMJ upon GAD1 silencing in neurons. GluRIIA was severely affected by GAD1 silencing in neurons (Elav-GADi) in comparison to the control (Elav-ctrl). On the left: confocal microscopy acquisition of the motoneuron laying on the muscles 6/7 of the second abdominal segment of third instar larvae. The nerve cell was stained with anti-HRP (green, merged to GluRIIA) and anti-GluRIIA (red). On the right: quantification of GluRIIA/Hrp intensity. Genotypes: Elav-ctrl (uasLACZ/Elav-GAL4), Elav-GADi (Elav-GAL4/+; uasGAD-RNAi). Quantification was done in GraphPad Prism 7.0, ***$p < 0.001$ calculated by T-Test. Error bars SEM. Scale bar: 5 µm. Number of examined synaptic boutons was per genotype <200.

7) The role of GAD1 in the glia

7.1) GAD1 reintroduction in the glia rescues TBPH null motility defects and the clustering of GluRIIA at the post-synaptic membranes

In the past we demonstrated that TBPH plays a strong role in glial homeostasis[145]. The silencing of TBPH in this tissue provoked strong motility problems and induced glial retractions, uncovering the neuronal terminals[145]. To investigate if GAD1 was involved in these processes, we reintroduced the enzyme in the glia using two glial drivers, Repo-GAL4 and Gliotactin-GAL4. We observed that GAD1 reintroduction in the glia rescued the locomotion impairments of TBPH null third instar larvae (Fig. 34) concluding that GAD1 had an important role in the glia.

We then examined the NMJ. First, we investigated if the wrapping of the glia was ameliorating. The driver we utilized was Repo-GAL4 recombined to GFP to constitutively express GFP in the glia, enabling us to individualize these tissues around the motoneurons. We measured the area that the glia was occupying but no significant improvement in the glial wrapping was noticed upon GAD1 reintroduction. We then analysed if motoneuron integrity was modified. We measured neuronal branching and the shape of the synaptic boutons but none of these structures were

ameliorating upon GAD1 reintroduction (Fig. 35). As both glial wrapping and motoneurons branching depend strictly on the organization of microtubules, we feel to suggest that nor the glial GAD1 (or the neuronal GAD1, as seen in previous experiments) could replace TBPH functions related to the morphology organization of these tissues. Finally, we measured the clustering of Bruchpilot, Syntaxin, Disc Large and GluRIIA. Similarly as before, we labelled these markers in the NMJ of TBPH null third instar larvae and measured their distribution. We noticed that GAD1 reintroduction was rescuing the clustering of the GluRIIA (Fig. 39) but not modified Disc Large (Fig. 38) and Syntaxin (Fig. 37). Bruchpilot was used as internal control (Fig. 36). Here, glial GAD1 was able to recover GluRIIA clustering, suggesting a strong role of this enzyme in both neurons and glia regarding the synaptic communication homeostasis at the post-synaptic terminals. As Disc Large was not recovering this time, we speculate that glial GAD1 is less specific to Disc Large in comparison to its neuronal counterpart, although more elucidation will be required in this matter. We concluded that GAD1 played an important role in the glia by controlling fly motility through the regulation of GluRIIA clustering at the post-synaptic membranes.

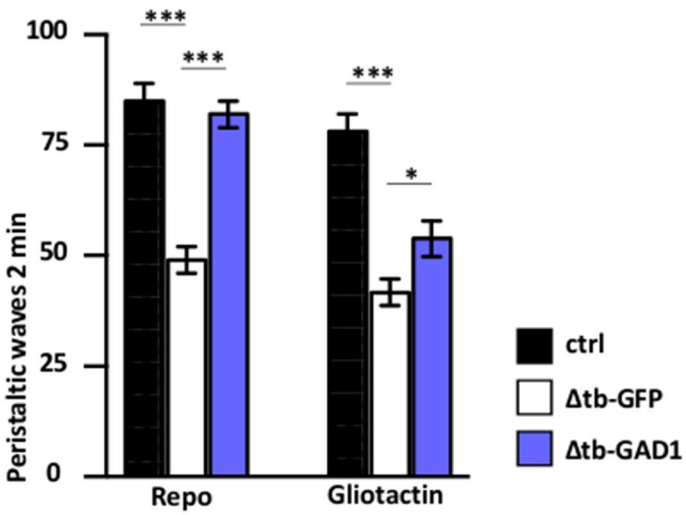

Fig. 34) GAD1 overexpression in the glia of TBPH null larvae. GAD1 reintroduction (Δtb-GAD1) in the glia by Repo-GAL4 and Gliotactin-GAL4 drivers have significantly recovered the motility defects of TBPH null third instar larvae compared to the negative control (Δtb-GFP). Performance was calculated as the number of peristaltic waves performed in 2 min by third instar larvae. Genotype: ctrl (on the left: $TBPH^{\Delta 23}$/+; Repo-GFP, uasGFP/+ and on the right: $TBPH^{\Delta 23}$, Gliotactin-GAL4/+; uasGFP/+), Δtb-GFP (on the left: $TBPH^{\Delta 23}/TBPH^{\Delta 23}$; Repo-GFP, uasGFP/+ and on the right: $TBPH^{\Delta 23}$, Gliotactin-GAL4/$TBPH^{\Delta 23}$; uasGFP/+), Δtb-GAD1 (on the left: $TBPH^{\Delta 23}/TBPH^{\Delta 23}$; Repo-GFP, uasGFP/uasGAD1 and on the right: $TBPH^{\Delta 23}$, Gliotactin-GAL4/$TBPH^{\Delta 23}$; uasGAD1/+). Quantification was done in GraphPad Prism 7.0, *$p < 0.05$, ***$p < 0.001$ calculated by one-way ANOVA. Error bars SEM. Total number of examined larvae per genotype was 25.

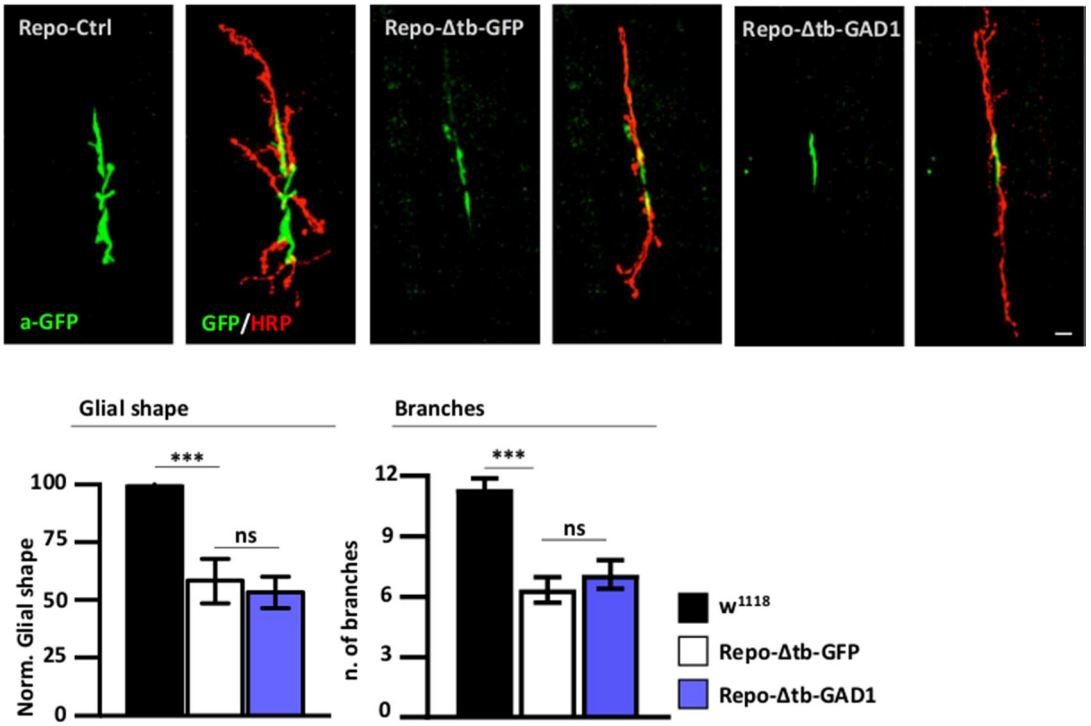

Fig. 35) Glial wrapping and motoneuron branching upon GAD1 overexpression in the glia of TBPH null larvae. Reintroduction of GAD1 in the glia (Repo-Δtb-GAD1) did not rescue glial wrapping and motoneuron branching in comparison to the negative control (Repo-Δtb-GFP). On the top: confocal microscopy acquisition of the motoneuron and supporting glia laying on the muscles 6/7 of the second abdominal segment of third instar larvae. The nerve cell was stained with anti-HRP (red) whereas the glia was labelled by a-GFP (green) that detects the constitutively expressing GFP under Repo driver. On the bottom: quantification of area covered by the glia over the motoneuron surface and quantification of the n. of branches of the motoneuron. Genotypes: Repo-ctrl ($TBPH^{\Delta 23}$/+; Repo-GFP, uasGFP/+), Repo-Δtb-GFP ($TBPH^{\Delta 23}$/$TBPH^{\Delta 23}$; Repo-GFP, uasGFP/+) and Repo-Δtb-GAD1 ($TBPH^{\Delta 23}$/$TBPH^{\Delta 23}$; Repo-GFP, uasGFP/uasGAD1). Quantification was done in GraphPad Prism 7.0, ns = ot significative, ***p < 0.001 calculated by one-way ANOVA. Error bars SEM. Scale bar: 10 µm. n>15 larvae per genotype.

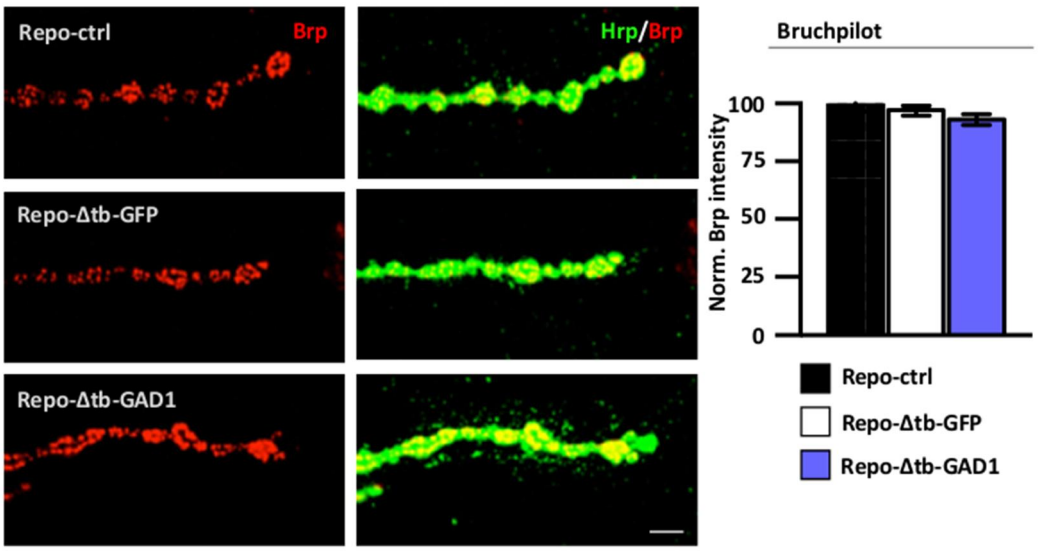

Fig. 36) Distribution of pre-synaptic protein Bruchpilot in the NMJ of TBPH null larvae upon GAD1 overexpression in the glia. Bruchpilot was used as internal control. Our quantification shows that Bruchpilot distribution did not change in the tested samples. On the left: confocal microscopy acquisition of the motoneuron laying on the muscles 6/7 of the second abdominal segment of third instar larvae. The nerve cell was stained with anti-HRP (green, merged to Brp) and anti-Brp (red). On the right: quantification of Brp/Hrp intensity. Genotypes: Repo-ctrl ($TBPH^{\Delta 23}$/+; Repo-GFP, uasGFP/+), Repo-Δtb-GFP ($TBPH^{\Delta 23}$/$TBPH^{\Delta 23}$; Repo-GFP, uasGFP/+) and Repo-Δtb-GAD1 ($TBPH^{\Delta 23}$/$TBPH^{\Delta 23}$; Repo-GFP, uasGFP/uasGAD1). Quantification was done in GraphPad Prism 7.0, ns = not significative (not shown) calculated by one-way ANOVA. Error bars SEM. Scale bar: 5 µm. n>200 synaptic boutons per genotype.

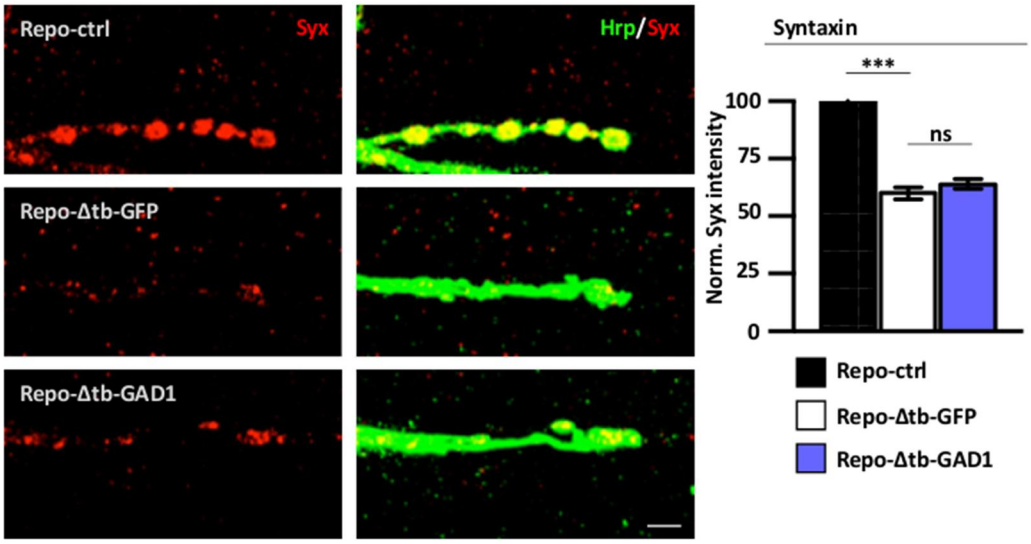

Fig. 37) Distribution of pre-synaptic protein Syntaxin in the NMJ of TBPH null larvae upon GAD1 overexpression in the glia. GAD1 reintroduction in the glia (Repo-Δtb-GAD1) did not rescue the distribution of neuronal Syntaxin in comparison to the negative control (Repo-Δtb-GFP). On the left: confocal microscopy acquisition of the motoneuron laying on the muscles 6/7 of the second abdominal segment of third instar larvae. The nerve cell was stained with anti-HRP (green, merged to Syx) and anti-Syx (red). On the right: quantification of Syx/Hrp intensity. Genotypes: Repo-ctrl ($TBPH^{\Delta 23}$/+; Repo-GFP, uasGFP/+), Repo-Δtb-GFP ($TBPH^{\Delta 23}$/$TBPH^{\Delta 23}$; Repo-GFP, uasGFP/+) and Repo-Δtb-GAD1 ($TBPH^{\Delta 23}$/$TBPH^{\Delta 23}$; Repo-GFP, uasGFP/uasGAD1). Quantification was done in GraphPad Prism 7.0, ns = not significative, ***$p < 0.001$ calculated by one-way ANOVA. Error bars SEM. Scale bar: 5 µm. n>200 synaptic boutons per genotype.

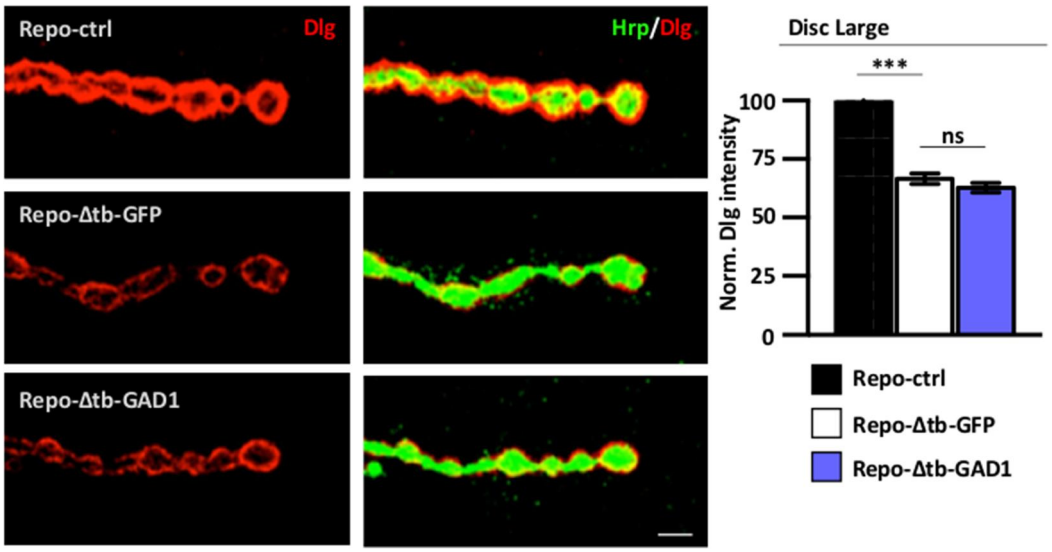

Fig. 38). Distribution of post-synaptic protein Disc Large in the NMJ of TBPH null larvae upon GAD1 overexpression in the glia. GAD1 reintroduction in the glia (Repo-Δtb-GAD1) did not rescue the distribution of neuronal Disc Large in comparison to the negative control (Repo-Δtb-GFP). On the left: confocal microscopy acquisition of the motoneuron laying on the muscles 6/7 of the second abdominal segment of third instar larvae. The nerve cell was stained with anti-HRP (green, merged to Dlg) and anti-Dlg (red). On the right: quantification of Dlg/Hrp intensity. Genotypes: Repo-ctrl ($TBPH^{\Delta 23}$/+; Repo-GFP, uasGFP/+), Repo-Δtb-GFP ($TBPH^{\Delta 23}$/$TBPH^{\Delta 23}$; Repo-GFP, uasGFP/+) and Repo-Δtb-GAD1 ($TBPH^{\Delta 23}$/$TBPH^{\Delta 23}$; Repo-GFP, uasGFP/uasGAD1). Quantification was done in GraphPad Prism 7.0, ns = not significative, ***$p < 0.001$ calculated by one-way ANOVA. Error bars SEM. Scale bar: 5 µm. n>200 synaptic boutons per genotype.

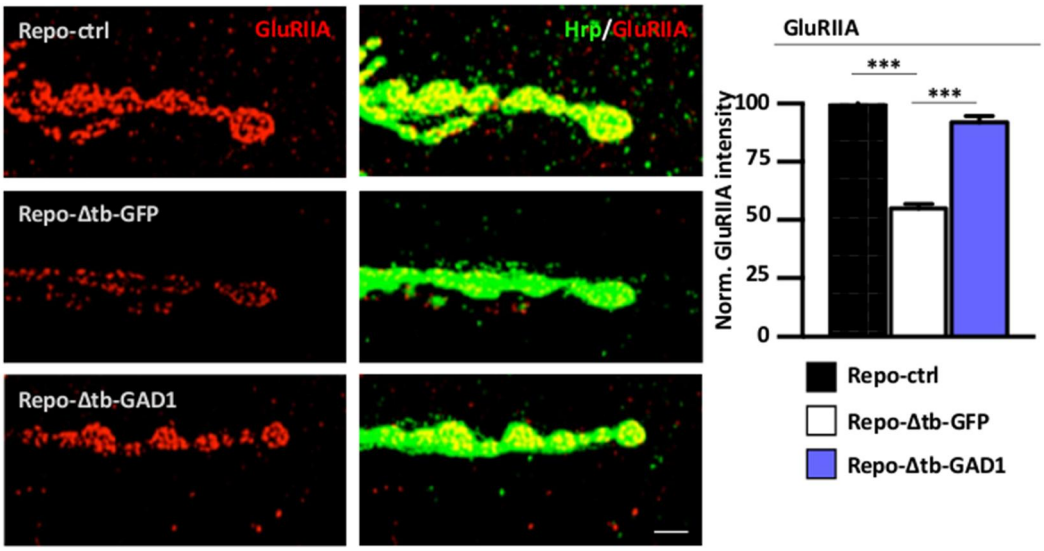

Fig. 39) Distribution of post-synaptic protein GluRIIA in the NMJ of TBPH null larvae upon GAD1 overexpression in the glia. GAD1 reintroduction in the glia (Repo-Δtb-GAD1) rescued (to wild type level) the distribution of neuronal GluRIIA in comparison to the negative control (Repo-Δtb-GFP). On the left: confocal microscopy acquisition of the motoneuron laying on the muscles 6/7 of the second abdominal segment of third instar larvae. The nerve cell was stained with anti-HRP (green, merged to GluRIIA) and anti-GluRIIA (red). On the right: quantification of GluRIIA/Hrp intensity. Genotypes: Repo-ctrl ($TBPH^{\Delta 23}$/+; Repo-GFP, uasGFP/+), Repo-Δtb-GFP ($TBPH^{\Delta 23}$/$TBPH^{\Delta 23}$; Repo-GFP, uasGFP/+) and Repo-Δtb-GAD1 ($TBPH^{\Delta 23}$/$TBPH^{\Delta 23}$; Repo-GFP, uasGFP/uasGAD1). Quantification was done in GraphPad Prism 7.0, ***$p < 0.001$ calculated by one-way ANOVA. Error bars SEM. Scale bar: 5 µm. n>200 synaptic boutons per genotype.

7.2) Glial GAD1 affects fly motility by regulating GluRIIA clustering at post-synaptic membrane

In the previous experiment, GAD1 reintroduction in the glia rescued TBPH null motility defects and GluRIIA clustering indicating that the presence of this enzyme was important in neurons as well as in the glia. To confirm that these effects were GAD1 specific, we silenced GAD1 in the glial tissue using Repo-GAL4 as a driver. We noticed strong locomotor deficits in third instar larvae (Fig. 40).

At the level of the NMJ, we noticed that motoneurons branching and synaptic bouton shape were not affected in third instar larvae (Fig. 41). This result was in agreement with our previous findings indicating that glial GAD1 did not promote morphological growth. Finally, we analysed the NMJ of third instar larvae for Bruchpilot, Syntaxin, Disc Large and GluRIIA distribution (Fig. 42-45). We noticed that GAD1 silencing in the glia strongly compromised GluRIIA clustering at the post-synaptic membranes. None of the other proteins were affected. These results suggested that GAD1 was specifically required in the glia to promote synaptic communication homeostasis by regulating GluRIIA distribution on the post-synaptic membranes.

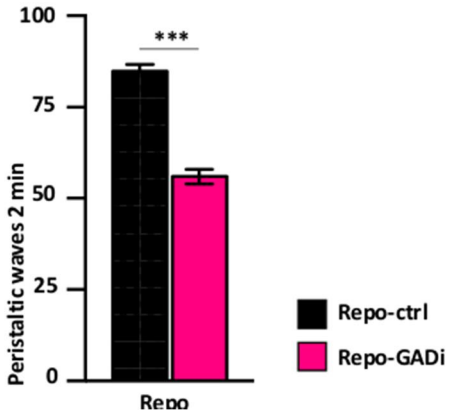

Fig. 40) Larval locomotion upon GAD1 silencing in glial tissue. GAD1 suppression with Repo-GAL4 driver (Repo-GADi) induced strong motility problems in comparison to the control (Repo-ctrl). The phenotype was calculated by measuring the number of peristaltic movements third instar larvae were able to perform in 2 min. Genotypes: Repo-ctrl (+/uasGFP; Repo-GAL4/+) and Repo-GADi (+/+; Repo-GAL4/uasGAD1 RNAi). Quantification was done in GraphPad Prism 7.0, ***$p < 0.001$ calculated by T-Test. Error bars SEM. n=20 larvae per genotype.

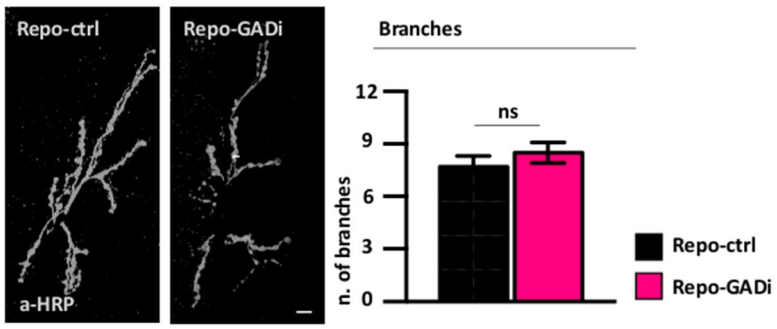

Fig. 41) Motoneuron branching upon GAD1 silencing in the glia. Silencing of GAD1 in the glia by Repo-GAL4 driver (Repo-GADi) did not affect the structural ramification of the motoneuron over the muscles. On the left: confocal microscopy acquisition of the motoneuron laying on the muscles 6/7 of the second abdominal segment of third instar larvae. On the right: quantification of synaptic branches ramification. The motoneuron was labelled anti-HRP. Genotypes: Repo-ctrl (+/uasGFP; Repo-GAL4/+) and Repo-GADi (+/+; Repo-GAL4/uasGAD1 RNAi). Quantification was done in GraphPad Prism 7.0, ns = not significative, calculated by T-Test. Error bars SEM. Scale bar: 10 µm. n=15 larvae per genotype.

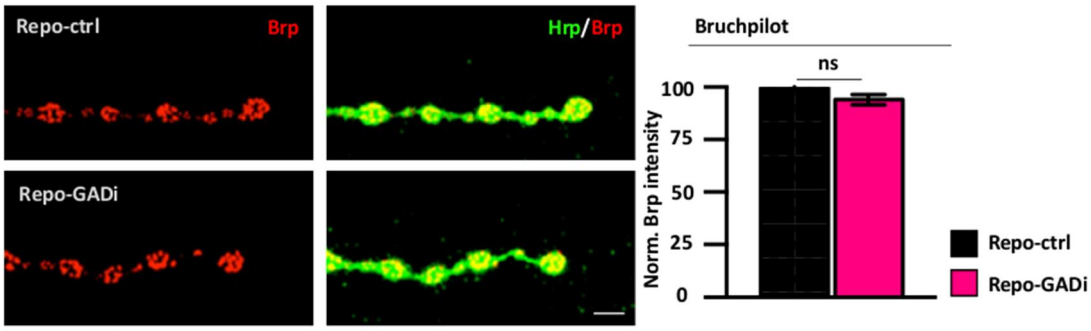

Fig. 42) Bruchpilot distribution in the NMJ upon GAD1 silencing in the glia. Bruchpilot was used as an internal control. Bruchpilot distribution did not change upon GAD1 silencing in the glia (Repo-GADi). On the left: confocal microscopy acquisition of the motoneuron laying on the muscles 6/7 of the second abdominal segment of third instar larvae. The nerve cell was stained with anti-HRP (green, merged to Brp) and anti-Brp (red). On the right: quantification of Brp/Hrp intensity. Genotypes: Repo-ctrl (+/uasGFP; Repo-GAL4/+) and Repo-GADi (+/+; Repo-GAL4/uasGAD1 RNAi). Quantification was done in GraphPad Prism 7.0, ns = not significative, calculated by T-Test. Error bars SEM. Scale bar: 5 µm. Number of examined synaptic boutons per genotype was <200.

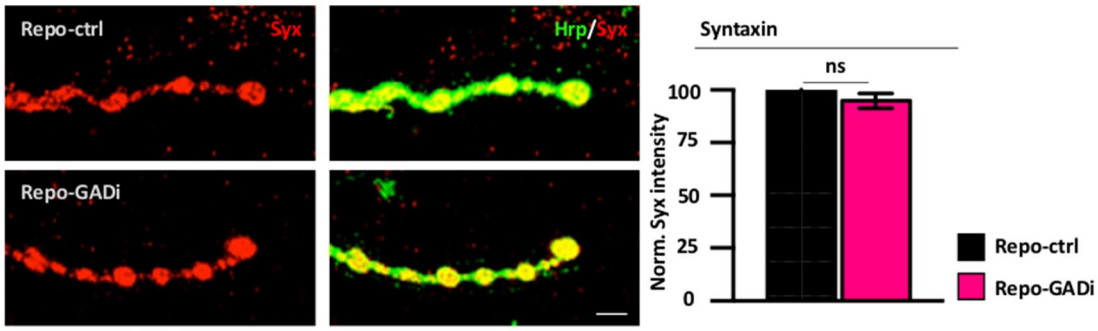

Fig. 43) Distribution of pre-synaptic protein Syntaxin in the NMJ upon GAD1 silencing in the glia. Syntaxin was downregulated in TBPH null flies. Glial GAD1 silencing (Repo-GADi) did not affect Syx distribution in the synapse. On the left: confocal microscopy acquisition of the motoneuron laying on the muscles 6/7 of the second abdominal segment of third instar larvae. The nerve cell was stained with anti-HRP (green, merged to Syx) and anti-Syx (red). On the right: quantification of Syx/Hrp intensity. Genotypes: Repo-ctrl (+/uasGFP; Repo-GAL4/+) and Repo-GADi (+/+; Repo-GAL4/uasGAD1 RNAi). Quantification was done in GraphPad Prism 7.0, ns = not significative, calculated by T-Test. Error bars SEM. Scale bar: 5 µm. Number of examined synaptic boutons per genotype was <200.

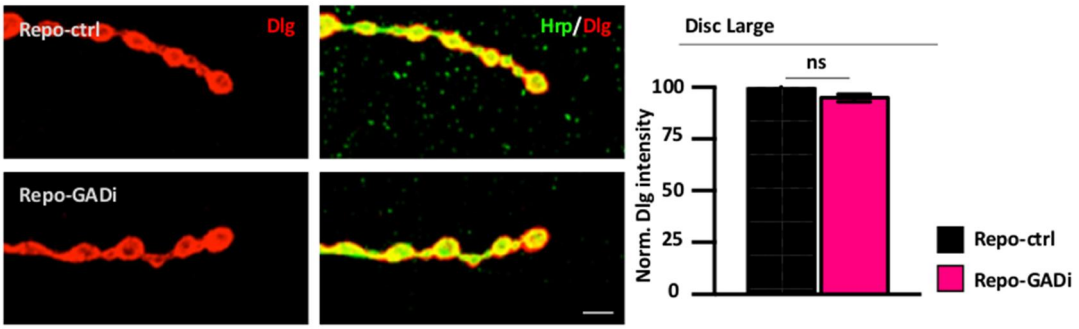

Fig. 44) Distribution of post-synaptic protein Disc Large in the NMJ upon GAD1 silencing in the glia. Glial GAD1 silencing (Repo-GADi) did not affect Disc Large distribution in the synapse. On the left: confocal microscopy acquisition of the motoneuron laying on the muscles 6/7 of the second abdominal segment of third instar larvae. The nerve cell was stained with anti-HRP (green, merged to Dlg) and anti-Dlg (red). On the right: quantification of Dlg/Hrp intensity. Genotypes: Repo-ctrl (+/uasGFP; Repo-GAL4/+) and Repo-GADi (+/+; Repo-GAL4/uasGAD1 RNAi). Quantification was done in GraphPad Prism 7.0, ns = not significative, calculated by T-Test. Error bars SEM. Scale bar: 5 µm. Number of examined synaptic boutons per genotype was <200.

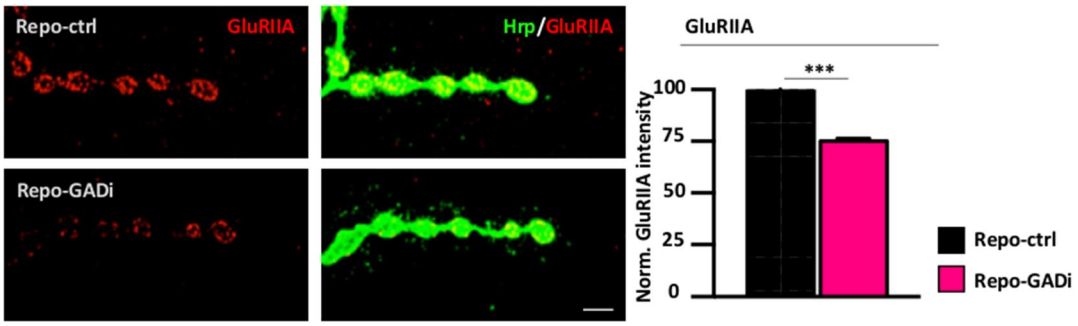

Fig. 45) Distribution of post-synaptic protein GluRIIA in the NMJ upon GAD1 silencing in the glia. Glial GAD1 silencing (Repo-GADi) affected GluRIIA distribution on the post-synaptic membrane in comparison to the control (Repo-ctrl). On the left: confocal microscopy acquisition of the motoneuron laying on the muscles 6/7 of the second abdominal segment of third instar larvae. The nerve cell was stained with anti-HRP (green, merged to GluRIIA) and anti-GluRIIA (red). On the right: quantification of GluRIIA/Hrp intensity. Genotypes: Repo-ctrl (+/uasGFP; Repo-GAL4/+) and Repo-GADi (+/+; Repo-GAL4/uasGAD1 RNAi). Quantification was done in GraphPad Prism 7.0, ***$p < 0.001$ calculated by T-Test. Error bars SEM. Scale bar: 5 µm. Number of examined synaptic boutons per genotype was <200.

8) Role of GAD1 in neurotransmitter balance and neurodegeneration

8.1) Glutamate concentration is high in the extracellular space of TBPH null flies

Our findings indicated that GAD1 was downregulated in TBPH null flies and this modification provoked serious motility problems that were caused by alterations in the clustering of the proteins Disc Large and GluRIIA in the post-synaptic membranes. We discovered that GAD1 influenced these proteins and GAD1 reintroduction in neurons or glia rescued Disc Large and GluRIIA distribution. Given that GAD1 cellular function is to convert Glutamate to GABA, as this enzyme was downregulated in TBPH mutants, we expected less enzymatic activity to convert one neurotransmitter into the other, with a consequent increase of Glutamate and decrease of GABA. Importantly, previous studies have shown that high Glutamate levels directly affect the sensitivity and distribution of the GluRIIA receptors causing excitotoxicity[138]. Therefore, to test the levels of Glutamate in TBPH mutant flies, we extracted the haemolymph of third instar larvae and performed a Liquid Chromatography followed by Mass Spectrometry (LC-MS) analysis. The results clearly indicated that there was an excess of Glutamate in TBPH

null flies in comparison to wild type (Fig. 46). Similar levels of Glutamate were observed when GAD1 was silenced in neurons (Elav-GADi). In addition, since our earlier experiments showed that GAD1 was required in both neurons and glia, we introduced for the first time a fly that allows the parallel overexpression of GAD1 in both tissues (Elav-Repo-Δtb-GAD1) and compared it to GFP expression alone (Elav-Repo-Δtb-GFP), in both cases in a TBPH null background. We observed that Elav-Repo-Δtb-GFP had similar Glutamate levels as TBPH null flies and that the parallel overexpression of GAD1 in neurons and glia was able to reduce Glutamate concentration to almost the wild type range. These results indicated that, due to the downregulation of GAD1 expression, TBPH null flies presented excessive levels of Glutamate in their extracellular space and suggested that the abundance of this neurotransmitter could cause excitotoxicity.

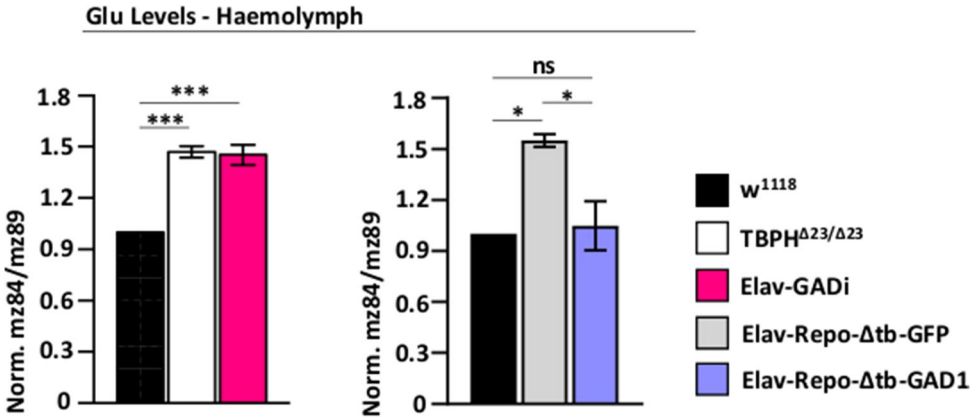

Fig. 46) Glutamate concentration in the haemolymph of TBPH null third instar larvae. We performed LC-MS to measure Glutamate concentration in the haemolymph of third instar larvae. Our results indicated excessive Glutamate levels in the haemolymph of TBPH null third instar larvae ($TBPH^{\Delta 23/\Delta 23}$). Similar levels were obtained by GAD1 silencing in neurons (Elav-GADi). Glutamate concentration went down in our TBPH null GAD1 rescue experiments (Elav-Repo-Δtb-GAD1) in comparison to the negative control (Elav-Repo-Δtb-GFP). Genotypes: w^{1118}, $TBPH^{\Delta 23/\Delta 23}$, Elav-GADi (Elav/+; +/uasGAD1 RNAi), Elav-Repo-Δtb-GFP (Elav-GAL4, $TBPH^{\Delta 23/\Delta 23}$; Repo-GAL4/uasGFP), Elav-Repo-Δtb-GAD1 (Elav-GAL4, $TBPH^{\Delta 23/\Delta 23}$; Repo-GAL4/uasGAD1). Quantification was done by measuring the ratio between the chosen fragment of the fragmentation spectra of Glutamic acid and isotopic labelled Glutamic acid. Quantification was done in GraphPad Prism 7.0, *$p < 0.05$, ***$p < 0.001$ calculated by one-way ANOVA. Error bars SEM. n=15-18 per genotype. Courtesy of Dr. Giulia Romano and Dr. Corrado Guarnaccia.

8.2) Treatment with GluRs inhibitors rescues motility problems in TBPH deficient flies

In the previous experiment, we have shown that TBPH null flies suffered from an excess of Glutamate in their haemolymph. It is believed that this condition might be detrimental due to the increased stimulation of the GluRs, provoking over-firing and neuronal death. To test this hypothesis, we fed TBPH null larvae with different concentration of Memantine, a very specific GluRs antagonist and Lithium Chloride (LiCl), a less specific antagonist of GluRs. The drug was diluted in water and mixed with regular fly food. TBPH null flies were fed with the drug from embryogenesis till late larval stage, when the locomotion assays were performed. We found that 50 µM of Memantine was sufficient to partially rescue the motility problems observed in TBPH null larvae (Fig. 47). Similar rescue was observed in TBPH null larvae treated with 5 mM of LiCl (Fig. 48). In addition, we observed that 50 µM of Memantine completely rescued the motility defects of TBPH-minus hypomorphic alleles generated after the silencing of the protein in neurons by RNAi (Fig. 49).

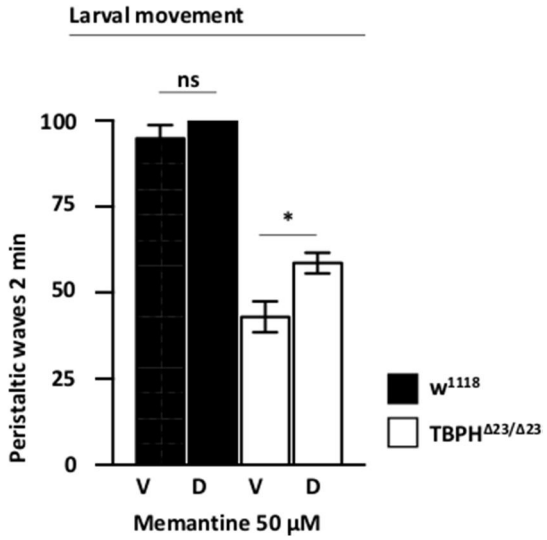

Fig. 47) Motility assays of TBPH null larvae after Memantine treatment. TBPH null third instar ($TBPH^{\Delta23/\Delta23}$) larvae fed with 50 µM of Memantine (D) ameliorated locomotion performance in comparison to untreated animals (V), measured by the number of peristaltic movements performed in 2 min. Genotypes: w^{1118}, $TBPH^{\Delta23}/^{\Delta23}$. V-vehicle, D-Drug. Quantification was done in GraphPad Prism 7.0, *p < 0.05, ***p < 0.001 calculated by one-way ANOVA. Error bars SEM. n=20 per genotype.

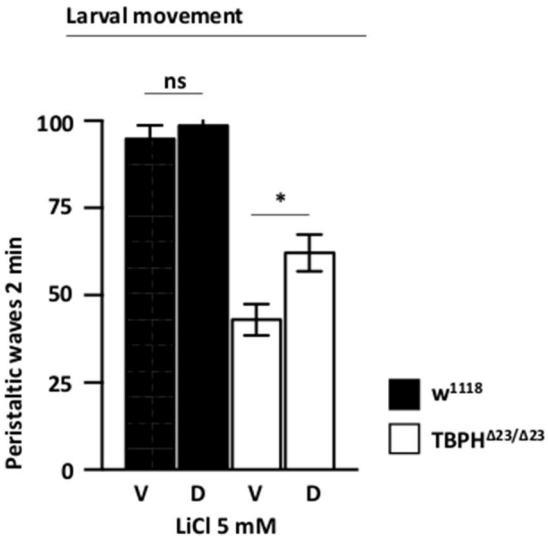

Fig. 48) Motility assays of TBPH null third instar larvae after LiCl treatment. TBPH null larvae ($TBPH^{\Delta23/\Delta23}$) fed with 5 mM of LiCl (D) ameliorated locomotion performance in comparison to untreated animals (V), measured by the number of peristaltic movements performed in 2

min. Genotypes: w^{1118}, $TBPH^{\Delta 23}/^{\Delta 23}$. V-vehicle, D-Drug. Quantification was done in GraphPad Prism 7.0, *p < 0.05, ***p < 0.001 calculated by one-way ANOVA. Error bars SEM. n=20 per genotype.

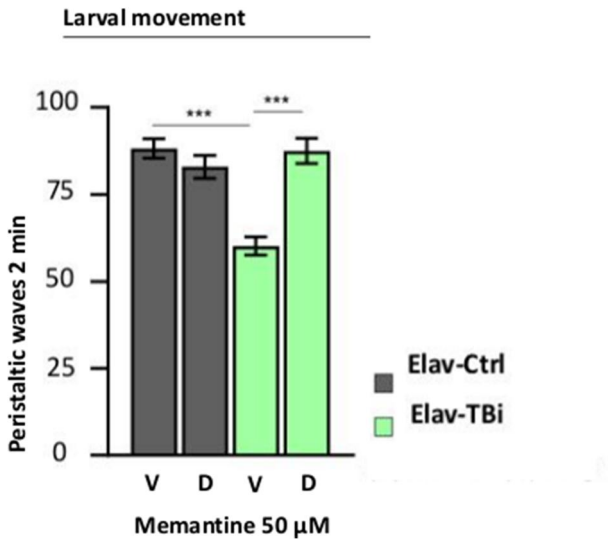

Fig. 49) Motility assay after Memantine treatment of larvae with reduced levels of TBPH expression in neurons. Third instar larvae expressing TBPH RNAi in neurons (Elav-TBi) and fed with 50 µM of Memantine (D) ameliorated locomotion performance in comparison to untreated animals (V), measured by the number of peristaltic movements performed in 2 min. Genotypes: Elav-Ctrl (Elav-GAL4/uasGFP), Elav-TBi (Elav-GAL4/uasTBPH RNAi). Quantification was done in GraphPad Prism 7.0, ***p < 0.001 calculated by one-way ANOVA. Error bars SEM. V-vehicle, D-Drug. n=20 per genotype

8.3) Treatment with Memantine rescues completely the GluRIIA clustering defects described in larvae with reduced levels of TBPH expression in neurons

We have discovered that the treatment with GluRs antagonist Memantine rescued the locomotion problems described in larvae with reduced levels of TBPH expression in neurons. We suggested that this rescue was due to the limitation in the binding excess of Glutamate to GluRs. Importantly, previous studies have shown that over-activation of GluRs was not only inducing excitotoxicity but, more interestingly, GluRIIA clustering downregulation[138]. Therefore, to test whether Memantine was able to revert this condition, we measured the levels of the GluRIIA in larvae with reduced levels of TBPH fed with Memantine 50 µM (Fig. 50). We found that Memantine was able to completely rescue the clustering of GluRIIA at NMJ of larvae with reduced expression of TBPH in neurons, suggesting that Glutamate-GluRs over-activation was leading to GluRIIA clustering alterations.

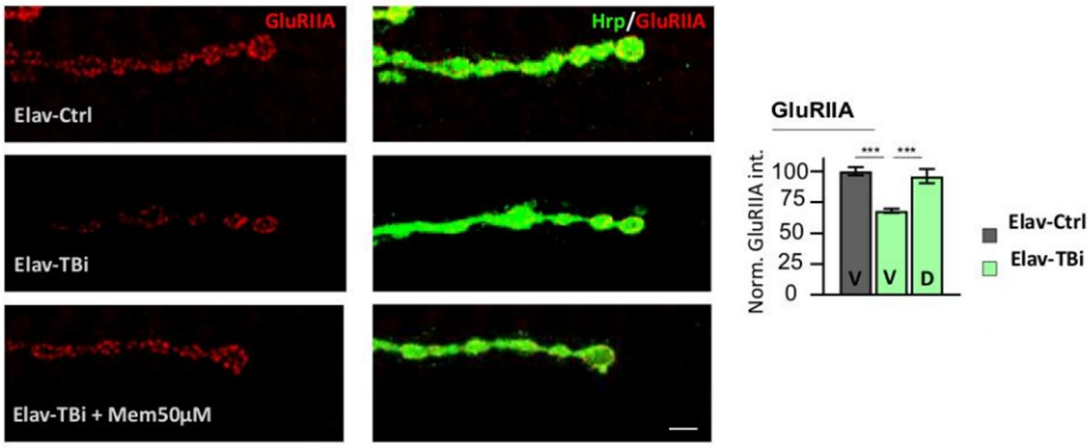

Fig. 50) GluRIIA clustering of larvae with TBPH deficiency in neurons after Memantine treatment. Distribution of post-synaptic protein GluRIIA ameliorated in the NMJ of larvae with reduced levels of TBPH expression in neurons (Elav-TBi) after 50 µM treatment with Memantine (D) in comparison to untreated animals (V). On the left: confocal microscopy acquisition of the motoneuron laying on the muscles 6/7 of the second abdominal segment of third instar larvae. The nerve cell was stained with anti-HRP (green, merged to GluRIIA) and anti-GluRIIA (red). On the right: quantification of GluRIIA/Hrp intensity. Genotypes: Elav-Ctrl (Elav-GAL4/uasGFP), Elav-TBi (Elav-GAL4/uasTBPH RNAi). V-vehicle, D-Drug. Quantification was done in GraphPad Prism 7.0, ***$p < 0.001$ calculated by one-way ANOVA. Error bars SEM. Scale Bar: 5 µm. n=20 per genotype

8.4) GABA is strongly downregulated in TBPH null larval brains

We demonstrated that TBPH null flies presented high levels of Glutamate and suggested that this alteration could be causing motility problems and neurodegeneration. However, the role of GABA, supposedly downregulated in TBPH mutant flies, was not specified. To test this

hypothesis, we stained with anti-GABA the NMJs and brains of TBPH null third instar larvae. GABA was barely detectable at Drosophila's NMJs (Fig. 51) indicating that the flies may not require GABA for NMJ transmission. Next, we measured the levels of GABA in the brains of TBPH null third instar larvae. Here, we analysed the whole brain intensity ratio between GABA and Elav, a nuclear protein of neurons shown to be unaffected in TBPH mutants (data not shown). We discovered that TBPH null larval brains presented a strong reduction in the levels of GABA in comparison to wild type flies (Fig. 52). This finding supported our hypothesis and indicated that GABA downregulation could play an important role in TBPH null phenotypes.

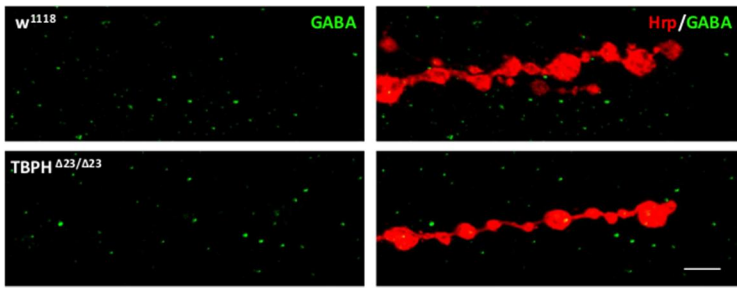

Fig. 51) GABA levels in Drosophila's NMJ of TBPH null larvae. GABA was barely detectable at the level of NMJs of both wild type and TBPH null larvae. Confocal microscopy acquisition of the motoneuron laying on the muscles 6/7 of the second abdominal segment of third instar larvae. The nerve cell was stained with anti-HRP (red) and anti-GABA (green). Genotypes: w^{1118}, $TBPH^{\Delta 23}/^{\Delta 23}$. Scale bar: 5 µm. Number of examined larvae per genotype was >20.

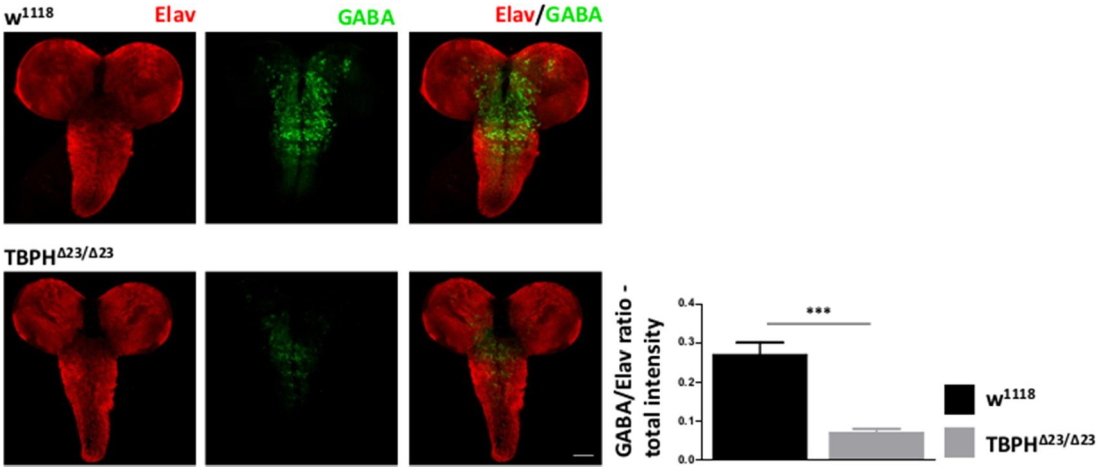

Fig. 52) GABA levels in Drosophila's brain of TBPH null third instar larvae. GABA was strongly downregulated in the brains of TBPH null larvae ($TBPH^{\Delta 23/\Delta 23}$) in comparison to wild type (w^{1118}). On the left: confocal microscopy acquisition of third instar larval brains stained for anti-GABA (green), anti-Elav (red) and merged (Elav/GABA). On the right: Quantification of whole brain intensity GABA/Elav ratio. Genotypes: w^{1118}, $TBPH^{\Delta 23}/^{\Delta 23}$. Quantification was done in GraphPad Prism 7.0, ns = not significative (not shown), ***$p < 0.001$ calculated by T-Test. Error bars SEM. Scale bar: 50 µm. Number of examined brains per genotype was >10.

8.5) Feeding of GABA does not rescue locomotion

To test whether GABA downregulation had any involvement in TBPH mutants locomotion impairments, we fed TBPH null third instar larvae with different concentration of GABA, ranging from 20 mM to 200 mM (data shown only for 40 mM). No recovery of the locomotion impairments was observed in the treated animals (Fig. 53). Although this result could indicate that GABA may not be involved in TBPH null locomotion phenotypes, its role cannot be completely excluded. It is

possible that our feeding methodology was not efficient enough to test this hypothesis and more sensitive methodologies are necessary to reach definitive conclusions.

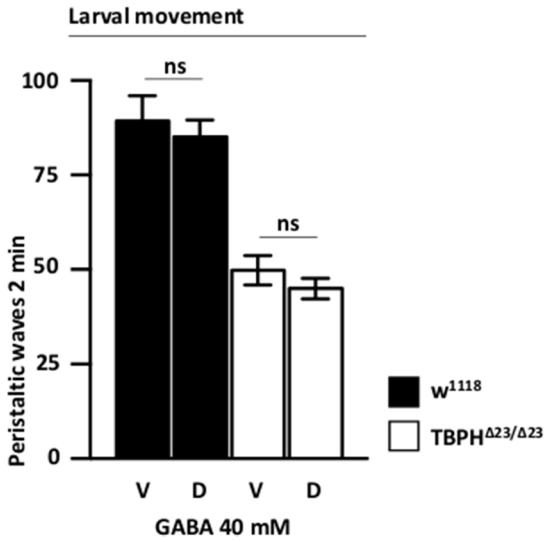

Fig. 53) Motility assays of TBPH null larvae after GABA treatment. TBPH null third instar larvae ($TBPH^{\Delta23/\Delta23}$) fed with 40 mM GABA (D) did not ameliorate in locomotion performance in comparison to untreated animals (V), measured by the number of peristaltic movements performed in 2 min. Genotypes: w^{1118}, $TBPH^{\Delta23}/^{\Delta23}$. V-vehicle, D-Drug. Quantification was done in GraphPad Prism 7.0, ns = not significative, calculated by one-way ANOVA. Error bars SEM. n=20 per genotype.

9) GAD1 defects in humans and ALS patients

9.1) TDP43-GAD1 relationships are conserved in humans

The downregulation of GAD1 in TBPH null flies was a crucial event responsible for the synaptic alterations described in ALS fly models. To test if these regulatory defects were conserved through the evolution, we silenced TDP-43 in human neuroblastoma SK-N-BE cells and observed a strong downregulation of GAD67 (Fig. 54), the GAD1 homolog protein in humans, suggesting that these mechanisms were conserved in human tissues.

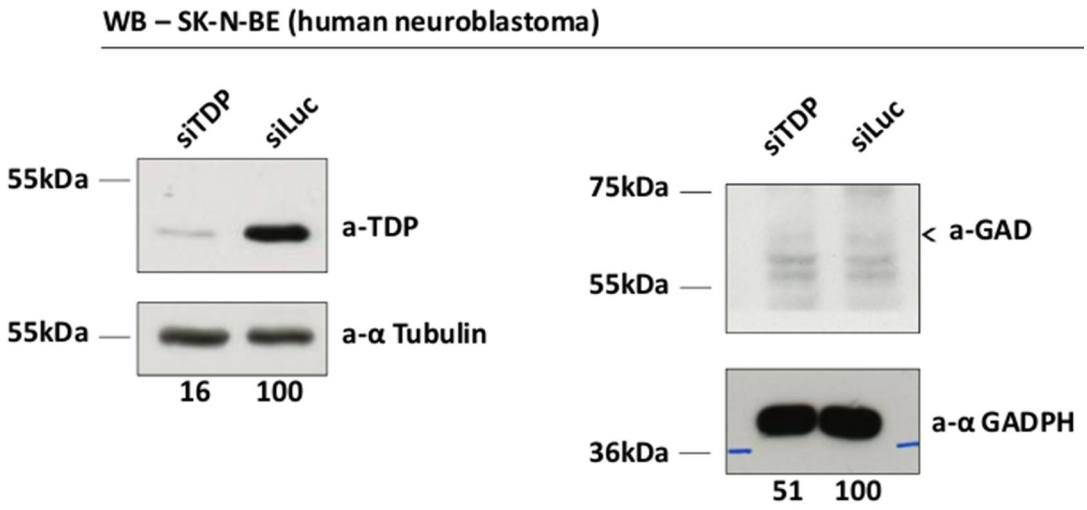

Fig. 54) GAD67 expression values upon silencing of TDP-43 in human neuroblastoma cells. TDP-43 suppression induced GAD67 downregulation at protein level, measured by western blot analysis. Cells were transfected with TDP43 RNAi, lysed and prepared for western blot analysis (explained in detail in the Material and Methods section). Samples were run on polyacrylamide gels, transferred on nitrocellulose membranes and labelled with the appropriate primary antibodies. On the left: the membrane was labelled anti-TDP and anti-

Tubulin. On the right: membrane was labelled anti-GAD67 and anti-GADPH. Beneath are the intensity quantification of Tubulin/TDP and GAPDH/GAD done in ImageJ. Courtesy of Dr. Raffaella Klima.

9.2) GAD1 defects in ALS patients

In the previous experiment, we have shown that TDP43-GAD1 relationship was conserved through evolution suggesting that ALS patients could harbour similar defects in the regulation of the protein levels of GAD1. To test this hypothesis, we took advantage of iPSC lines reprogrammed from primary fibroblasts derived from ALS-patients carrying mutations in TDP-43 (patient #1 was carrying the mutation G287S, patient #2: G294V and patient #3: G378S)[146]. These cell lines were compared with lines derived from unaffected individuals (control #1 and control #2) in western blot analysis using anti-GAD67. We noticed that the protein levels of GAD67 were strongly reduced in all three ALS samples in comparison to controls (Fig. 55). Furthermore, we found that iPSC derived motoneurons (MNs) from patient #3 and control #1 (differentiated in MNs following the protocol described in [147]) showed similar defects in GAD67 expression at the protein and mRNA levels (Fig.

56 and 57) indicating that GAD1 misregulation was present in ALS patients and suggesting this enzyme could play an important role in ALS.

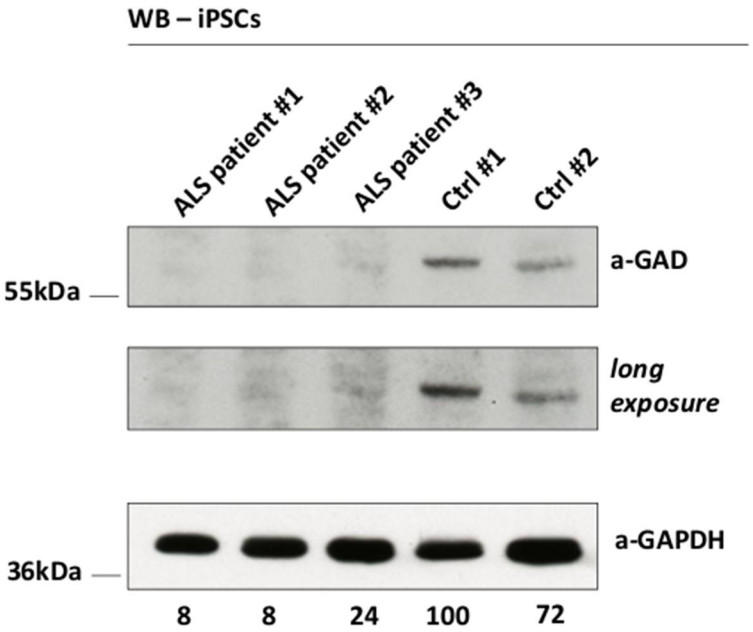

Fig. 55) GAD67 protein expression in iPSC derived from ALS patients. GAD67 expression was downregulated in ALS patients in comparison to control # 1 and #2, measured by western blot analysis. iPSC were lysed and prepared for western blot analysis. Samples were run on polyacrylamide gel, transferred on nitrocellulose membrane and labelled with anti-GAD67 and anti-GADPH. Beneath are the intensity quantification GAPDH/GAD done in ImageJ. Courtesy of Dr. Raffaella Klima.

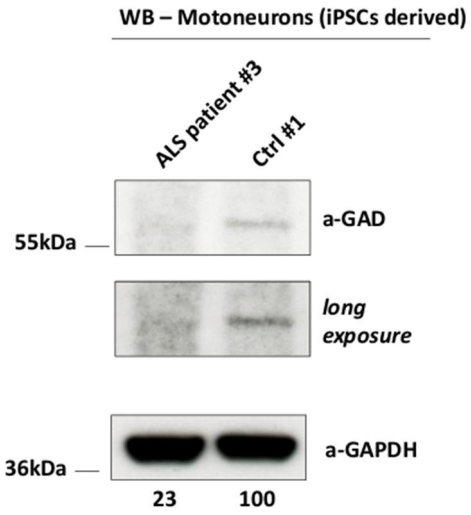

Fig. 56) GAD67 protein expression in motoneurons derived from iPSC of ALS patient #3 in comparison to control #1. GAD67 protein was downregulated in motoneurons of ALS patients as measured by western blot analysis. iPSC were lysed and prepared for western blot (as explained in the Material and Methods section). Samples were run on polyacrylamide gel, transferred on nitrocellulose membrane and labelled with anti-GAD67 and anti-GADPH. Beneath are the intensity quantification GAPDH/GAD done in ImageJ. Courtesy of Dr. Raffaella Klima.

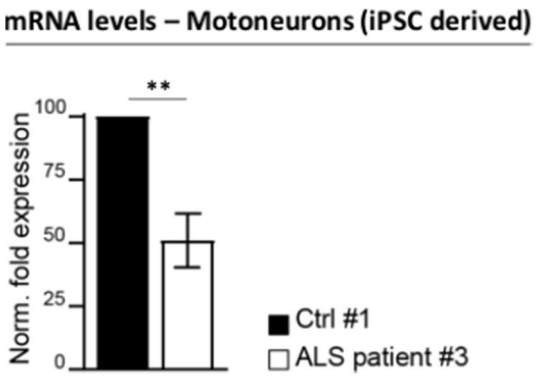

Fig. 57) Expression of GAD67 mRNA in motoneurons derived from iPSC of ALS patient #3 in comparison to control #1. GAD67 mRNA was downregulated in motoneurons of ALS patients as measured by RT-PCR. Samples were prepared for RT-PCR analysis as explained in the Material and Methods section. Courtesy of Dr. Raffaella Klima.

DISCUSSION

10) TDP-43 influences GAD expression

Thanks to wide genome proteomic analysis we found that GAD1, the enzyme that converts Glutamate to GABA, was translationally downregulated in flies lacking TBPH protein expression. These findings were later confirmed by western blot and RT-PCR, indicating that GAD1 was both transcriptionally and translationally downregulated in TBPH null flies. As TBPH is a RNA binding protein, we suspected that TBPH was directly binding and regulating GAD1 mRNA. Thus, we performed immunoprecipitation studies (data not shown) but we did not see any binding interaction between the two molecules. As these experiments were done on the mature form of GAD1 mRNA, these results indicated that TBPH did not promote GAD1 mRNA transport or stability but left unanswered question about the steps that preceded, the transcription and processing of GAD1 pre-mRNA. Interestingly, our preliminary data (not shown) indicated that TBPH affects the stability of GAD1 pre-mRNA. However, we still do not know whether this regulation is performed at the pre-mRNA processing level (which is very likely given that TBPH is primarily a splicing factor) or if it is instead achieved by the assembly of the transcriptional machinery on the GAD1 promoter region, thus promoting the transcription of GAD1 gene.

11) GAD1 is required in both neurons and glia to maintain synaptic stability

We have previously observed that several synaptic proteins, including the pre-synaptic protein Syntaxin and the post-synaptic proteins Disc Large and GluRIIA, were translationally downregulated and did not clusterize properly at synaptic terminals in TBPH null flies[143]. As GAD1 was previously shown to regulate the clustering of the GluRIIA[138], we reintroduced GAD1 gene by the UAS-GAL4 expression system, in both the neurons and the glia of TBPH null flies. We observed that GAD1 was required in both tissues to maintain the proper clustering of the GluRIIA. In addition, neuronal GAD1 was also promoting the clustering of Disc Large, the GluRIIA associated protein. For what concerned the metabolism of pre-synaptic proteins, we observed that in our rescue experiments the neuronal GAD1 was able to induce a weak recovery of Syntaxin. However, subsequent experiments did not confirm that the effect on Syntaxin was GAD1 specific. In addition, GAD1 was not able to rescue the morphology of pre-synaptic terminals, which was not surprising given that TBPH was shown to promote microtubule organization by directly regulating Futsch, the microtubule associated protein[61], and many other proteins related to synapse structure and

function. To note, however, that the measurements related to the neuronal growth, the count of the number of branches and regular synaptic boutons in particular, were done manually and are appropriate only to detect gross changes in synaptic morphology: these measurements are way too simplistic and arbitrary to observe any subtle changes. The development of software able to count automatically these parameters would be of great help in the future. In absence of more sophisticated methods, our results indicated, all together, that although GAD1 could partially rescue the synaptic communication deficits in TBPH null flies, it was unable to compensate for the regulatory events TBPH is responsible for, especially the ones related to neuronal growth.

12) GAD1 downregulation causes elevate levels of Glutamate and reduced levels of GABA

Although we demonstrated that GAD1 promotes GluRIIA and Disc Large clustering, we could not explain the nature of this regulation. Many years back, Featherstone et al[136, 138], suggested that high levels of Glutamate promoted the downregulation of GluRs field on post-syanptic membranes, a phenomenon associated with excitotoxicity prevention. Obviously, the downregulation of GAD1 would suggest such scenario.

Thus, we have found by LC-MS that the haemolymph of TBPH null larvae presented high levels of Glutamate. In addition, we observed that GAD1 silencing in neurons could induce Glutamate levels that were equally high as those seen in TBPH mutants, indicating that this effect was GAD1 specific. Finally, the simultaneous overexpression of GAD1 in both the neurons and glia in TBPH null larvae recovered Glutamate levels to wild type. However, it remains to be understood whether the silencing of GAD1 specifically in the glia would induce similar raises in Glutamate. As the glia is associated with Glutamate re-uptake from the synaptic cleft, glial GAD1 must have a fundamental role in excitotoxicity prevention. In contrast, the neuronal GAD (at least in humans) is primarily associated with the outer membranes of synaptic vesicles where it serves to convert Glutamate and pump GABA in. Interestingly though, as crucial proteins, such as Syntaxin, that relate to vesicle exocytosis are downregulated in TBPH mutants, Glutamate release in the synaptic cleft must be mediated by mechanisms that are not dependent of vesicular release. Indeed, Featherstone[138] found that GluR field depended strictly on non-vesicular release of Glutamate. In this direction, we have seen that Memantine and LiCl, two widely recognized GluRs antagonists, ameliorated the locomotion phenotypes and rescued GluRIIA clustering in TBPH

deficiency larvae indicating that Glutamate-GluRs overstimulation leaded to synaptic instability. Regarding to that, it would be interesting to understand the effects that the binding excesses have on muscles and if this effects can, in some retroactive way, affect pre-synaptic homeostasis. Also, the increased binding of Glutamate to the pre-synaptic GluRs should be experimented.

Not surprisingly, we have found that GABA levels were compromised in TBPH null larval brains. The fruit fly seemed not to use GABA for NMJ transmission, so we could conclude that NMJ synaptic instability in TBPH null flies were primarily caused by Glutamate excess. However, as GABA is present at large concentrations in certain brain regions, where it acts as an inhibitory molecule for neuronal circuits, GABA downregulation could still play a fundamental role in TBPH null phenotype. We tried, unsuccessfully, to rescue TBPH null larvae by feeding them with different concentration of GABA. Nevertheless, we couldn't be sure that GABA was able to get to the right regions of the brain after these treatments. More sensitive methodologies for GABA administration would allow definitive conclusions.

13) The TDP43-GAD1 relationship is conserved in humans and ALS patients may suffer from GAD67 downregulation

GAD65 and GAD67, the human orthologs of GAD1, were previously found misregulated in AD, Parkinson and Huntington's disease. In ALS, however, different observations were made regarding the role of this enzyme and its enzymatic products in relation to neurodegenerative processes. As we have demonstrated a strong link between Glutamate metabolism and TBPH in fruit flies, we questioned whether this relationship was conserved in humans. Thus, we silenced TDP-43 by RNAi in human neuroblastoma cells and observed a consequent downregulation of GAD67. More strikingly, we obtained iPSC derived from fibroblast of ALS patients harbouring mutations inside TDP-43 protein and observed that these individuals were suffering from GAD67 downregulation at both the protein and mRNA level. These findings were of crucial significance because they coupled, for the first time, two pathological mechanism, TDP-43 proteinopathy and Glutamate excitotoxicity, widely recognized in ALS disease and opened the path to the development of pharmaceutical compounds against a previously unexplored molecular target (GAD67). In this sense, the development of "drugs" able to stimulate GAD67 enzymatic activity would mimic the

effects seen in our genetic rescue experiments preventing excitoxicity and promoting synaptic stabilization.

14) Future plans

The lack of an appropriate antibody for GAD1 protein detection renders that study of the function and regulation of this gene troublesome. Our previous biochemical studies were done on $GAD1^{MIMIC}$, that is the endogenous gene that has the mimic cassette (EGFP-FlAsH-StrepII-TEV-3xFlag-tag) inserted in the middle of the coding sequence of the protein. However, this methodology has some drawbacks: first, we believe that the position of the insert disturbs the proper folding, thus regulation and function of the protein. In this sense, we performed immunohistochemistry using an anti-EGFP to study the localization of the protein and whether it changed in TBPH null flies and noticed that GAD1 was not co-localizing with GABA expressing cells in the brain (data not shown), which was strange given the function of this protein. In addition, as the enzyme must dimerize to be activated, the mutated form of the protein might also disturb the functional, non-mutated, copy. Moreover, as the enzyme is downregulated in TBPH null flies, it was unfavourable to perform additional studies in this genetic background.

In this respect, we decided to clone a gene that would harbour tags on both the N-terminal and C-terminal of the protein and be under UAS control. This construct could help us understand more about GAD1 metabolism. We will study GAD1 protein stability, localization and interactome. For instance, despite its very likely that TBPH regulates GAD1 pre-mRNA, GAD1 protein downregulation could initially be triggered by other cellular or environmental factors and, as this would result in Glutamate excitoxicity and stress, it could be the first trigger to TBPH downregulation, eventually leading to further problems in GAD1 expression in a feedback mechanism. Secondary, this construct could allow us to find ways (either drugs or induced post-translational changes) that would boost the natural function of the GAD1 enzyme, as this would mimic our rescue experiments. However, since the cloned gene would be under UAS control, we will not be able to determine which cells naturally express the protein and to what extent. For this purpose, it will be required to insert a tag at the end of the endogenous gene. This can be done, nowadays, with Crispr/CAS9 technology. Otherwise an antibody that detects the endogenous protein can be made, but this approach can be more costly and troublesome.

Concluding remarks

ALS is a devastating disease of the motor system. Poor diagnosis and treatment are consequent to the little understanding of the pathogenesis. For a long time, Glutamate metabolism disorders have been linked to disease onset and progression. Glutamate levels are high in ALS patients, which is believed to cause excitotoxicity. Another important contributor to ALS is TDP-43, a nuclear and RNA binding protein that is found cytosolically aggregated and post-translationally modified in the great majority of the patients.

In this PhD thesis we have demonstrated a link between TDP-43 and Glutamate metabolism. Thanks to wide screen proteomic analysis, we found that TBPH null flies had downregulated levels of GAD1. This in turn caused an excess of Glutamate and lack of GABA, promoting excitotoxicity, downregulation of GluRs and the GluR-associated proteins. Importantly, we observed that TDP43-GAD1 relationship was conserved in humans and that ALS patients carrying mutations in TDP-43 presented defects in GAD67 gene expression.

MATERIAL AND METHODS

Fly strains

The following genotypes were used:

w[1118], w[1118];TBPH$^{\Delta 23}$/CyO-GFP, w[1118];TBPH$^{\Delta 142}$/CyO-GFP, w[1118];Elav-GAL4/CyO-GFP, w[1118];D42-GAL4/D42-GAL4, w[1118];Repo-GAL4/TM3Sb, w[1118];Gliotactin-GAL4/CyO-GFP, w[1118];GMR-GAL4/GMR-GAL4, w[1118];UAS-GFP(mCD8), w[1118];UAS-TBPH/UAS-TBPH, w[1118];Mi[MIC]GAD1^{MI09277}/TM3Sb, UAS-GAD1/TM3Sb, UAS-GAD1 RNAi (#28079)/Tm3Sb, UAS-TBPH RNAi (#ID38377, VDRC), UAS-LacZ/CyO.

Fly genotypes used in figures

Fig. 18-19, 21)

- w^{1118}
- TBPH$^{\Delta 23/\Delta 23}$
- TBPH$^{\Delta 142/\ \Delta 142}$

Fig. 20)

- w^{1118}
- TBPH$^{+/+}$; GAD1^{MIMIC}/GAD1
- TBPH$^{\Delta 23/\Delta 23}$; GAD1^{MIMIC}/GAD1

Fig. 22)

- w^{1118}
- Elav-GAL4, TBPH$^{\Delta 23/\Delta 23}$; uasGFP/+
- Elav-GAL4, TBPH$^{\Delta 23/\Delta 23}$; uasGAD1/+
- Elav-GAL4, TBPH$^{\Delta 23/\Delta 23}$; uasTBPH/+

- w^{1118}
- $TBPH^{\Delta 23/\Delta 23}$; uasGFP/D42-GAL4
- $TBPH^{\Delta 23/\Delta 23}$; uasGAD1/D42-GAL4
- $TBPH^{\Delta 23/\Delta 23}$; uasTBPH/D42-GAL4

Fig. 23-27)

- w^{1118}
- Elav-GAL4, $TBPH^{\Delta 23/\Delta 23}$; uasGFP/+
- Elav-GAL4, $TBPH^{\Delta 23/\Delta 23}$; uasGAD1/+

Fig. 28)

- uasLACZ/Elav-GAL4
- Elav-GAL4/+; uasGAD1-RNAi
- uasLACZ/+; +/D42-GAL4
- D42-GAL4/uasGAD1-RNAi

Fig. 29-33)

- uasLACZ/Elav-GAL4
- Elav-GAL4/+; uasGAD1-RNAi

Fig. 34)

- $TBPH^{\Delta 23}$/+; Repo-GFP, uasGFP/+
- $TBPH^{\Delta 23}/TBPH^{\Delta 23}$; Repo-GFP, uasGFP/+
- $TBPH^{\Delta 23}/TBPH^{\Delta 23}$; Repo-GFP, uasGFP/uasGAD1
- $TBPH^{\Delta 23}$, Gliotactin-GAL4/+; uasGFP/+
- $TBPH^{\Delta 23}$, Gliotactin-GAL4/$TBPH^{\Delta 23}$; uasGFP/+
- $TBPH^{\Delta 23}$, Gliotactin-GAL4/$TBPH^{\Delta 23}$; uasGAD1/+

Fig. 35-39)

- $TBPH^{\Delta 23}$/+; Repo-GFP, uasGFP/+
- $TBPH^{\Delta 23}/TBPH^{\Delta 23}$; Repo-GFP, uasGFP/+
- $TBPH^{\Delta 23}/TBPH^{\Delta 23}$; Repo-GFP, uasGFP/uasGAD1

Fig. 40-45)

- +/uasGFP; Repo-GAL4/+
- +/+; Repo-GAL4/uasGAD1 RNAi

Fig. 46)

- w^{1118}
- $TBPH^{\Delta 23/\Delta 23}$
- Elav-GAL4/+; uasGAD1-RNAi
- Elav-GAL4, $TBPH^{\Delta 23/\Delta 23}$; Repo-GAL4/uasGFP
- Elav-GAL4, $TBPH^{\Delta 23/\Delta 23}$; Repo-GAL4/uasGAD1

Fig. 47-48)

- w^{1118} + Vehicle
- w^{1118} + Drug
- $TBPH^{\Delta 23/\Delta 23}$ + Vehicle
- $TBPH^{\Delta 23/\Delta 23}$ + Drug

Fig. 49-50)

- Elav-GAL4/uasGFP + Vehicle
- Elav-GAL4/uasTBPH RNAi + Vehicle
- Elav-GAL4/uasTBPH RNAi + Drug

Fig. 51-53)

- w^{1118}
- $TBPH^{\Delta 23/\Delta 23}$

Protein separation by two-dimensional gel (IEF/SDS PAGE) and analysis by mass spectrometry

Three independent protein extracts from fly heads were prepared for the two TBPH null mutants and the wild type strain. After Bradford quantification equal protein amounts were precipitated by TCA, and further solubilized in iso-electro-focusing (IEF) rehydration solution with 0.6% IPG buffer pH 3-11 NL (from GE Healthcare Bio-sciences AB). The

extracts were then subjected to isoelectrofocusing with nonlinear immobilized pH-gradient strips (pH3-11 NL), 13 cm in lenght. The isoelectrofocusing was programmed at: 4 h at 50V, 1 h at 500V, 2 h at 1000V up to h x 48000V. After equilibration of the focused strips in 6 M urea, 30% glycerol, 50 mM Tris-HCL (pH 8.8), 2% SDS, 62.5 mg iodoacetamide and bromophenol blue, strips were subjected to electrophoretic separation on a 14% SDS polyacrylamide gels (of the following dimensions: 18 x 20 x 0.15 cm) run overnight at 12 mA. After run, gels were fixed (1hr 10%(v/v) ethanol-7% (v/v) acetic acid) and stained with 0.12% Colloidal G-250 Coomassie Blue before acquisition of spot intensity (300 dpi-linear response conditions) with an Epson Expression 1680 Pro Scanner. pI values were calculated according to the pH curve of the pH gradient strips that the supplier provided (GE life Sciences), whereas molecular masses of proteins were determined according to semi-logarithmic curves of $\log_{10}$ molecular mass versus migration distance. Image acquisition was done for all nine gels (analysis done in triplicate for any strain) and analysed with Redfin 3 program (Ludesi AB, Lund, Sweden) that includes all to all spot matching and normalization according to total protein content. If the difference of the mean spot intensity was greater than 1.5-fold between the groups ($p <$

0.05), the protein was considered differentially expressed and were excised from gel and sent to mass spectrometry analysis performed by Proteome Factory AG in Germany for nano LC-ESI-MS/MS analysis.

Western blot analysis

Third instar larval brains, or S2 cells, were lysed in lysis buffer (10mM Tris, 150 mM NaCl, 5 mM EDTA, 5 mM EGTA, 10% Glycerol, 50 mM NaF, 5 mM DTT, 4 M Urea, pH 7.4, protease inhibitors (Roche, #11836170001)) and after protein quantification of lysates by Qubit (Q#33211, Invitrogen), samples were separated on 10% SDS-PAGE and transfer to 0,22um nitrocellulose membranes (#NBA083C Whatman Protran). Membrane were blocked in 5% non-fat dry milk in Tris Buffered Saline + 0.1 % Tween 20 (TBS-T).

SK-N-BE and iPSC were resuspended in ice cold PBS + Protease Inhibitors, followed by sonification (Biorupture, Diagenode).

Primary antibodies were used with the following concentration: anti-Flag M5 (1:10000, Sigma F4042), anti-cMyc (1:3000, Santa Cruz 9E10), anti-HA (1:6000, Cell Signalling, 6E2), anti-tubulin DM1A (1:4000, Calbiochem #CP06), anti-GADPH (1:2000, Santa Cruz 47724 SC), anti-GAD1 (#5305

Cell Signaling 1:2,000). Secondary antibodies concentration: anti-rabbit HRP conjugated (1:10000, Pierce #32460), anti-mouse HRP conjugated (1:10000, Pierce # 32430). For detection, SuperSignal West Femto Maximum Sensitivity Substrate Kit (Pierce, #PR34095) was used. Quantification was performed by ImageJ after acquisition of the autoradiographic films with an Epson Expression 1680 Pro Scanner.

RT-PCR

RNA of third instar larval brains and of IPS derived motoneurons were extracted with RNeasy Microarray MiniKit (Qiagen, #73304) plus QIAshredder (Qiagen, #79654), and after DNase treatment (Promega, #M6101) were retro-transcribed with oligo-dT and SuperScript III First-Strand Synthesis (TermoFischer, #18080051). Primers were specifically designed for the Gad1 gene of drosophila and human origin, while as housekeeping we select a set of primers for RpL11 and GAPDH for drosophila and human respectively:

GAD1: 5'GAATTCAGAGCATAGAAGCCACCG3' and

5'CAACTGGCTCTTCATCTTCTCCTG3'

Rpl11: 5'CCATCGGTATCTATGGTCTGGA3' and 5'CATCGTATTTCTGCTGGAACCA3'

Gapdh: 5'CTGGGCTACACTGAGCACC3' and 5'AAGTGGTCGTTGAGGGCAATG3'

GAD67: 5'CCTCAACTATGTCCGCAAGAC3' and 5'TGTGCGAACCCCATACTTCAA3'

The samples were quantified according to the $\Delta\Delta C_T$ equation and normalized on the genotype of control.

Larval movement

Larvae at 3rd instar stage (120h old) were carefully picked from fly vials, washed in a drop of water, selected against GFP balancer under UV lamp and collected into 0.6% agar plates. One larva at the time was picked, transferred to 10 cm diameter agar plate, and after a period of adaptation of 30 s, the number of peristaltic waves were counted for a period of 120 s. To confirm the right genotype of the selected and tested larvae, after crawling they were transferred to a fresh food vial, for pupae metamorphosis and enclosure into adult fly. Approximately 20 larvae per genotype were tested.

Larval NMJ immunohistochemistry

Larvae at 3rd instar stage were selected against GFP balancer under the UV lamp and kept in small 0.6% agar plates as described earlier. Larvae were then picked up individually, dissected on sylgard plates in HL-3[149],

and fixed for 20 min in 4% formaldehyde (for anti-GluRIIA larvae were fixed 5 min in methanol at -20°C). After formaldehyde fixation, larvae were transferred in 0,5 ml tubes and kept in HL-3 buffer in ice. After the dissection was over for all genotypes, dissected larvae were washed 15 min (3 x 5 min) in PBST (0.1% Tween 20 in Phosphate Buffer Saline), and a blocking step of 30 min in 5% Normal Goat Serum (NGS) in PBST (NGS-PBST) preceded the overnight incubation at 4°C with primary antibodies in 5% NGS-PBST. Primary antibodies were removed by 30 min (3 x 10 min) washes in PBST, and a second blocking step of 5% NGS-PBST of 30 min was performed before the incubation with the secondary antibodies that last 2h at room temperature. After a 1h wash (3 x 20 min) in PBST, samples were incubated overnight at 4°C in 30 µl of the mounting medium Slow Fade (S36936 Thermofisher). The next day, for mounting, larvae were transferred to the microscope slide, brain and gut were removed, and larvae were properly positioned, overlaid with Slow Fade, closed with a coverslip and sealed with nail polish. The microscope slides stored at 4°C were acquired on confocal microscope. Primary antibodies concentration: anti-Syx 8C3s (1:15, DSBH), anti-BRP (1:50, DSHB), anti-DLG 4F3c (1:250, DSHB), anti-GluRIIA 8B4D2c (1:15, DSHB), anti-GFP (1:200, Life Technologies), anti-HRP (1:150, Jackson). Secondary

antibodies concentration: Alexa Fluor 488 (1:500, rabbit and mouse, Life Technologies), Alexa Fluor 555 (555, rabbit, mouse, rat, Life Technologies).

Larval brain immunohistochemistry

Larvae, selected as previously described, were put in a drop of PB, where brains were extracted to be subsequently transferred in 0,5 ml tubes containing 4% formaldehyde in PBT (0.3% Triton X100 in Phosphate Buffer) in ice. After all brains were extracted, samples were removed form ice and fixed for 20 min at room temperature. After a wash of 60 min (3 x 20 min), brains were subjected to a blocking step of 30 min in 5% NGS-PBT before an overnight incubation at 4°C, with primary antibodies diluted in 5% NGS-PBT. The day after, a washing step of 60 min (3 x 20 min) precede an incubation with secondary antibodies in 5% NGS-PBT for 2h at RT. Three further washing steps in PBT, 20 min each, were performed before the overnight incubation with the mounting media Slow Fade at 4°C. The day after, brains were mounted on microscope slide. Primary antibodies concentration: anti-GABA (1:500, Sigma), anti-Elav (1:250, DSHB). Secondary antibodies concentration:

Alexa Fluor 488 (1:500, rabbit, Life Technologies), Alexa Fluor 555 (555, rat, Life Technologies).

Image acquisition and quantification

The images were acquired using a 63x oil lens on a Zeiss 510 Meta confocal microscope and processed with the Zeiss LSM software. Microscope and computer settings were maintained equal for all acquired larvae. Images of whole motoneurons laying on muscles 6 and 7 of the second abdominal segment were taken with a 2-fold magnification and analysed with ImageJ. For the quantification of pre- and post-synaptic proteins all samples were always labelled with both an anti-HRP and with the antibody against the protein of interest and the ratio between the mean intensity of their respective signals was measured for each synaptic bouton in the motoneuron's terminal. Glial area quantification was done by measuring the area that glia was occupying versus the area of the presynaptic terminal. Quantification of the number of branches was done at 0.7-fold magnification counting the number of motoneuron's extensions from the main branch. The regularity of synaptic boutons was calculated by measuring the number of big synaptic boutons with spherical shape. All statistical analysis was

performed with GraphPad Prism 7.0 applying Unpaired Student's T-Test or three-way ANOVA test (Bonferroni post-test).

Drug feeding

All drugs tested, were dissolved in melted regular fly food at the proper final concentration (stocks: Memantine 4.6 mM, Lithium Chloride 1 M and GABA 8 M). Parental flies were kept in drug-added-food for a period of time of 24h and were subsequently discarded. The embryos, laid in that period of time, were allowed to reach the third instar stage before performing larval movements assays.

Extraction of larval haemolymph

Haemolymph was extracted from 15-18 larvae at third instar stage for a total volume of 2 µl per genotype in the following manner: third instar larvae were pinned at the extremities and inserted in 0.5 ml tube that was cut on the bottom with a 3 mm incision, inserted in a 1.5 ml tube and centrifuged at top speed for 20 seconds approximately. The haemolymph extracted was stored at – 80 °C for further analysis. 4 µl of the haemolymph extract, were mixed with 200 µl of internal standard

solutions (10µM of L-Glutamic acid-2,3,3,4,4-d_5 from Merck KGaA, Germany) in acetonitrile : water (60 : 40) with 10 mM of NH_4OAc. After a centrifugation step, 5 µl of sample solution was run into LC-MS/MS.

Gradient elution profile and instrument

Two mobile phases, A and B, were constituted of 0.1% of formic acid in water and 0.1% of formic acid in acetonitrile respectively. The profile of gradient elution was the following: 0 min for 10% A, 3 min for 10% A, 13 min for 100% A, 20 min for 100% A, 21 min for 10% A, 31 min for 10% A. The HPLC instrument used was the Gilson 234 autosampler (from Gilson Inc., Middleton, WI), 306 Binary Pump and a Thermostatted Compartment Column (from Agilent Technologies, Morges, Switzerland). The retention of the chromatography was obtained with a hydrophilic liquid chromatography interaction (HILIC) column (ZIC®-HILIC, 150 × 2.1 mm i.d., 3.5µm, from Merck KGaA, Germany), run at 250 µl/min at 30 °C. The detection of eluates was done by amaZonSL ion trap MS (from Bruker Daltonik GmbH, Germany) in the positive electrospray ionization (ESI) mode. The voltage of the ion spray was set at 4500 V with a source temperature of 200 °C. Data were acquired according to m/z 148.1/84.1 transition of L-Glutamate and 153.1/89.1 transition of d5-L-Glutamate

(internal standard), followed by Compass Data Analysis 4.2 analysis (Bruker).

Cellular cultures and RNAi silencing

Standard conditions in DMEM-Glutamax (ThermoFisher Scientific, #31966-021) with the addition of 10% fetal bovine serum and 1X antibiotic-antimycotic solution (Sigma, #A5955) were used for SK-N-BE neuroblastoma cell culturing. TDP-43 silencing was done with HiPerfect Transfection Reagent following manufacturer instructions (Qiagen, #301705). The RNA interference sequences were the following: siRNA specific for human TDP-43 - (5'-gcaaagccaagaugagccu-3'); siRNA specific for Luciferase (Sigma, 5'-uaaggcuaugaagagauac-3'). Before transfection, 2-4 x 10^5 cells per well, in a total volume of 1.4 ml of medium containing 10% fetal serum were seeded in a 6-well plate. 3 µl of each siRNA (stock 40 µM in water), was diluted in 91 µl of Opti-MEM1 (ThermoFisher, # 51985-026), after a 5 min incubation at RT, 6 µl of HiPerfect Transfection Reagent were added, incubation of 10 minutes was done to allow formation of the complexes and finally the mixture was drop-wise added to cells. Silencing procedure was repeated after 24h and 48h.

iPS cell cultures and differentiation to MN

Dermal biopsies were used to obtain fibroblasts from ALS patients (patient # 1 was carrying G287S mutation, patient # 2: G294V mutation and patient # 3: G378S; all mutations were inside TDP-43 gene, as schematically shown in the figure 58, found below) and unaffected individuals (control # 1 and #2) which were reprogrammed in iPS cell by CytoTune iPS 2.0 Sendai Reprogramming Kit (Life Technologies)[146], based on the Sendai virus (SeV) vectors in addition to OCT4, SOX2, c-Myc an KLF4, the four reprogramming factors cloned inside the virus. iPSCs with an embryonic stem cell (ESC) like morphology were cultured on Matrigel-coated dishes (BD Biosciences) inside Essential E8 media (Life Technologies) and maintained at 37°C with 5% CO_2. iPS cells differentiation in MNs was done as described in [147].

All studies that involved human samples were performed in accordance with the Code of Ethics of the World Medical Association (Helsinki Declaration) and in compliance with national legislations and institutional guidelines. Dermal biopsies (Eurobiobank) were consented by the ethical committee of the IRCCS Foundation Ca' Grande Ospedale Maggiore Policlinico).

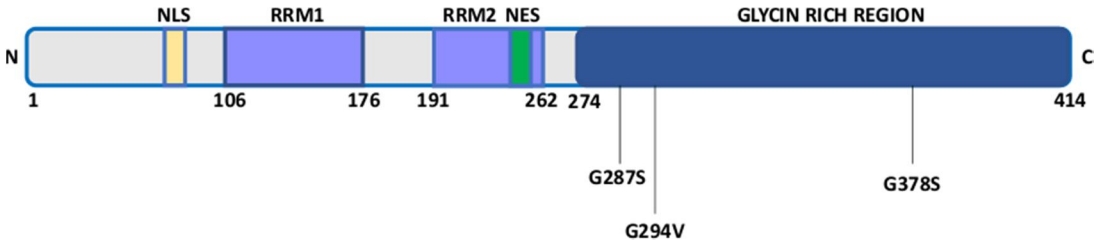

Fig. 58) Schematic representation of the positions of TDP-43 mutations, derived from ALS patient #1, #2 and #3, used in figures 55, 56 and 57. Detailed explanation in the text.

Statistical analysis

All data analysis was done with GraphPad Prism 7.0.

LITERATURE

1. Turner, M. R. & Swash, M. The expanding syndrome of amyotrophic lateral sclerosis: a clinical and molecular odyssey. *J. Neurol. Neurosurg. Psychiatry* 86, 667–673 (2015).
2. Kumar, D. R., Aslinia, F., Yale, S. H. & Mazza, J. J. Jean-Martin Charcot: The Father of Neurology. *Clin. Med. Res.* 9, 46–49 (2011).
3. Tan, S. Y. & Shigaki, D. Jean-Martin Charcot (1825-1893): pathologist who shaped modern neurology. *Singapore Med. J.* 48, 383–384 (2007).
4. Rowland, L. P. How Amyotrophic Lateral Sclerosis Got Its Name: The Clinical-Pathologic Genius of Jean-Martin Charcot. *Arch. Neurol.* 58, 512–515 (2001).
5. Goetz, C. G. Amyotrophic lateral sclerosis: early contributions of Jean-Martin Charcot. *Muscle Nerve* 23, 336–343 (2000).
6. Robberecht, W. & Philips, T. The changing scene of amyotrophic lateral sclerosis. *Nat. Rev. Neurosci.* 14, 248–264 (2013).
7. Kiernan, M. C. *et al.* Amyotrophic lateral sclerosis. *Lancet Lond. Engl.* 377, 942–955 (2011).
8. Tapia, R. Cellular and molecular mechanisms of motor neuron death in amyotrophic lateral sclerosis: a perspective. *Front. Cell. Neurosci.* 8, (2014).

9. Gordon, P. H. Amyotrophic Lateral Sclerosis: An update for 2013 Clinical Features, Pathophysiology, Management and Therapeutic Trials. *Aging Dis.* 4, 295–310 (2013).
10. Lomen-Hoerth, C. *et al.* Are amyotrophic lateral sclerosis patients cognitively normal? *Neurology* 60, 1094–1097 (2003).
11. Olney RK, Murphy J, Forshew D, Garwood E, Miller BL, Langmore S, Kohn MA, Lomen-Hoerth C. The effects of executive and behavioral dysfunction on the course of ALS. Neurology (2005)
12. Rabkin JG, Albert SM, Rowland LP and Mitsumoto H. How common is depression among ALS caregivers? A longitudinal study. Amyotrophic Lateral Sclerosis (2009).
13. Lou, J.-S., Reeves, A., Benice, T. & Sexton, G. Fatigue and depression are associated with poor quality of life in ALS. *Neurology* 60, 122–123 (2003).
14. Leone, M., Chandra, V. & Schoenberg, B. S. Motor neuron disease in the United States, 1971 and 1973-1978: patterns of mortality and associated conditions at the time of death. *Neurology* 37, 1339–1343 (1987).

15. Manjaly, Z. R. *et al.* The sex ratio in amyotrophic lateral sclerosis: A population based study. *Amyotroph. Lateral Scler. Off. Publ. World Fed. Neurol. Res. Group Mot. Neuron Dis.* 11, 439–442 (2010).
16. Corcia, P. *et al.* Causes of death in a post-mortem series of ALS patients. *Amyotroph. Lateral Scler. Off. Publ. World Fed. Neurol. Res. Group Mot. Neuron Dis.* 9, 59–62 (2008).
17. Couratier, P. *et al.* Epidemiology of amyotrophic lateral sclerosis: A review of literature. *Rev. Neurol. (Paris)* 172, 37–45 (2016).
18. Talbot, K. Motor neuron disease: the bare essentials. *Pract. Neurol.* 9, 303–309 (2009).
19. Miller, R. G., Munsat, T. L., Swash, M. & Brooks, B. R. Consensus guidelines for the design and implementation of clinical trials in ALS. World Federation of Neurology committee on Research. *J. Neurol. Sci.* 169, 2–12 (1999).
20. Brooks, B. R. El Escorial World Federation of Neurology criteria for the diagnosis of amyotrophic lateral sclerosis. Subcommittee on Motor Neuron Diseases/Amyotrophic Lateral Sclerosis of the World Federation of Neurology Research Group on Neuromuscular Diseases and the El Escorial 'Clinical limits of amyotrophic lateral

sclerosis' workshop contributors. *J. Neurol. Sci.* 124 Suppl, 96–107 (1994).

21. Ludolph, A. *et al.* A revision of the El Escorial criteria - 2015. *Amyotroph. Lateral Scler. Front. Degener.* 16, 291–292 (2015).
22. Agosta, F. *et al.* The El Escorial criteria: strengths and weaknesses. *Amyotroph. Lateral Scler. Front. Degener.* 16, 1–7 (2015).
23. Chiò A, Mora G, Leone M, Mazzini L, Cocito D, Giordana MT, Bottacchi E, Mutani R. Early symptom progression rate is related to ALS outcome: a prospective population-based study. Neurology (2002).
24. Miller, R. G. *et al.* Practice parameter update: the care of the patient with amyotrophic lateral sclerosis: multidisciplinary care, symptom management, and cognitive/behavioral impairment (an evidence-based review): report of the Quality Standards Subcommittee of the American Academy of Neurology. *Neurology* 73, 1227–1233 (2009).
25. Chiò, A., Bottacchi, E., Buffa, C., Mutani, R. & Mora, G. Positive effects of tertiary centres for amyotrophic lateral sclerosis on outcome and use of hospital facilities. *J. Neurol. Neurosurg. Psychiatry* 77, 948–950 (2006).

26. Zoccolella, S. *et al.* Riluzole and amyotrophic lateral sclerosis survival: a population-based study in southern Italy. *Eur. J. Neurol.* 14, 262–268 (2007).

27. Petrov, D., Mansfield, C., Moussy, A. & Hermine, O. ALS Clinical Trials Review: 20 Years of Failure. Are We Any Closer to Registering a New Treatment? *Front. Aging Neurosci.* 9, (2017).

28. Chiò, A. *et al.* Global epidemiology of amyotrophic lateral sclerosis: a systematic review of the published literature. *Neuroepidemiology* 41, 118–130 (2013).

29. Régal, L. *et al.* The G93C mutation in superoxide dismutase 1: clinicopathologic phenotype and prognosis. *Arch. Neurol.* 63, 262–267 (2006).

30. Rosen, D. R. *et al.* Mutations in Cu/Zn superoxide dismutase gene are associated with familial amyotrophic lateral sclerosis. *Nature* 362, 59–62 (1993).

31. Bendotti, C. *et al.* Dysfunction of constitutive and inducible ubiquitin-proteasome system in amyotrophic lateral sclerosis: implication for protein aggregation and immune response. *Prog. Neurobiol.* 97, 101–126 (2012).

32. Ezzi, S. A., Urushitani, M. & Julien, J.-P. Wild-type superoxide dismutase acquires binding and toxic properties of ALS-linked mutant forms through oxidation. *J. Neurochem.* 102, 170–178 (2007).

33. Andersen, J. K. Oxidative stress in neurodegeneration: cause or consequence? *Nat. Med.* 10 Suppl, S18-25 (2004).

34. Neumann, M. *et al.* Ubiquitinated TDP-43 in frontotemporal lobar degeneration and amyotrophic lateral sclerosis. *Science* 314, 130–133 (2006).

35. Lee, E. B., Lee, V. M.-Y. & Trojanowski, J. Q. Gains or losses: molecular mechanisms of TDP43-mediated neurodegeneration. *Nat. Rev. Neurosci.* 13, 38–50 (2011).

36. Renton, A. E. *et al.* A hexanucleotide repeat expansion in C9ORF72 is the cause of chromosome 9p21-linked ALS-FTD. *Neuron* 72, 257–268 (2011).

37. Weisskopf, M. G. *et al.* Prospective study of chemical exposures and amyotrophic lateral sclerosis. *J. Neurol. Neurosurg. Psychiatry* 80, 558–561 (2009).

38. Simkó, M. & Mattsson, M.-O. Extremely low frequency electromagnetic fields as effectors of cellular responses in vitro: possible immune cell activation. *J. Cell. Biochem.* 93, 83–92 (2004).
39. Huisman, M. H. B. *et al.* Population based epidemiology of amyotrophic lateral sclerosis using capture-recapture methodology. *J. Neurol. Neurosurg. Psychiatry* 82, 1165–1170 (2011).
40. Morozova, N. *et al.* Diet and amyotrophic lateral sclerosis. *Epidemiol. Camb. Mass* 19, 324–337 (2008).
41. Veldink, J. H. *et al.* Intake of polyunsaturated fatty acids and vitamin E reduces the risk of developing amyotrophic lateral sclerosis. *J. Neurol. Neurosurg. Psychiatry* 78, 367–371 (2007).
42. Zarei, S. *et al.* A comprehensive review of amyotrophic lateral sclerosis. *Surg. Neurol. Int.* 6, 171 (2015).
43. Lin, C. L. *et al.* Aberrant RNA processing in a neurodegenerative disease: the cause for absent EAAT2, a glutamate transporter, in amyotrophic lateral sclerosis. *Neuron* 20, 589–602 (1998).
44. Shaw, P. J. & Eggett, C. J. Molecular factors underlying selective vulnerability of motor neurons to neurodegeneration in amyotrophic lateral sclerosis. *J. Neurol.* 247 Suppl 1, I17-27 (2000).

45. Lezi, E. & Swerdlow, R. H. Mitochondria in neurodegeneration. *Adv. Exp. Med. Biol.* 942, 269–286 (2012).

46. Martin, L. J. Mitochondrial pathobiology in ALS. *J. Bioenerg. Biomembr.* 43, 569–579 (2011).

47. Menzies, F. M., Ince, P. G. & Shaw, P. J. Mitochondrial involvement in amyotrophic lateral sclerosis. *Neurochem. Int.* 40, 543–551 (2002).

48. Pasinelli, P. *et al.* Amyotrophic lateral sclerosis-associated SOD1 mutant proteins bind and aggregate with Bcl-2 in spinal cord mitochondria. *Neuron* 43, 19–30 (2004).

49. Liu, J. *et al.* Toxicity of familial ALS-linked SOD1 mutants from selective recruitment to spinal mitochondria. *Neuron* 43, 5–17 (2004).

50. Ikenaka, K. *et al.* Disruption of axonal transport in motor neuron diseases. *Int. J. Mol. Sci.* 13, 1225–1238 (2012).

51. Jin Hee Shin, Jae Keun Lee. Multiple Routes of Motor Neuron Degeneration in ALS. IntechOpen. (2013)

52. Ou, S. H., Wu, F., Harrich, D., García-Martínez, L. F. & Gaynor, R. B. Cloning and characterization of a novel cellular protein, TDP-43, that

binds to human immunodeficiency virus type 1 TAR DNA sequence motifs. *J. Virol.* 69, 3584–3596 (1995).

53. Wang, H.-Y., Wang, I.-F., Bose, J. & Shen, C.-K. J. Structural diversity and functional implications of the eukaryotic TDP gene family. *Genomics* 83, 130–139 (2004).
54. Buratti, E. *et al.* Nuclear factor TDP-43 and SR proteins promote in vitro and in vivo CFTR exon 9 skipping. *EMBO J.* 20, 1774–1784 (2001).
55. Krecic, A. M. & Swanson, M. S. hnRNP complexes: composition, structure, and function. *Curr. Opin. Cell Biol.* 11, 363–371 (1999).
56. Ayala, Y. M. *et al.* Human, Drosophila, and C.elegans TDP43: nucleic acid binding properties and splicing regulatory function. *J. Mol. Biol.* 348, 575–588 (2005).
57. Tollervey, J. R. *et al.* Characterizing the RNA targets and position-dependent splicing regulation by TDP-43. *Nat. Neurosci.* 14, 452–458 (2011).
58. Mercado, P. A., Ayala, Y. M., Romano, M., Buratti, E. & Baralle, F. E. Depletion of TDP 43 overrides the need for exonic and intronic splicing enhancers in the human apoA-II gene. *Nucleic Acids Res.* 33, 6000–6010 (2005).

59. Ayala, Y. M., Misteli, T. & Baralle, F. E. TDP-43 regulates retinoblastoma protein phosphorylation through the repression of cyclin-dependent kinase 6 expression. *Proc. Natl. Acad. Sci. U. S. A.* 105, 3785–3789 (2008).

60. Fiesel, F. C. *et al.* Knockdown of transactive response DNA-binding protein (TDP-43) downregulates histone deacetylase 6. *EMBO J.* 29, 209–221 (2010).

61. Godena, V. K. *et al.* TDP-43 Regulates Drosophila Neuromuscular Junctions Growth by Modulating Futsch/MAP1B Levels and Synaptic Microtubules Organization. *PLoS ONE* 6, (2011).

62. Strong, M. J. *et al.* TDP43 is a human low molecular weight neurofilament (hNFL) mRNA-binding protein. *Mol. Cell. Neurosci.* 35, 320–327 (2007).

63. Barmada, S. J. *et al.* Cytoplasmic mislocalization of TDP-43 is toxic to neurons and enhanced by a mutation associated with familial amyotrophic lateral sclerosis. *J. Neurosci. Off. J. Soc. Neurosci.* 30, 639–649 (2010).

64. Alami, N. H. *et al.* Axonal transport of TDP-43 mRNA granules is impaired by ALS-causing mutations. *Neuron* 81, 536–543 (2014).

65. Wang, I.-F., Wu, L.-S., Chang, H.-Y. & Shen, C.-K. J. TDP-43, the signature protein of FTLD-U, is a neuronal activity-responsive factor. *J. Neurochem.* 105, 797–806 (2008).

66. Buratti, E. *et al.* Nuclear factor TDP-43 can affect selected microRNA levels. *FEBS J.* 277, 2268–2281 (2010).

67. Ayala, Y. M. *et al.* TDP-43 regulates its mRNA levels through a negative feedback loop. *EMBO J.* 30, 277–288 (2011).

68. Buratti, E. & Baralle, F. E. TDP-43: gumming up neurons through protein-protein and protein-RNA interactions. *Trends Biochem. Sci.* 37, 237–247 (2012).

69. Leigh, P. N. *et al.* Ubiquitin-immunoreactive intraneuronal inclusions in amyotrophic lateral sclerosis. Morphology, distribution, and specificity. *Brain J. Neurol.* 114 (Pt 2), 775–788 (1991).

70. Okamoto, K. *et al.* Ubiquitin-positive intraneuronal inclusions in the extramotor cortices of presenile dementia patients with motor neuron disease. *J. Neurol.* 239, 426–430 (1992).

71. Arai, T. *et al.* TDP-43 is a component of ubiquitin-positive tau-negative inclusions in frontotemporal lobar degeneration and amyotrophic lateral sclerosis. *Biochem. Biophys. Res. Commun.* 351, 602–611 (2006).

72. Neumann, M. *et al.* TDP-43-positive white matter pathology in frontotemporal lobar degeneration with ubiquitin-positive inclusions. *J. Neuropathol. Exp. Neurol.* 66, 177–183 (2007).
73. Mackenzie, I. R. A. *et al.* Pathological TDP-43 distinguishes sporadic amyotrophic lateral sclerosis from amyotrophic lateral sclerosis with SOD1 mutations. *Ann. Neurol.* 61, 427–434 (2007).
74. Amador-Ortiz, C. *et al.* TDP-43 immunoreactivity in hippocampal sclerosis and Alzheimer's disease. *Ann. Neurol.* 61, 435–445 (2007).
75. Higashi, S. *et al.* Concurrence of TDP-43, tau and alpha-synuclein pathology in brains of Alzheimer's disease and dementia with Lewy bodies. *Brain Res.* 1184, 284–294 (2007).
76. Willard, S. S. & Koochekpour, S. Glutamate, glutamate receptors, and downstream signaling pathways. *Int. J. Biol. Sci.* 9, 948–959 (2013).
77. Watkins, J. C. & Jane, D. E. The glutamate story. *Br. J. Pharmacol.* 147 Suppl 1, S100-108 (2006).
78. Kelly, A. & Stanley, C. A. Disorders of glutamate metabolism. *Ment. Retard. Dev. Disabil. Res. Rev.* 7, 287–295 (2001).

79. Boeree G. Neurotransmitters. http://webspace.ship.edu/cgboer/genpsyneurotransmitters.html

80. Birnbaumer, L. *et al.* The naming of voltage-gated calcium channels. *Neuron* 13, 505–506 (1994).

81. Walls, A. B., Waagepetersen, H. S., Bak, L. K., Schousboe, A. & Sonnewald, U. The glutamine-glutamate/GABA cycle: function, regional differences in glutamate and GABA production and effects of interference with GABA metabolism. *Neurochem. Res.* 40, 402–409 (2015).

82. Schousboe, A., Bak, L. K. & Waagepetersen, H. S. Astrocytic Control of Biosynthesis and Turnover of the Neurotransmitters Glutamate and GABA. *Front. Endocrinol.* 4, 102 (2013).

83. Erlander, M. G. & Tobin, A. J. The structural and functional heterogeneity of glutamic acid decarboxylase: a review. *Neurochem. Res.* 16, 215–226 (1991).

84. Traynelis, S. F. *et al.* Glutamate receptor ion channels: structure, regulation, and function. *Pharmacol. Rev.* 62, 405–496 (2010).

85. Hermans, E. & Challiss, R. A. Structural, signalling and regulatory properties of the group I metabotropic glutamate receptors:

prototypic family C G-protein-coupled receptors. *Biochem. J.* 359, 465–484 (2001).

86. Niswender, C. M. & Conn, P. J. Metabotropic glutamate receptors: physiology, pharmacology, and disease. *Annu. Rev. Pharmacol. Toxicol.* 50, 295–322 (2010).
87. Shiraishi-Yamaguchi, Y. & Furuichi, T. The Homer family proteins. *Genome Biol.* 8, 206 (2007).
88. Julio-Pieper, M., Flor, P. J., Dinan, T. G. & Cryan, J. F. Exciting times beyond the brain: metabotropic glutamate receptors in peripheral and non-neural tissues. *Pharmacol. Rev.* 63, 35–58 (2011).
89. Levy, L. M., Warr, O. & Attwell, D. Stoichiometry of the glial glutamate transporter GLT-1 expressed inducibly in a Chinese hamster ovary cell line selected for low endogenous Na+-dependent glutamate uptake. *J. Neurosci. Off. J. Soc. Neurosci.* 18, 9620–9628 (1998).
90. Leigh, P. N. & Meldrum, B. S. Excitotoxicity in ALS. *Neurology* 47, S221-227 (1996).
91. Megumi Akamatsu, Takenari Yamashita, Naoki Hirose, Sayaka Teramoto, Shin Kwak. The AMPA receptor antagonist perampanel

robustly rescues amyotrophic lateral sclerosis (ALS) pathology in sporadic ALS model mice. Scientific Reports (2016).

92. Maas, S., Kawahara, Y., Tamburro, K. M. & Nishikura, K. A-to-I RNA Editing and Human Disease. *RNA Biol.* 3, 1–9 (2006).
93. Sanelli, T., Ge, W., Leystra-Lantz, C. & Strong, M. J. Calcium mediated excitotoxicity in neurofilament aggregate-bearing neurons in vitro is NMDA receptor dependant. *J. Neurol. Sci.* 256, 39–51 (2007).
94. Ozyurt, E., Graham, D. I., Woodruff, G. N. & McCulloch, J. Protective effect of the glutamate antagonist, MK-801 in focal cerebral ischemia in the cat. *J. Cereb. Blood Flow Metab. Off. J. Int. Soc. Cereb. Blood Flow Metab.* 8, 138–143 (1988).
95. Mukhin, A., Fan, L. & Faden, A. I. Activation of metabotropic glutamate receptor subtype mGluR1 contributes to post-traumatic neuronal injury. *J. Neurosci. Off. J. Soc. Neurosci.* 16, 6012–6020 (1996).
96. Bruno, V. *et al.* The neuroprotective activity of group-II metabotropic glutamate receptors requires new protein synthesis and involves a glial-neuronal signaling. *J. Neurosci. Off. J. Soc. Neurosci.* 17, 1891–1897 (1997).

97. Ren, K., Iadarola, M. J. & Dubner, R. An isobolographic analysis of the effects of N-methyl-D-aspartate and NK1 tachykinin receptor antagonists on inflammatory hyperalgesia in the rat. *Br. J. Pharmacol.* 117, 196–202 (1996).

98. Rothstein, J. D., Van Kammen, M., Levey, A. I., Martin, L. J. & Kuncl, R. W. Selective loss of glial glutamate transporter GLT-1 in amyotrophic lateral sclerosis. *Ann. Neurol.* 38, 73–84 (1995).

99. Roth, F. C. & Draguhn, A. GABA Metabolism and Transport: Effects on Synaptic Efficacy. *Neural Plasticity* (2012). doi:10.1155/2012/805830

100. Haugstad, T. S., Hegstad, E. & Langmoen, I. A. Calcium dependent release of gamma-aminobutyric acid (GABA) from human cerebral cortex. *Neurosci. Lett.* 141, 61–64 (1992).

101. Flores-Soto, M. E. *et al.* Structure and function of NMDA-type glutamate receptor subunits. *Neurol. Engl. Ed.* 301–310 doi:10.1016/j.nrleng.2011.10.003

102. Wu, C. & Sun, D. GABA receptors in brain development, function, and injury. *Metab. Brain Dis.* 30, 367–379 (2015).

103. Langendorf, C. G. *et al.* Structural characterization of the mechanism through which human glutamic acid decarboxylase auto-activates. *Biosci. Rep.* 33, (2013).

104. Soghomonian, J. J. & Martin, D. L. Two isoforms of glutamate decarboxylase: why? *Trends Pharmacol. Sci.* 19, 500–505 (1998).

105. Pinal, C. S. & Tobin, A. J. Uniqueness and redundancy in GABA production. *Perspect. Dev. Neurobiol.* 5, 109–118 (1998).

106. Gustavo Fenalti, Ruby H P Law, Ashley M Buckle, Christopher Langendorf, Kellie Tuck, Carlos J Rosado, Noel G Faux, Khalid Mahmood, Christiane S Hampe, J Paul Banga, Matthew Wilce, Jason Schmidberger, Jamie Rossjohn, Ossama El-Kabbani, Robert N Pike, A Ian Smith, Ian R Mackay, Merrill J Rowley & James C Whisstock. GABA production by glutamic acid decarboxylase is regulated by a dynamic catalytic loop. Nature Structural and Molecular Biology (2007).

107. Akbarian, S. & Huang, H.-S. Molecular and cellular mechanisms of altered GAD1/GAD67 expression in schizophrenia and related disorders. *Brain Res. Rev.* 52, 293–304 (2006).

108. Saiz, A. *et al.* Spectrum of neurological syndromes associated with glutamic acid decarboxylase antibodies: diagnostic clues for this association. *Brain J. Neurol.* 131, 2553–2563 (2008).

109. Jennings, B. H. Drosophila – a versatile model in biology & medicine. *Mater. Today* 14, 190–195 (2011).

110. Maynard, J. Identification of Essential Functions of GRP94 in Metazoan Growth Control and Epithelial Homeostasis. (2018).

111. Robertson, H. M. *et al.* A stable genomic source of P element transposase in *Drosophila melanogaster*. *Genetics* 118, 461–470 (1988).

112. Bischof, J., Maeda, R. K., Hediger, M., Karch, F. & Basler, K. An optimized transgenesis system for Drosophila using germ-line-specific phiC31 integrases. *Proc. Natl. Acad. Sci. U. S. A.* 104, 3312–3317 (2007).

113. Brand, A. H. & Perrimon, N. Targeted gene expression as a means of altering cell fates and generating dominant phenotypes. *Dev. Camb. Engl.* 118, 401–415 (1993).

114. Nassif, C., Noveen, A. & Hartenstein, V. Early development of the Drosophila brain: III. The pattern of neuropile founder tracts during the larval period. *J. Comp. Neurol.* 455, 417–434 (2003).

115. Hummel, T., Schimmelpfeng, K. & Klämbt, C. Commissure Formation in the Embryonic CNS ofDrosophila: I. Identification of the Required Gene Functions. *Dev. Biol.* 209, 381–398 (1999).

116. Hartenstein, V. & Wodarz, A. Initial neurogenesis in Drosophila. *Wiley Interdiscip. Rev. Dev. Biol.* 2, 701–721 (2013).

117. Spindler, S. R. & Hartenstein, V. The Drosophila neural lineages: a model system to study brain development and circuitry. *Dev. Genes Evol.* 220, 1–10 (2010).

118. Neumüller, R. A. & Knoblich, J. A. Dividing cellular asymmetry: asymmetric cell division and its implications for stem cells and cancer. *Genes Dev.* 23, 2675–2699 (2009).

119. Broadie, K. *et al.* From growth cone to synapse: the life history of the RP3 motor neuron. *Development* 119, 227–238 (1993).

120. Keshishian, H., Broadie, K., Chiba, A. & Bate, M. The drosophila neuromuscular junction: a model system for studying synaptic development and function. *Annu. Rev. Neurosci.* 19, 545–575 (1996).

121. Gramates, L. S. & Budnik, V. Assembly and maturation of the Drosophila larval neuromuscular junction. *Int. Rev. Neurobiol.* 43, 93–117 (1999).

122. Halpern, M. E., Chiba, A., Johansen, J. & Keshishian, H. Growth cone behavior underlying the development of stereotypic synaptic connections in Drosophila embryos. *J. Neurosci. Off. J. Soc. Neurosci.* 11, 3227–3238 (1991).

123. Prokop, A., Landgraf, M., Rushton, E., Broadie, K. & Bate, M. Presynaptic development at the Drosophila neuromuscular junction: assembly and localization of presynaptic active zones. *Neuron* 17, 617–626 (1996).

124. Stork, T., Bernardos, R. & Freeman, M. R. Analysis of Glial Cell Development and Function in Drosophila. *Cold Spring Harb. Protoc.* 2012, 1–17 (2012).

125. Hartenstein, V. Structure and Development of Glia in Drosophila. *Glia* 59, 1237–1252 (2011).

126. Banerjee, S. & Bhat, M. A. Glial Ensheathment of Peripheral Axons in Drosophila. *J. Neurosci. Res.* 86, 1189–1198 (2008).

127. Akbergenova, Y. & Bykhovskaia, M. Synapsin regulates vesicle organization and activity-dependent recycling at Drosophila motor boutons. *Neuroscience* 170, 441–452 (2010).

128. Ilardi, J. M., Mochida, S. & Sheng, Z. H. Snapin: a SNARE-associated protein implicated in synaptic transmission. *Nat. Neurosci.* 2, 119–124 (1999).

129. Wagh, D. A. *et al.* Bruchpilot, a protein with homology to ELKS/CAST, is required for structural integrity and function of synaptic active zones in Drosophila. *Neuron* 49, 833–844 (2006).

130. Mays, T. A., Sanford, J. L., Hanada, T., Chishti, A. H. & Rafael-Fortney, J. A. Glutamate receptors localize postsynaptically at neuromuscular junctions in mice. *Muscle Nerve* 39, 343–349 (2009).

131. Ultsch, A., Schuster, C. M., Laube, B., Betz, H. & Schmitt, B. Glutamate receptors of *Drosophila melanogaster*. Primary structure of a putative NMDA receptor protein expressed in the head of the adult fly. *FEBS Lett.* 324, 171–177 (1993).

132. Han, T. H., Dharkar, P., Mayer, M. L. & Serpe, M. Functional reconstitution of *Drosophila melanogaster* NMJ glutamate receptors. *Proc. Natl. Acad. Sci. U. S. A.* 112, 6182–6187 (2015).

133. Mitri, C., Parmentier, M.-L., Pin, J.-P., Bockaert, J. & Grau, Y. Divergent evolution in metabotropic glutamate receptors. A new receptor activated by an endogenous ligand different from glutamate in insects. *J. Biol. Chem.* 279, 9313–9320 (2004).

134. Astorga, C. *et al.* Presynaptic DLG regulates synaptic function through the localization of voltage-activated Ca(2+) Channels. *Sci. Rep.* 6, 32132 (2016).

135. Jackson, F. R., Newby, L. M. & Kulkarni, S. J. Drosophila GABAergic systems: sequence and expression of glutamic acid decarboxylase. *J. Neurochem.* 54, 1068–1078 (1990).

136. Featherstone, D. E. *et al.* Presynaptic Glutamic Acid Decarboxylase Is Required for Induction of the Postsynaptic Receptor Field at a Glutamatergic Synapse. *Neuron* 27, 71–84 (2000).

137. Phillips, A. M., Salkoff, L. B. & Kelly, L. E. A neural gene from *Drosophila melanogaster* with homology to vertebrate and invertebrate glutamate decarboxylases. *J. Neurochem.* 61, 1291–1301 (1993).

138. Featherstone, D. E., Rushton, E. & Broadie, K. Developmental regulation of glutamate receptor field size by nonvesicular glutamate release. *Nat. Neurosci.* 5, 141–146 (2002).

139. Mizielinska, S. *et al.* C9orf72 repeat expansions cause neurodegeneration in Drosophila through arginine-rich proteins. *Science* 345, 1192–1194 (2014).

140. Li, Y. *et al.* A Drosophila model for TDP-43 proteinopathy. *Proc. Natl. Acad. Sci. U. S. A.* 107, 3169–3174 (2010).

141. Watson, M. R., Lagow, R. D., Xu, K., Zhang, B. & Bonini, N. M. A drosophila model for amyotrophic lateral sclerosis reveals motor neuron damage by human SOD1. *J. Biol. Chem.* 283, 24972–24981 (2008).

142. Feiguin, F. *et al.* Depletion of TDP-43 affects Drosophila motoneurons terminal synapsis and locomotive behavior. *FEBS Lett.* 583, 1586–1592 (2009).

143. Romano, G. *et al.* Chronological requirements of TDP-43 function in synaptic organization and locomotive control. *Neurobiol. Dis.* 71, 95–109 (2014).

144. Straus W. Cytochemical detection of mannose-specific receptors for glycoproteins with horseradish peroxidase as a ligand. Histochemistry (1981).

145. Romano, G. *et al.* Glial TDP-43 regulates axon wrapping, GluRIIA clustering and fly motility by autonomous and non-autonomous mechanisms. *Hum. Mol. Genet.* 24, 6134–6145 (2015).

146. Fusaki, N., Ban, H., Nishiyama, A., Saeki, K. & Hasegawa, M. Efficient induction of transgene-free human pluripotent stem cells using a

vector based on Sendai virus, an RNA virus that does not integrate into the host genome. *Proc. Jpn. Acad. Ser. B Phys. Biol. Sci.* 85, 348–362 (2009).

147. Ng, S.-Y. *et al.* Genome-wide RNA-Seq of Human Motor Neurons Implicates Selective ER Stress Activation in Spinal Muscular Atrophy. *Cell Stem Cell* 17, 569–584 (2015).

148. Feng, Y., Ueda, A. & Wu, C.-F. A modified minimal hemolymph-like solution, HL3.1, for physiological recordings at the neuromuscular junctions of normal and mutant Drosophila larvae. *J. Neurogenet.* 18, 377–402 (2004).